AD-751 055

THE YIELD BEHAVIOUR OF RIGID POLYMERS

J. A. Jukes

Ministry of Defence
London, England

June 1972

UNLIMITED

BR 28227

D Mat Report No 180

PROCUREMENT EXECUTIVE, MINISTRY OF DEFENCE

AD751055

THE YIELD BEHAVIOUR OF RIGID POLYMERS

J. A. Jukes

Trinity College, University of Cambridge

JUNE 1972

UNLIMITED

D Mat Report No 180

D Mat Ref ZB/107/4

PROCUREMENT EXECUTIVE, MINISTRY OF DEFENCE

THE YIELD BEHAVIOUR OF RIGID POLYMERS

J A Jukes

JUNE 1972

Report to Director of Research Materials 3 (Air Systems) under former Ministry of Technology Research Agreement No FD 129/050/ADM

FOREWORD

This report was prepared by J A Jukes, Trinity College, University of Cambridge for the Director of Research Materials 2 (Air Systems), Procurement Executive, Ministry of Defence, under Research Agreement PD 129/70/ADM.

The work was initiated on 1 October 1966 and administered by Mat(O)1 under the direction of ADR/MAT 2(O), Procurement Executive, Ministry of Defence. This report covers the period October 1966 to October 1969.

SUMMARY

The yield behaviour of solid polymers has been examined, with especial reference to that of the glassy amorphous polymers. Considering polymethyl methacrylate to be a typical glassy amorphous polymer, the effects of strain rate and temperature on the yield stress have been determined by taking stress-strain curves in simple plane strain compression.

The variation of the plane strain compressive yield stress with applied tension and compression has also been determined for polymethyl methacrylate and several other polymers.

It was shown that the hydrostatic component of stress had a significant effect on the yield behaviour of the polymers studied. This has been considered in terms of the Tresca and von Mises yield criteria modified for pressure dependence. It was found that a relation of the form $K = Ko - \mu P$ could be used to explain the observed pressure dependence of yielding for the stress states studied, where K is the critical yield stress, Ko is a constant termed the cohesion, μ a constant termed the coefficient of internal friction and P the hydrostatic stress component. It was found, however, that the polymers were sensitive to the testing conditions employed and that the relatively simple yield criteria of Tresca and von Mises only have application to a specified structure and set of testing conditions.

By considering yielding as an equilibrium between the applied strain rate and the rate at which units of the structure move, an equation has been derived allowing interpretation of the yield condition in terms of the molecular processes associated with yielding or flow in polymers. The interpretation of yield as a rate process was confirmed for polymethyl methacrylate when it was found that Ko increased linearly with the logarithm of the strain rate over three decades at room temperature.

It was shown that μ was a parameter expressing the sensitivity of a polymer to the hydrostatic stress component.

In polymethyl methacrylate it was found that μ was constant over the temperature range 20° to 70° suggesting that the various effects giving rise to pressure dependent yielding are overall independent of temperature.

It was shown that increasing the crystallinity of a polymer causes the value of Ko to increase, whereas addition of plasticiser decreases the value, similar changes occuring with μ. From these effects and the range of values observed for Ko and μ for different polymers a qualitative indication of the effects of different polymer structures on yield behaviour was obtained.

LIST OF SYMBOLS AND ABBREVIATIONS

D - deviatoric stress tensor

$J_{1,2,3}$ - first invariants of stress tensor

J'_2 - second invariant of deviatoric stress tensor

J'_3 - third invariant of deviatoric stress tensor

σ - stress under dies

σ' - measured stress

σ'' - stress with no friction between dies and specimen

σ_1 - compressive stress

σ_2 - tensile stress

$\sigma_{1,2,3}$ - principal components of stress

σ_x - normal stress

σ_n - normal stress across shear plane

σ^u - fully corrected uniaxial yield stress

σ^p - fully corrected plane yield stress

σ_y - yield stress

$\tau_{xy,yz,zx}$ - shearing stresses

S - applied stress

P - hydrostatic stress

k - shear yield stress in pure shear

F - average force in direction of applied stress

ε - nominal strain

ε'_1 - compressive strain after relaxation

ε'_2 - tensile strain after relaxation

e - true or natural strain

e_a - nominal applied strain

e_r - nominal residual strain

e_x - strain in x direction

ε_y - yield strain

ε_y - strain in y direction

γ_{xy} - shear strain

$\dot{\varepsilon}_{1,2,3}$ - principal strain rates

$\dot{G}$ - shear strain rate

$\varepsilon' x$ - volume expansion

f - vibrational jump frequency

f_o - basic frequency

f_{nett} - nett frequency

F_o - natural jump frequency at zero hydrostatic pressure

p - pressure

$\bar{p}$ - mean pressure on dies

W - total work absorbed

W_σ - work done against normal stress

W_τ - work done by shearing stress

x - bulk modulus

E' - yield modulus

Y' - Young's modulus for uniaxial compression

V - Poisson's ratio

ϕ - angle of shear plane (angle of internal friction $\tan^{-1} \mu$)

α - angle of inclination of shear zones after unloading

α' - angle of inclination of shear zones at instant of yield

β - $90^\circ - \alpha$

d - measured density

d_a - density of amorphous material

d_c - density of crystalline material

C' - weight percent crystallinity

λ' - component of volume expansion normal to shear direction (displacement normal to the shear direction)

μ - coefficient of internal friction

K_o - cohesion

V_a - activation volume

T_g - glass transition temperature

λ - distance between equilibrium positions (shear displacement)

T - absolute temperature

E_o - energy barrier height

ϕ_s - coefficient of surface friction

R - part of total load per unit specimen width provided by elastically deforming the material outside the test section

K_B - Boltzmann's constant

A - effective cross sectional area of the deforming unit

w - specimen width

b - specimen breadth

h_o - original specimen thickness

h - specimen thickness

a - specimen radius

A')
B)
C) - constants
c)
m)

PMMA - Polymethyl methacrylate

PS - Polystyrene

PVC - Polyvinylchloride

PET - Polyethylene terephthalate

LDPE - Low density polyethylene

HDPE - High density polyethylene

CONTENTS

1 INTRODUCTION AND PROGRAMME

In addition to elasticity and viscoelasticity, which are observed at low stress levels, one of the fundamental types of stress response in rigid polymers is plastic yield. At the present time this important phenomenon is not as well understood for polymers as for metals.

In general, plastic yielding in metals takes place by slip on crystallographic planes by dislocation movement. Deformation occurs in shear when the maximum shear stress or the elastic shear strain energy density reaches a critical value. In either case the critical shear stress for yield is independent of the hydrostatic stress component, and deformation takes place at essentially constant volume.

The deformation of amorphous polymers has no known simple mechanism analogous to dislocation movement, and in view of the complex structure of these materials the process by which plastic yielding occurs is likely to be more complicated. It is therefore improbable that the critical shear stress to produce deformation is a well defined parameter as in metals. Volume changes in polymers appear to be more pronounced, and it is unlikely that the shear stress for yield is independent of the hydrostatic stress component.

Usually studies of yield, and yield criteria, involve tensile testing of rods or flat strips and thin walled tubes subjected to torsion or internal pressure. In the present work plane strain compression was used to study yield phenomena in a number of polymers, as this type of test avoids many of the difficulties associated with tensile testing at large strains. To investigate the yield criterion, sheet specimens compressed in plane strain were also subjected to a tensile stress in the plane of the sheet, and the compressive yield stress determined as a function of the applied tension. Since plane strain conditions were used, it was also possible to take sections from the plane of deformation and observe the development of plastic strains within a specimen.

For these experiments a loading system in which biaxial tensile or compressive stresses could be applied to a sheet specimen was designed and built. Facilities were also included for measurement of the large strains involved, and for testing up to a temperature of 70°C.

Initially the yield behaviour of glassy amorphous polymers was considered, as the complicating variable of crystalline morphology could be avoided. Prime consideration was given to polymethyl methacrylate (PMMA), as this material typifies many of the characteristics of glassy amorphous polymers, and is readily available commercially as "Perspex" sheet. Stress-strain curves were determined in simple plane strain compression in order to define a yield point for this material, and the effects of strain rate and temperature on the yield stress were investigated. Tests under combined stress illustrated a significant effect of the hydrostatic stress component on yielding, and these results are discussed in terms of some of the more important yield criteria used for other materials.

The yield behaviour in simple plane strain compression, and under combined stress states was also investigated for polystyrene, rigid polyvinyl choride, polyethylene terephthalate, two epoxy resins, and low and high density polyethylene. Similar effects were observed in all these polymers, and two parameters are used to describe the yield behaviour in each case.

Some of the current ideas on the mechanism of yielding in solid polymers are discussed, and the Eyring rate theory used to suggest an explanation of the main features of the observed yield behaviour.

2 WORK CARRIED OUT AND RESULTS OBTAINED

2.1 Specimen preparation and experimental technique

2.1.1 Specimen preparation

Flat, parallel sided, sheet specimens 114mm long and 38mm wide were cut out and prepared for testing in a variety of ways depending upon the type of polymer, and these are mentioned below. To ensure comparable results from one test to the next, specimens were, as far as possible, all taken from the same sheet, and a number of specimens sufficient to cover the needs of any one series of tests all given the same preparative treatment.

2.1.1.1 Polymethyl methacrylate (PMMA)

Commercial ICI "Perspex" cast acrylic sheet, approximately 1.6mm thick, was used. This material had a weight average molecular weight of the order of 2.3×10^5, and contained no plasticiser. Its glass transition temperature was given as in the range 105-110°C. Specimens were cut from the sheet using a band saw, then milled to size, and the edges polished to remove any remaining scratches. These samples contained a small amount of residual moulding strain which was removed, together with moisture and excess monomer, by annealing. This was accomplished by laying them on talc, in an air oven maintained at 110°C, for 24 hours, and then slow cooling over a further period of 24 hours. After this treatment the specimens appeared to be isotropic under polarised light. They were stored in a dessicator until required.

2.1.1.2 Polystyrene (PS)

Granular polystyrene was supplied by Shell as Carinex QP crystal, which had a weight average molecular weight of the order of 10^5, and contained a small amount of plasticiser (less than 1%). The glass transition temperature was given as approximately 100°C. The granules supplied were compression moulded at 170°C into amorphous, unoriented sheets, approximately 3.2mm thick, and standard size specimens were taken from the sheets as described for PMMA. The specimens were annealed on talc for 24 hours at 100°C, followed by slow cooling. Before storing the specimens in the dessicator, they were carefully checked for crazes which readily occurred during preparation.

2.1.1.3 Polyvinyl chloride (PVC)

The specimens which were cut and polished as described for PMMA were taken from a commercial grade rigid polyvinyl chloride, manufactured by ICI as "Darvic" sheet. The material was in the form of clear sheet, approximately 1.6mm thick, which was unlikely to be plasticised, but probably did contain a small amount of stabiliser. The specimens contained a small amount of orientation from the fabrication process, but no annealing treatment was given.

2.1.1.4 Epoxy resins

Two types of "Araldite" epoxy resin in the form of cast 1.6mm thick sheet, were supplied by Ciba (ARL) Limited, and were given code letters C and D. Epoxy resin C was made from Ciba MY 750 with 20 parts by weight of DY 040 plasticiser. The approximate

deflection temperature of this resin was 75°C. Epoxy resin D was made from Ciba MY 750 with 40 parts by weight of DY 040 plasticiser, and the approximate deflection temperature was 45°C. Specimens were cut from the sheets with a saw and polished in the usual way.

2.1.1.5 Polyethylene terephthalate (PET)

This was supplied by ICI Runcorn, as transparent sheet approximately 0.8mm thick. The material was essentially amorphous and unoriented, and had a density of 1.337 Mg/m^3 at 23°C*. The amorphous polymer is made by quenching from the melt to below the glass transition temperature, and crystallinity can be developed by heating the amorphous material. There was a surface ripple on one side of the sheet from the fabrication process, which caused a small variation in specimen thickness of approximately 3%, but this did not appear to affect is behaviour under stress. The specimens were cut out with a sharp razor blade as this material shattered like glass under the saw, but it was able to withstand the usual polishing techniques.

2.1.1.6 Low density polyethylene (LDPE)

"Alkathene" WJG 11 granules, of melt flow index 2.0 and density 0.918 Mg/m^3 at 23°C, were supplied by ICI. These were compression moulded at the Royal College of Aeronautics, Cranfield, into crystalline unoriented sheets approximately 1.6mm thick. Low density polyethylene contains branched chains, and has a crystallinity of the order of 50-60%. Specimens were cut from the moulded sheets with a razor blade, and polished in the usual way.

2.1.1.7 High density polyethylene (HDPE)

This polymer was supplied by British Hydrocarbon Chemicals Limited as "Rigidex 50" (melt flow index 5.0), in the form of granules, which were moulded by ICI Runcorn into crystalline unoriented sheets approximately 1.6mm thick. The polymer has an essentially linear structure, and a crystallinity of the order of 80-90%. Specimens were cut out with a razor blade and polished as before.

2.1.2 Experimental techniques

The factor controlling the conditions of plane strain in the double indentation test are outlined in Appendix 1. Details of the design of the apparatus and of its calibration are given in Appendix 2 and the problem of friction between the dies and the specimen during compression is discussed in Appendix 3.

2.1.2.1 Simple plane strain compression

Except for special tests, experiments were conducted at room temperature, and in general tests were completed in as short a time as possible to minimise variations in environment such as temperature and humidity. Molybdenum disulphide grease ("Molyslip") was used as lubricant between the die faces and the

* "Precursor Melinex", with undetectable crystallinity by X-rays.

specimen, as this has been shown to be an effective lubricant for these materials (Ford and Williams (1964)). See also Section 2.3. After each compression the dies were cleaned and polished, and fresh grease applied, as Molyslip drying on the dies could cause an increase in friction. With the specimen placed squarely between the dies, a small load (100N) was applied to allow compaction of the rig, and the dial gauges were then zeroed. Compression took place at a constant crosshead speed of the order of 0.1mm/min, which in general gave specimen strain rates around 0.002/sec. A trace of load against time was automatically produced by the testing machine.

To measure the strain during loading, readings of the two dial gauges against time were taken, and this was achieved in one of two ways. Dial gauge readings were noted at time intervals measured on a clock synchronised with the machine chart; or by recording gauge readings onto magnetic tape, which was later replayed in synchronisation with a clock. The mean of the two gauge readings, determined by one of these methods, was taken, and allowing for rig deflection, a plot of specimen deflection against time corresponding to the trace of load against time produced by the machine, could be obtained. If excess tilting of the dies was observed, greater than 0.002in (0.05mm), the test was stopped, and shims placed between the top die and the compression anvil, until even loading was achieved. These procedures produced stress-strain data for a constant crosshead speed. Although often quoted as such, this was not the same as constant strain rate data, as the specimen strain rate was observed to change throughout the course of the compression (See Section 2.2)

2.1.2.2 Plane strain compression with additional tension

Tensile stresses (σ_2) in addition to the compressive stress (σ_1), were applied using the tensile rig described earlier. A small tensile load (50N) was applied to allow the rig to settle in, and by using the levelling screws on the supporting frame, the specimen was levelled onto the bottom die so that it was just in contact with it. Under a small compressive load applied to the dies, the tensile load was increased to some pre-determined value, and held constant by monitoring the pressure in the hydraulic system to ± 5 lb/in^2 (0.034N/mm^2). Loading in compression then took place as described before, and dial gauge readings were recorded. In this way values of the plane strain compressive yield stress (σ_1) were measured for various values of applied tension (σ_2). For the glassy polymers, tensile fracture intervened before tensile yield, and only a limited range of applied tensions could be investigated.

2.1.2.3 Plane strain compression with additional compression

Small compressive stresses (σ_2) were applied in addition to the compressive stress (σ_1), using the compression rig described earlier. These compression-with-compression tests were performed on PMMA and PS. Specimens were prepared as before, but the length was reduced to 25mm so that no buckling would occur when the specimen was loaded. Using the holders described in Appendix 2.3, the specimen was loaded in compression in the plane of the sheet by using the same technique as described above for

tension, and in this way the variation of the plane strain compressive yield stress, with the additional compressive stress (σ_2) was investigated.

2.1.3 Observation of the mode of deformation by sectioning

For the glassy polymers studied here, there exists a relationship between strain and birefringence which, in the absence of a knowledge of the exact nature of this relationship, allows qualitative observation of the strains remaining in the polymer after deformation. Since these strains for the tests used here are confined to a single plane, it is possible to cut sections from deformed specimens parallel to this plane, and by observation of the pattern of birefringence, to study the mode of deformation. Sections were cut from the centre deformed specimens as shown in Figure 1, using a saw or razor blade. These were carefully polished down to less than 0.5mm thickness with wet emery polishing wheels, and either diamond paste polishing wheels or Silvo, to give a final polish. The birefringent patterns in these sections seen in plane polarised white light were photographed in an optical microscope. Some thinner sections, down to 10 μm, were taken from PET, and PS, using a MSE base sledge microtome, and these sections photographed in the microscope as before.

2.2 The stress-strain curve of polymethyl methacrylate

2.2.1 Determination of the stress-strain curve in simple plane strain compression

During the simple plane strain compression of a specimen at constant crosshead speed, two sets of measurements were taken from which it was possible to construct a stress-strain curve for the material. The variation of the load with time was recorded directly by the testing machine, while the readings of the two dial gauges with time allowed calculation of the specimen deflection rate. These two sets of measurements are shown in Figure 2, for a standard size PMMA specimen compressed at room temperature, with a constant crosshead speed of 0.2mm/min. The shape of these curves is typical of all the glassy polymers studied here, with a characteristic maximum in the loading curve, followed by a load drop. The specimen deflection curve shows a changing slope related to the load maximum and minimum. These curves indicate that this type of test is neither a constant loading rate, nor constant strain rate test, and that some care is needed in their interpretation. This will be discussed in a later section.

To obtain values of nominal stress from the load time curve, the load readings are divided by the initial area of specimen under load, which is the original width of the specimen (w), multiplied by the die breadth (b). True stress values are calculated by dividing the applied load by the current area of the specimen during deformation. Nominal strains are obtained from the specimen displacement curve, by dividing the displacement by the original specimen thickness h_o, so that $\varepsilon = (h_o - h)/h_o$ where ε is nominal strain, and h the final specimen thickness. The true or natural strain is defined by $e = \int_h^{ho} dh/h$ which may be written $\ln ho/h = \ln 1/(1-\varepsilon)$. Therefore, as the height of the specimen approaches zero, $e \to \infty$ while $\varepsilon \to 1$. The nominal stress - nominal strain curve derived from Figure 2 is shown in Figure 3.

One advantage of this type of plane strain compression test, is that the area under load should remain constant during the deformation, so that the distinction between nominal and true stress is unnecessary. However. the large elastic strains in polymeric materials cause the ends of the deformed section to be bulged outwards to a far greater extent than in metals. This results in an increase in the effective area on which the load acts, and hence a possible error in taking nominal stress instead of true stress. By measuring the width of a deformed PMMA specimen immediately after unloading, an estimate of this error was made. Referring to Figure 3 for a specimen loaded to a nominal strain of 0.14, an 0.5% increase in specimen width was estimated, while for a specimen loaded to a nominal strain of approximately 0.25, a 1.5% increase in width was estimated. Therefore, up to nominal strains of approximately 0.25, the error in taking nominal stress instead of true stress was a maximum of 1.5%, which was within the experimental error.

A similar argument holds for taking nominal strain instead of true strain. The nominal stress-true strain curve derived from the curves in Figure 2 is also shown in Figure 3, and it can be seen that nominal strain only becomes significantly smaller than true strain at large values.

The majority of the stress and strain data considered here is concerned with the yield point, which was always found to occur within the range of stress and strain for which negligible error was incurred in taking nominal values instead of true values. For this reason nominal stress and strain have been used except where otherwise stated.

Referring to the nominal stress - nominal strain curve in Figure 3, some non linearity is still apparent near the origin even after the correction for rig deflection has been applied. This occurs because for each test it is impossible to ensure that the same amount of grease is applied, and consequently there is still some error due to grease being squeezed out from between the dies at low loads. This is corrected for by extrapolating back the initial straight line portion of the stress-strain curve to give a new effective origin.

2.2.2 The shape of the curve up to the yield point

During the initial linear portion of the stress-strain curve, up to approximately 0.03 strain, the material is behaving like a Hookean elastic solid with stress proportional to strain. For this early part of the deformation stress and strain values are small, and times relatively short at the testing speed of 0.2mm/min. Therefore, the time and rate effects to which polymers are so sensitive are negligible and Hookean response is achieved from a viscoelastic solid. The elastic modulus of the material, for a given temperature and rate of testing, can be calculated from the initial linear portion of the curve, and the moduli quoted in the text are obtained in this way. Beyond 0.03 strain, which is analogous to the proportional limit in metals, non linear behaviour appears. Unlike metals, this is not necessarily due to the presence of plastic or irreversible strains in the material but is partly due to the presence of time dependent viscoelasticity.

To illustrate this point, and to determine the strain for which plastic strains appear in the material, a series of standard size PMMA specimens were compressed between 6.4mm dies, at room temperature, with a constant crosshead speed of 0.2mm/min. The specimens were given a range of applied strains up to approximately 0.40 and the residual strain immediately after unloading was measured. The resulting plot of nominal applied strain against residual strain immediately after unloading, is shown in Figure 4. Up to applied strains of approximately 0.10 a small non linear increase of residual strain with applied strain was observed. This was followed by a larger linear increase of residual strain above 0.10. The specimens were allowed to relax for a week in a dessicator at room temperature, and the residual strains remeasured. The shape of the curve in Figure 4 was essentially unaltered, except that the origin along the residual strain axis was shifted to a strain of approximately 0.039.

Reading the curve in Figure 4 in conjunction with the stress-strain curve in Figure 3 it can be seen that during the initial linear portion of the stress-strain curve, negligible residual strain was produced in the specimen immediately after unloading, and the Hookean elasticity suggested by the stress-strain curve is verified. Between approximately 0.03 and 0.10 applied strain, significant residual strains are measured in the specimen which relax out over a period of time and thereby demonstrate the basic viscoelastic nature of the material. For applied strains greater than approximately 0.10, residual specimen strains persist after several days relaxation period. These residual strains, still present after relaxation, will be called plastic strains by analogy with metals, and they will be considered as permanent at the temperature of deformation since they did not recover appreciably over any further period at this temperature.

2.2.3 Definition of the yield point

For an ideal elastic-plastic body which deforms homogeneously, the yield point would be that point on the stress-strain curve where plastic strains are first produced. However, this ideal situation rarely occurs in practice, and a closer understanding of the relation between the stress-strain curve measured on the bulk sample, and the strains within the deforming specimen, is necessary in order to define the yield point. To study the development of deformation in a PMMA specimen, sections were taken from the deformed specimens used to construct Figure 4. Thin sections were cut from the centre of the relaxed specimens in the plane of deformation, as described in Section 2.1, and then studied in plane polarised light. The photographs in Figure 5 show sections from specimens given increasing applied strains, and the values of applied strain quoted relate the specimen sections to the stress-strain curve in Figure 3.

Zones of plastically deformed material begin at each of the four die corners which are singular stress points (Nadai 1950), and as the applied strain increases, wedge shaped regions of sheared material extend into the inside of the specimen and propagate across the whole specimen by reflection at the die faces. As straining proceeds beyond the maximum point on the stress-strain curve, deformation continues by widening of the shear zones, until strains in the region of the minimum point on the stress-strain curve are reached, when the deformation becomes homogeneous, and continues only at higher stresses. This type of strain field has been analysed by Green (1951) for an ideal rigid plastic, and a similar type of deformation was assumed by Hill (1950) in his analysis of compression of a block between rough plates.

By careful study of the deformed sections in relation to the stress-strain curve for PMMA, it was concluded that the maximum stress point on the stress-strain curve corresponded to the condition that a plastic zone covered the whole of the specimen. Before this point elastic material is still present, and the dies can only move together by an elastic order of magnitude. Beyond the maximum stress point a complete plastic zone across the specimen allows the dies to move together to a greater extent, causing large plastic strains within the specimen. Therefore, although permanent plastic strains do occur before the maximum stress point (Figure 4), these arise because of the stress concentrations causing imhomogeneous straining, and the true yield stress of the bulk material will be the maximum stress on the stress-strain curve. The nomenclature used here to describe aspects of the stress-strain curve of PMMA and similar glassy polymers is shown in Figure 6.

2.2.4 The load drop after the yield point

The nominal stress-strain curve for PMMA in Figure 3 shows a drop in stress of approximately $8N/mm^2$ for an increase in strain of approximately 0.13 beyond the yield point. This phenomenon known as strain softening has been investigated by Ender (1968) for PMMA yielding under constant load, and he has shown that the effect is related to the molecular processes associated with straining. Brown and Ward (1968) have also studied a similar load drop seen with PET over a variety of test conditions, and they concluded that the load drop is an intrinsic material property associated with the dynamic relationship between the molecular processes and the applied strain rate. Further work is necessary to relate the load drop seen here to the applied testing conditions, but these results do show that the fall in stress after yield is not a geometrical effect as in tensile testing, for in the plane strain compression test the area under load increases if it changes at all, and the true stress will be lower than the nominal stress.

2.2.5 The effect of machine elasticity

It was shown in section 2.2.1 that for constant crosshead speed the specimen strain rate varies throughout the course of the test, and it was important to determine how this behaviour was affecting the value of the yield stress measured in these tests.

The cause of the variable strain rate prior to yield, in these constant crosshead speed tests, can be ascribed to the elastic deflections of the testing machine. Ideally the machine should show no deflection under load, and in this case all of the crosshead movement would appear as strain in the sample under test. In practice, however, finite deflections of the machine under load do occur, and the displacement of the crosshead in any given time will be divided between the specimen and the machine, in proportion to their moduli. If the modulus of the specimen changes, the proportions of the displacement will change, and in particular if the modulus of the specimen becomes zero, the machine will relax its displacement into the specimen at a rate depending upon the imposed crosshead speed and the ratio of the moduli. It can be seen therefore that the specimen strain rate will vary throughout the test, as the modulus changes.

To investigate these effects two different tests were run on PMMA in which the area of specimen under load was changed, so that two widely different yield loads were obtained. In the case where the yield load was high (50KN), deflections in the machine were large, and the effects of machine elasticity were pronounced, while for a lower yield load (3KN) these effects were reduced. It was concluded from these tests that reducing the effects of machine elasticity decreased the changes in strain rate up to the yield point. The yield stress was unchanged, and a yield drop in load was still observed. These conclusions are important when comparing the stress-strain curves, determined at constant crosshead speed, for different polymers with markedly different yield loads.

2.2.6 Constant nominal strain rate tests

The constant crosshead speed test is often quoted in the literature as a constant strain rate test, but this has been shown here to be untrue for the plane strain compression test. An attempt was made therefore to maintain the specimen deflection rate, and hence the nominal strain rate, constant throughout the course of a plane strain compression test. Keeping the nominal strain rate constant meant that the true strain rate would be continually changing, but apart from the experimental difficulties in maintaining a constant true strain rate, the differences would only become significant for nominal strains in excess of 0.15 as mentioned earlier, and the yield point strain was generally lower than this value.

To determine a stress-strain curve at constant strain rate, the specimen deflection against time was first determined at constant crosshead speed in the usual way. From this curve the changes in crosshead speed required to maintain the strain rate constant throughout yield were calculated. The test was then repeated under identical conditions, except that the crosshead speed was continuously changed as calculated. This process was achieved experimentally by using the variable speed control incorporated in the Tensometer testing machine, and dial gauge readings were taken using the magnetic tape method described earlier.

The results of such a constant strain rate test at 0.27mm/min specimen deflection rate, together with the results of a constant crosshead speed test at the same speed, are shown in Figures 7 and 8. The most important observation from these curves was that the yield stresses for each curve 149.6 ± 2.3 N/mm^2 at constant crosshead speed, and 145.4 ± 2.2 N/mm^2 at constant strain rate were equal within the experimental error, and the yield stress appeared to be unaffected by the strain rate behaviour prior to yield. Sets of curves similar to those shown in Figures 7 and 8 were produced for three different speeds from 0.05mm/min to 0.3mm/min and in each case it was apparent that the yield stress at constant strain rate was the same as the yield stress at the equivalent constant crosshead speed, within the experimental error.

In conclusion therefore, despite the fact that the effects of machine elasticity and variable strain rate complicate an interpretation of a constant crosshead speed test, the yield stress is determined by the strain rate at the moment of yield alone. The curve in Figure 7 and similar curves taken throughout the course of this project, indicated that the strain rate precisely at the upper yield point was equivalent to the applied crosshead speed, and yield stress values can therefore be quoted at the strain rate as determined from the crosshead speed. Yield strain values however, are noticeably influenced by the strain rate behaviour prior to yield (Figure 8), and will therefore depend not only on the crosshead speed used but also on the elasticity of the testing machine.

2.2.7 The variation of the yield stress with strain rate

To determine the change in the plane strain compressive yield stress of PMMA with applied strain rate, a series of tests were run using crosshead speeds in the range 20-0.025 mm/min. Specimens were compressed in the usual way at room temperature using 6.4 mm dies, and at each speed a load maximum followed by a yield drop was observed as described in Section 2.2.1. The nominal yield stress was calculated in each case. The nominal strain rate at the yield point was found by dividing the crosshead speed by the original specimen thickness (h_o). Yield stress values were plotted against the natural logarithm of the strain rate, and a linear variation shown in Figure 9 was found. Similar results for the variation of yield stress with strain rate have been given by Roetling (1965), and Andrews and Whitney (1964), for PMMA tested in tension. These results will be discussed in terms of the mechanism of yielding in a later section.

2.3 The yield behaviour of PMMA and other polymers

2.3.1 Introduction

In the previous section the stress-strain curve for PMMA was described in some detail in order to define the yield point. In the light of these results stress-strain curves were produced for all the polymers studied, and a yield point defined for each material. Using these definitions the variation of the plane strain compressive yield stress with applied tension or compression was measured for each material, as described in Section 2.1 with a view to producing a yield criterion for these stress states. A detailed analysis of the plane strain compressive yield stress, and the uniaxial compressive yield stress of PMMA, was also carried out, in order to extend the discussion of the yield criterion for this material to more general, non plane strain, stress states.

2.3.2 Stress-strain curves for other polymers

The stress-strain curves shown in Figures 10 and 11 were all determined as described previously for PMMA in Section 2.2.1. The specimens were compressed between 6.4mm dies with a constant crosshead speed of 0.2mm/min, and at room temperature. Nominal stress is plotted against natural or true strain, as large strains are considered. The variation of the strain rate, for each material, during compression at constant crosshead speed, was similar to that described for PMMA. However, for the reasons given in Section 2.2.5 the changes in strain rate became less pronounced for those polymers yielding at lower stresses, so that for HDPE and LDPE the test was essentially a constant strain rate test. The strain hardening after the yield point shown by all the materials may not be as large as indicated since the stress is plotted as nominal stress, and for large strains the true stress will be significantly lower than the nominal stress.

For all the glassy polymers, including PET, the stress-strain curves are similar to that shown by PMMA, with an initial linear portion at low stresses followed by a stress maximum and a load drop. Therefore by analogy with PMMA the yield stress in each case will be taken as the first maximum on the stress-strain curve. In truth the maximum stress point is not necessarily the actual yield stress of the bulk material, as for example in PS where deformation bands appear before the maximum stress point which is associated with initiation and propagation of such bands (see Section 2.3.4). However the yield stress as defined here will be directly related to the true yield stress of the bulk

material through some constant factor such as a stress concentration term, and a useful indication of the yield behaviour can be obtained with this definition.

For the polyethylenes there was no maximum stress point on the stress-strain curve, and the mode of deformation cannot be studied in polarised light as these materials are opaque. The yield point cannot therefore be so readily defined for these materials. However, the yield stress for materials which show no load drop after the yield point is often taken as the value at the intersection of the extrapolations of the linear portions of the curve before and after the yield point (Nadai (1950)), and this definition will be used here. For HDPE this point corresponded to the point of inflexion in the stress-strain curve as shown in Figure 11. Further justification for using this definition of the yield point was obtained from the stress-strain curves for plane strain compression with applied tension (see Figure 12) when a load drop appeared at higher tensions, and the extrapolated yield stress became the maximum stress point.

2.3.3 Yield stress and strain values and moduli

The modulus was determined for each material from the slope of the initial linear portion of the stress-strain curve. As already described, the nominal strain rate during this portion of the curve was generally constant but less than the strain rate at the yield point. The various moduli quoted in Table 1 are therefore given at the nominal strain rate measured during the initial part of the stress-strain curve. In this region viscoelastic effects will be small, and the material will behave like a Hookean elastic solid (Bowden (1968)). Therefore applying linear elasticity theory to the stress system in plane strain compression (see Appendix 1.5), it can be shown that the modulus measured from these stress-strain curves $E' = \frac{Y}{(1-\nu^2)}$, where Y is Young's Modulus for uniaxial compression and ν is Poisson's ratio.

The yield stress values given in Table 1 are quoted at the strain rate at the yield point as calculated from the crosshead speed. Yield strain values are included for a qualitative comparison only, as these have been shown to vary noticeably with the strain rate behaviour prior to yield.

The errors quoted for the moduli were estimated from the range of lines that could be constructed through the early points of the stress-strain curve, while the errors on the yield strain were estimated from the stress-strain curve around the yield point. The errors on the yield stresses were computed from the known experimental errors.

2.3.4 The mode of deformation

In Appendix 1.6 the theoretical mode of deformation of an ideal rigid plastic in plane strain compression is discussed, and the deformation is shown to take place inhomogeneously as a number of independent rigid wedges which slide along a criss-cross of slip lines. Apart from the polyethylenes which were opaque, sections taken from deformed specimens showed that in every case the deformation was inhomogeneous. Figures 13-17 show the types of deformation observed in the various materials.

The section of PVC showed most clearly the mode of deformation proposed by Green; as a zig-zag shape zone of plastically deformed material crossed the whole specimen width, dividing it into a number of undeformed wedges. A similar form of deformation was seen in the PMMA section but the plastic zones are more diffuse, while in PS the same zig-zag plastic zone was present but made up of smaller bands of intense shear. The sections shown for Epoxy resin D and PET do not show the overall zig-zag pattern, as yielding has been more readily initiated at surface irregularities than at the die corners.

Inhomogeneous yielding in tension has been well reported in the literature for many materials. Nadai (1950) discusses the formation of narrow plastic zones in mild steel plates, and shows how the applied stresses cause the plastic zone to be obliquely inclined at 55° to the tensile axis. Brown and Ward (1968) have investigated plastic shear zones containing up to 2.0 shear strain formed in oriented PET in tension, and have explained the main features of such regions by considerations of the polymer structure. Rider and Hargreaves (1969) explained the direction of the plastic zone formed in oriented PVC in tension, in terms of an anisotropic yield criterion derived from the von Mises yield criterion, and Argon et al. (1968) have observed bands in unoriented PS in compression, and in oriented PS in tension and torsion, and proposed a structural model for PS to explain the main features.

Although the shear zones formed in tension originated for different reasons to those formed in these plane strain compression tests, the general features, such as limiting width and the shear strains contained, are likely to be controlled by the same structural parameters in each case. The two extreme cases of PMMA with broad diffuse zones containing relatively low shear strains (0.10) and PS with narrow well defined bands containing large shear strains (~2.0), have been shown to be related through the effect of temperature, when PS can be made to behave like PMMA at high temperatures (greater than 65°C) and PMMA like PS at low temperatures (near -196°C) - Private communication Bowden and Raha. It is apparent that the characteristics of the band are directly related to the underlying molecular mechanisms taking place at yield. However, this requires much more detailed investigation, and apart from a qualitative description of the plastic shear zones, the parameter considered here will be the angle the zone makes with the compression axis.

The initiation and propagation of shear zones in PMMA has already been described in Section 2.2. For PVC and epoxy resins the zones are less diffuse than those in PMMA, although increasing strains beyond the yield point are incorporated in the same way, namely by widening of the zones until deformation is practically homogeneous at the lower yield stress. PET shows two types of zone intermediate between an epoxy resin type of broad zone, and sharp well defined bands a few micrometres thick similar to those seen in polystyrene (see Figure 18). Continued straining of a PET sample beyond the yield point results in some widening of the broader zones together with a proliferation of the smaller bands. In PS the deformation proceeds by formation of narrow bands (~1 μm wide) containing shear strains of up to 2.0. As straining continues beyond the yield point the bands do not widen but propagate along the shear direction and multiply in number leaving the surrounding material undeformed (see Figure 19).

2.3.5 Measurement of the angle of a shear zone

In the plane strain compression test deformation is restricted to a single plane, and this is the plane from which the sections shown in Figures 13-17 were cut. In this plane, the direction of maximum shear stress is inclined at 45° to the compression axis, and for a material which fails in shear alone, yielding would take place by shear along these directions. For materials such as soils, deformation in shear is accompanied by changes in volume (Terzaghi and Peck (1948)), and for these materials the angle of the plane in which deformation begins differs noticeably from 45°. The angle of the shear plane is therefore a useful parameter in a study of conditions of failure, and for glassy polymers there is the important advantage that the directions of deformation can be directly studied by viewing in polarised light, unlike metals for which complex etching techniques are necessary.

In PS and PET the large number of narrow shear bands allow measurement of their inclination to the compression axis with reasonable accuracy but in the remaining polymers the more diffuse nature of the zones, particularly with PMMA, prevents accurate measurements. However, it can be seen with these materials that small stress concentrations at the surfaces produce smaller zones of yielded material, from which it is possible that accurate measurements can be made. To accentuate this affect, and thereby permit more accurate determination of the shear direction, a series of fine scratches approximately 50 μm deep were made on one surface of the specimen, parallel to the length of the dies. These scratches did not change the yield stress within the experimental error, but the effect on the mode of deformation was to produce a number of smaller shear zones as shown in Figure 20 for PMMA. These zones were used to measure the angle of inclination to the compression axis.

Measurements of the shear zone angles were made on photographs of sections of specimens which had been taken just to the yield point and then unloaded and allowed to relax for at least 24 hours at room temperature. The inclination of several shear zones were measured in each specimen, and a standard deviation calculated for the mean value. In general the permanent deformation in the specimen, measured after relaxation, was small in comparison with the yield strain, and the inclination of the zones at the instant of yield will therefore be less than when measurements were made on sections cut from the specimens after recovery. If the values of the strains ε_1' and ε_2' recovered after relaxation are known (see Figure 21), an estimate of the inclination of the zones at the instant of yield α', can be found from the inclination of the zones measured after unloading α, using the equation:-

$$\tan \alpha' = \frac{(1+\varepsilon_2')}{(1+\varepsilon_1')} \tan \alpha \qquad (1)$$

where ε_1', which is a compressive strain, will be a negative number, and ε_2' will be a positive number. The value of ε_1' can be found by measuring the residual strain after deformation, and subtracting this from the yield strain for the material. The value of ε_2' was not measured directly but can be estimated, with limited precision, by measuring the width of the die imprint on the surface of the specimen after relaxation. The measured values of α°, together with the

corrected values α'^{o} estimated using Equation (1) are shown in Table 2.

The errors involved in determining the values ε_1' and ε_2' were abnormally large, but only an estimate of the effect of elastic recovery was required. For this reason the maximum correction has been applied to calculate α', and the errors quoted on this quantity are those involved in measuring α, and do not include the errors involved in the correction procedure.

These calculations show that for all the materials except PS, the large elastic strains at yield can account for the deviation of the measured angle from 45^{o}, while for PS deformation has definitely taken place on planes steeper than 45^{o}. These results will be discussed in relation to the stress data and yield condition in a later section.

2.3.6 Factors affecting the measurement of the yield stress of PMMA in plane strain compression

There are a number of factors inherent in the type of test used here which could influence the measured values of yield stress. These factors were given detailed investigation for PMMA in order to estimate the magnitude of the various effects, and to determine a fully corrected value of the plane strain compressive yield stress.

A series of PMMA specimens all of the same thickness but of various widths in the range 6.4 mm - 51 mm were compressed in the usual way at a constant crosshead speed of 0.2 mm/min using four different die breadths. The strain rate in every case was 0.0011/sec. These results were used to investigate the effects mentioned below.

2.3.6.1 End effects

The large elastic strains in PMMA cause the material at the ends of the deformed section to be bulged outwards to a far greater extent than in metals. This has a twofold effect. The load bearing area will be increased, and the true stress may be less than the nominal stress; the deformation at the ends of the compressed section will be non planar, and the measured yield stress may be less than the true plane strain yield stress. The difference between true stress and nominal stress at the yield point has already been shown to be small (Section 2.2). The tests mentioned above showed that for specimen widths greater than four times the die breadth, the yield stress was constant within the experimental error, and the material under the dies was effectively constrained. It was therefore concluded that in the standard test where a 38 mm specimen was compressed between 6.4 mm dies, end effects are not important.

2.3.6.2 Friction and shoulder restraint

Although the dies were well lubricated, it is possible that the friction between the specimen and dies was sufficient to restrict flow, and to lead to an increase in pressure under the central region of the dies (Bishop (1958)). It can be shown that (see Appendix 3) the mean pressure on the dies $\bar{p}$ is given by

$$\bar{p} = \sigma'' \left[1 + \frac{b\phi_s}{2h} \frac{(1+\mu)}{(1-\mu)} \right]$$

where σ'' is the stress with no friction between the die and the specimen, b is the die breadth, h the specimen thickness at yield, ϕ_s the coefficient of surface friction, and μ a material constant (coefficient of internal friction, see Section 3.1).

The elastic material alongside the dies will exert an appreciable restraint to deformation of the material under the dies, and this shoulder restraint has been analysed by Williams (1967). Following his analysis, if R be the part of the total load per unit specimen width provided by elastically deforming the material outside the test section, σ' the measured stress, and σ the actual stress under the dies, we have:-

$$\sigma'' = \sigma + \frac{R}{b} \text{ per unit width, and therefore}$$

$$\sigma' b = \left[\sigma + \frac{R}{b}\right]\left[b + \frac{\phi_s' b^2}{2h}\,\frac{(1+\mu)}{(1-\mu)}\right] = \bar{p}\, b$$

and if both ϕ_s and R are small

$$\sigma' = \sigma + \frac{R}{b} + \frac{\phi_s b \sigma}{2h}\,\frac{(1+\mu)}{(1-\mu)} \qquad (2)$$

Therefore, for a given specimen width and thickness, a plot of the measured yield stress (σ') against $\frac{1}{b}$ will show a minimum, and if friction is small, extrapolation of the linear part $\sigma' = \sigma + \frac{R}{b}$ to $b = \infty$ will give σ, the true yield stress.

Plots of yield stress against $\frac{1}{b}$ for three specimen widths 25.4 mm, 38.1 mm and 50.8 mm were made, and no minimum was observed for the largest die breadth 9.5 mm and specimen width 51 mm. Extrapolation of the plots to $b = \infty$ were made for each specimen width, and the mean yield stress was found to be 140.3 ± 2.7 N/mm^2.

A maximum value for the coefficient of surface friction ϕ_s can be estimated from the fact that no minimum was observed in the plot of σ' against $\frac{1}{b}$. Referring to Equation (2) a minimum will occur

$$\text{when } \sigma' = \sigma\left[1 + \frac{\phi_s b}{h}\,\frac{(1+\mu)}{(1-\mu)}\right]$$

No minimum was detected for $\frac{b}{h}$ ratios as large as 3.74, and assuming $\mu = 0.25$ (see Section 3.1)

$$\sigma' = \sigma\,(1 + \phi_s \times 3.74 \times 1.67).$$

For the effect of friction to be noticeable at this $\frac{b}{h}$ value, σ' should be approximately 4% higher than σ to place the difference outside the experimental error and $1 + \phi_s \times 6.23 = 1.04$.

$$\therefore\ \phi_s = 0.006$$

This value for the coefficient of surface friction is in agreement with that found by Williams (1967) for similar conditions.

2.3.6.3 Test geometry

The effect of the ratio of specimen thickness to die breadth has been investigated by Green (1951) for metals, and by Ford and Williams (1964) for polyethylene, and their results are discussed in Appendix 1. For a given specimen width stress values were plotted against the ratio $\frac{h}{b}$, where h is the specimen thickness at yield, and b is the die breadth. No significant maxima or minima were found within the experimental error, and the effects of test geometry were therefore assumed to be negligibly small.

2.3.7 Measurement of the yield stress of PMMA in uniaxial compression

The yield stress of PMMA was also measured in uniaxial compression in order to compare this value with the yield stress in plane strain compression, and thereby determine the effect of the hydrostatic component of stress on yielding (see Section 3.1). The uniaxial compressive yield stress was measured on cylindrical specimens cut from commercial ICI "Perspex" rod, which had been annealed for 24 hours at 110°C, and slow cooled. The rod was machined on a lathe to return it to a circular cross section after annealing, and various lengths were cut off and polished using metallographic techniques.

For the unconstrained yield stress measurements two corrections are necessary to determine the true yield stress. The load bearing area increases during straining, and a correction must be applied for the increase in diameter of the specimen under load. The surface friction between the dies and specimen causes an increase in pressure under the dies, and this can be corrected for as in the plane strain compression test.

To correct for changes in load bearing area during deformation it was assumed that the volume remained constant, so that the area of the specimen at yield could be computed from the measured contraction of the cylinder. Negligible barrelling was observed. The same lubrication conditions were used here as in the plane strain compression test. Friction was therefore known to be small and could be corrected for. It can be shown that the mean pressure on the ends of the cylindrical specimen is given by:-

$$\bar{p} = \sigma \left(1 + \phi_s \frac{a}{h} \cdot m\right) \qquad \text{(See Appendix 3)}$$

where σ is the true stress without friction, ϕ_s the coefficient of surface friction, a the radius of the specimen, h the height of the specimen at yield, and m a constant. Therefore, by measuring the yield stress for a range of $\frac{a}{h}$ values, and extrapolating to $\frac{a}{h} = 0$, the true yield stress can be found. Using $\frac{a}{h}$ values in the range 0.1 - 1.0, and a strain rate of 0.001 1/sec, the extrapolated value of the uniaxial compressive yield stress was found to be 104.0 ± 7.4 N/mm^2.

For comparison with this value one should ideally determine the plane strain yield stress on the same material. However, this would involve measurements on a large number of specimens to determine a fully

corrected value as described in section 2.3.6. The procedure used here was to measure the plane strain yield stress for a sheet specimen cut from the rod used to determine the uniaxial yield stress, and by comparison with the yield stress values determined in Section 2.3.6 for the same specimen dimensions and die breadth, apply the same percentage corrections as used there. That is, the plane strain yield stress measured on a normal sheet specimen, using 6.4 mm dies, a 38 mm specimen, and a strain rate of 0.0011/sec was 144.7 ± 1.9 N/mm^2 which when fully corrected became 140.3 ± 2.7 N/mm^2. This was a decrease of 3%. The plane strain yield stress measured on a section cut from the rod, at a strain rate of 0.0011/sec, was found to be 137.9 ± 1.7 N/mm^2 and decreasing this by 3% the fully corrected yield stress becomes 133.2 ± 1.6 N/mm^2. Therefore we have the plane strain and the uniaxial yield stresses, measured on the same material, as follows:-

The fully corrected uniaxial yield stress (σ^u) =

$$104.0 \pm 7.4 \text{ N/mm}^2$$

and the fully corrected plane strain yield stress (σ^p) =

$$133.2 \pm 1.6 \text{ N/mm}^2$$

$$\text{The ratio } \frac{\text{plane strain compressive yield stress}}{\text{uniaxial compressive yield stress}} = \frac{\sigma^p}{\sigma^u}$$

$$= 1.28 \pm 0.16$$

The importance of this result will be discussed in the next section.

2.3.8 Plane strain compression with applied tension

The technique used to measure the variation of the yield stress in plane strain compression with applied tension has been described in Section 2.1. For all the materials tested the compressive yield stress decreased with increasing applied tensions, and Figure 22 shows a typical series of stress-strain curves for epoxy resin D. The general effects of tension on the stress-strain curves of all the glassy polymers were similar, in that the overall shape of the curve remained the same with increasing tension, and the modulus and rate of strain softening were similar for all values of applied tension (σ_2). At higher strains the rate of strain hardening decreased with increasing tension, and in HDPE this had the effect of producing a load drop after yield (see Figure 12). The compressive yield load was determined from the trace of load against time, and the nominal yield stress (σ_1) calculated as before. The applied tensile load, which was maintained constant for a given test, was determined from the pressure in the hydraulic ram, and the nominal tensile stress could be found by dividing the load by the original cross sectional area of the specimen. However, the effective area over which the tensile load acts will decrease in proportion to the compressive strain (ε_1) and the true tensile stress will be noticeably larger than the nominal stress. The tensile stresses quoted are therefore true stress values calculated from the specimen area at yield and the applied load.

Figure 23 shows the experimentally determined variation of the compressive yield stress σ_1, with applied tensile stress σ_2 for PMMA using 6.4 mm and 3.2 mm dies and a crosshead speed of 0.2 mm/min. The

compressive yield stress σ_1 decreased linearly with the tensile stress σ_2. The lines drawn through the experimental points for which yielding occurred were obtained from a least squares calculation. It is evident that the compressive yield stress and the extrapolated tensile yield stress are not the same, indicating a significant effect of the hydrostatic component of the stress tensor on yielding. For tensile stresses greater than approximately 34 N/mm^2, tensile fracture intervened before yielding took place, and such fracture usually occurred at the die edges and along the length of the dies perpendicular to the tensile stress.

In Section 2.3.6 a number of factors affecting the value of the simple plane strain compressive yield stress were discussed, and these same factors could affect the experimental values in Figure 23 and hence the slope of the line. However, it has been shown that friction, end effects, and test geometry have negligible effect on the experimental values, and that shoulder restraint is the only major source of error. The latter effect can be corrected for by extrapolation to infinite die width (see Section 2.3.6), and this has been done using the results for 6.4 mm and 3.2 mm die widths shown in Figure 23. The corrected line for infinite die width is also constructed in Figure 23 and it is apparent that the change in slope is small. The equations for the three lines are:-

for nominal 3.2 mm dies: $\sigma_2 = 75.8\ (\pm\ 1.1) - 0.595\ (\pm\ 0.012)\sigma_1$ N/mm^2

for nominal 6.4 mm dies: $\sigma_2 = 73.8\ (\pm\ 0.98) - 0.619\ (\pm\ 0.011)\sigma_1$ N/mm^2

∞ dies: $\sigma_2 = 72.1\ (\pm\ 1.1) - 0.655\ (\pm\ 0.012)\sigma_1$ N/mm^2

For all the other materials tested the effect of shoulder restraint was never greater than that shown above for PMMA, and for convenience the results using 6.4 mm dies will be quoted in each case.

The variation of σ_1 with σ_2 for the range of polymers studied here at a crosshead speed 0.2 mm/min and room temperature is shown in Figures 24 and 25 and the data summarised in Table 3. For all the materials a linear variation was observed. In PS and PVC as in PMMA, fracture intervened at higher tensile stresses so that the whole of the diagram could not be investigated. The slope (a) of the lines in Table 3 is less than 1.0 for all the materials, showing that the compressive yield stress is significantly larger than the extrapolated tensile yield stress in every case. The dependence of yielding on pressure, illustrated by these results, has also been reported by several other workers, Whitney and Andrews (1967), Sternstein and Ongchin (1969), Sardar, Radcliffe, and Baer (1968), and these effects will be considered in the next section. The compressive strain rates for which the various lines were determined are shown in Table 3 and the effects of strain rate and temperature on the variation of σ_1 with σ_2 will also be discussed in a later section.

2.3.9 Plane strain compression with applied compression

Small values of compressive stress σ_2 were applied whilst loading in plane strain compression σ_1 as described earlier, in order to investigate the shape of the yield locus in the negative $-\sigma_1$ $-\sigma_2$ quadrant of the σ_1 σ_2 diagram. The techniques used both experimentally

and in the analysis of the results were the same as already described for compression-with-tension tests. To obtain consistent results, compression-with-tension tests were run on the same batch of material immediately after the compression-with-compression tests. The complete results obtained for PMMA and PS are shown in Figure 25. It can be seen that in each case the locus remains linear over the limited range of values of σ_2 investigated. The equations to the best straight lines in Table 4 show that the slopes determined in compression-with-compression are the same as with tension, within the error quoted.

2.4 Other parameters influencing yield behaviour

2.4.1 Introduction

In Section 3 it is shown that the yield behaviour of a number of polymers, subjected to various stress states, can be explained in terms of a Tresca or von Mises type yield criterion modified for pressure dependence. For the suggested yield condition to have wider application it is important to determine how the shape of the yield locus, and hence the parameters μ and k_o, will vary under different conditions. With this in mind a series of experiments were performed to demonstrate the effect of temperature in the range 20-70°C on the field behaviour of PMMA, and the effect of crystallinity on the yield behaviour of PET. Values of μ and k_o were also measured on two epoxy resins to demonstrate the consequence of increasing plasticiser content.

2.4.2 Measurement of the yield stress of PMMA at temperatures in the range 20-70°C

2.4.2.1 Apparatus

The apparatus described in Appendix 2 was modified to allow accurate temperature control of the specimen environment during straining. This was achieved by winding small 80 watt heaters around the sides of each of the dies, which were insulated from the rest of the compression rig by thin mica strips placed between the die, and the die block. STC M15 thermistors were carefully mounted close to the die faces as temperature sensing devices, and these were used in conjunction with a specially designed temperature controlling circuit shown in Figure 27. Two copper-constantan thermocouples were also mounted close to the die faces to allow accurate monitoring of the temperature of the die surface in contact with the specimen. A small enclosure was built between the top and bottom die blocks to contain the insulated dies, and preheated nitrogen gas at the test temperature was continually circulated through this enclosure to reduce heat losses and to ensure that the specimen outside the area under the dies was also at the test temperature.

2.4.2.2 Experimental technique

Due to the poor thermal conductivity of PMMA, it was necessary to allow a period of time for the specimen to reach the temperature of its environment and also to eliminate possible thermal gradients across the test sections. To investigate these effects four thermocouples were mounted within a trial specimen of PMMA at various positions around the compressed region. Molyslip grease was used on the dies as before, which were applied to the

trial specimen under a small load (≈250N), and preheated to a set temperature. The time taken for the temperature of the dies and specimen to equilibrate was noted, together with any thermal gradients produced. It was found that the temperature of the specimen under the dies and the temperature of the dies themselves were equal to within ± 0.5°C after approximately 5 minutes, and the temperature differences recorded by the thermocouples within the specimen were negligible (< 1°C) after approximately 10 minutes. Therefore the standard procedure was adopted of allowing each specimen to warm up to the pre-set temperature for at least 10 minutes before testing. Although the control of the initial temperature was to ± 0.5°C, larger variations occurred during straining which gave an accuracy of ± 1.0°C on the temperature readings at yield. The loading technique and measurement of strain were as described before in Section 2.1.

2.4.3 The stress-strain curves of PMMA in simple plane strain compression at various temperatures

Standard size specimens were compressed between 6.4 mm dies, using a constant crosshead speed of 0.2mm/min, at a series of temperatures in the range room temperature to 65°C. The stress-strain curves obtained from these tests are shown in Figure 28 where nominal stress is plotted against nominal strain. It can be seen that the elastic modulus determined at low strains, and the yield stress, both fall with increasing temperature. The yield strain also appears to decrease although this may be insignificant as this quantity has been shown to depend upon the strain rate behaviour prior to yield which could change noticeably with increasing temperature. In Figure 29 the yield stress is shown to decrease linearly with temperature within the experimental error, and to extrapolate to zero at approximately 120°C.

2.4.4 The variation of the coefficient of internal friction and the cohesion with temperature

Three sets of compression-with-tension tests were carried out at temperatures 22°C, 40°C, and 60°C. In each case 6.4 mm dies were used with a crosshead speed of 0.2 mm/min, and the variation of the compressive yield stress (σ_1), with applied tension (σ_2), was determined as described in Section 2.3. At each temperature σ_1 was linearly dependant on σ_2 as before, and the three lines were parallel within the experimental error (Figure 30). The value of μ was therefore constant in the range of temperatures investigated. Beardmore (1969) has also shown for PMMA that the yield stresses in uniaxial tension and compression are different by the same constant factor, over a range of temperatures from -43°C to + 77°C, confirming the above result for a different stress system over a wider range of temperatures. The value of the cohesion k_o is given by the expression $\sigma_1 = \frac{2k_o}{(1-\mu)}$ where σ_1 is the yield stress in simple plane strain compression (see Section 3.1), and as μ has been shown to be constant with temperature, the variation of σ_1 shown in Figure 29 now represents the variation of k_o with temperature. The implication of these results is that the yield surface in stress space should retain the same shape but become larger or smaller (expand or contract around the origin as focus) as temperature decreases or increases respectively.

In Section 3.1, Equation 35, it is shown that the yield stress is given by

$$k = \frac{2k_B T}{V_a} \ln \frac{\dot{G}}{CF_o} + \left(\frac{2k_B Tx}{V_a} + c\right) P$$

or $$k = k_o + \mu P$$

where the various terms are defined in Section 3.2. This equation cannot be readily extended to include the effect of temperature since it includes several parameters which could vary with temperature. Haward and Thackray (1968) quote activation volumes for several glassy polymers, which show that V_a may change with temperature, and Crowet and Homes (1964) suggest a linear increase of V_a with temperature for PMMA. The natural frequency F_o will also vary with temperature as may the compressibility term x. A simple approach would be to assume V_a is a linear function of temperature, when k_o would depend only on F_o according to the relation $k_o = \frac{2k_B T}{V_a} \ln \frac{\dot{G}}{CF_o}$, and μ would be constant for x and c constant. Further work is necessary however, to justify such an approach, and to extend the proposed model to include a comprenensive treatment of the effect of temperature.

2.4.5 The crystallisation of PET

To give some indication of the effects on k_o and μ of varying the percentage crystallinity, samples of PET, which were originally supplied as amorphous sheets (see Section 2.1), were subjected to various annealing treatments to produce partially crystallised structures, and these were tested in the usual way. The results presented in this section are not intended to be a rigorous treatment of crystallinity effects in PET but merely an indication of the general trends observed with a view to possible further work along these lines. Publications by Brown and Ward (1968 and 1968), and Allison and Ward (1967), have discussed many of the physical properties of PET in both the crystalline and amorphous state, and Thompson and Woods (1956) have described the effect of increasing crystallinity on dynamic mechanical properties. Astbury and Brown (1946), and Daubenny, Bunn and Brown (1954) have determined the crystal structure of PET.

A detailed investigation of the crystallisation characteristics of PET has been carried out by Keller, Lester and Morgan (1954) and Hartley, Lord and Morgan (1954). It is apparent from their work that the response of a particular sample of PET to crystallisation treatments is dependent upon many factors, such as the previous melt history, the limiting viscosity number (intrinsic viscosity), or any distortion of the sample. These observations, together with the size of the crystallised specimens required for compression-with-tension tests (102 mm. x 38 mm.), meant that it would be difficult to obtain a controlled degree of crystallinity and spherulite size. However, by using identical conditions for each batch of specimens and varying only the length of time for which the specimens were heated, it was hoped that comparative results for the effect of crystallinity on the yield behaviour could be obtained. Several attempts were made to observe the spherulitic structure of the crystallised specimens, and thereby define the crystallinity more closely. Unfortunately at the temperatures used here the spherulites were too small and large in number to allow any useful observations.

2.4.5.1 Apparatus

Specimens were crystallised on gauze trays stacked in a crystallising bath filled with silicone oil. Each sample was free to move on the tray, and the gauze allowed circulation of the silicone oil around each specimen. The outside of the bath was wound with a heater which was controlled by a Sunvic temperature controller, and this arrangement allowed regulation of the equilibrium temperature of the bath to $\pm$ 1.0°C. Two mechanical stirrers were used to circulate the oil around the specimens. Silicone oil was used as the confining liquid in which to crystallise the polymer samples; this having the least effect on the crystallisation processes (Keller et al. (1954)).

The crystallinity of the various samples was estimated by measuring their densities in a density gradient column. The column used was 0.7 m in length and thermostated to a temperature of 23.0°C. Carbon tetrachloride and p- Xylene were used as gradient liquids to give a density range of 1.3 - 1.5 Mg/m^3, and four calibration beads were used to determine the linearity of the column. The measurement of density with a density gradient column has been described by Boyer, Spencer and Wiley (1946), and Kilb and Izard (1949), and the details of this procedure will not be included here.

2.4.5.2 Crystallisation technique

To begin with the characteristic density against time-of-heating curves were determined for the particular sheet in use here. The silicone oil bath was first heated to the required temperature, and then a number of small pieces of PET (~2mm^2) were dropped in. Samples were removed after measured time intervals, quenched in silicone oil at room temperature, and washed with ether and dried. The density of these samples was then measured in the density gradient column, and a plot of density against time for a particular temperature was obtained. The curves obtained at five different temperatures are shown in Figure 31.

As the specimens required for the compression with tension tests were so large, it was important that the slowest possible crystallisation rate was used in order to allow uniform heating and hence uniform crystallisation of the samples. It was therefore decided to carry out crystallisations at temperatures around 95°C. To check for uniformity of crystallisation, a standard size test specimen was heated in the oil bath for 36 minutes at 99.0 $\pm$ 1.0°C, and small samples taken from several points within the specimen. These samples showed a scatter of density in the range $\pm$ 0.0025 Mg/m^3, which was equivalent to a scatter of percentage crystallinity of approximately $\pm$ 3%.

Values for the percentage crystallinity were calculated from density measurements using the equation

$$C' = \frac{d_c}{d} \frac{(d - d_a)}{(d_c - d_a)} \times 100$$

where C' is the weight percent crystallinity, d_c is the density of

the crystalline material, d_a the density of the amorphous material, and d the measured density (Baer (1964)). The amorphous density d_a was taken as 1.3350 Mg/m^3, and the crystalline density as 1.4550 Mg/m^3 (Miller and Hielsen (1961)).

2.4.6. The variation of the coefficient of internal friction and the cohesion with crystallinity

Samples were compressed in the usual way using 6.4 mm dies and a crosshead speed of 0.05 mm/min. Figure 32 shows the nominal stress-strain curve measured on a sample approximately 27% crystalline, in comparison with the uncrystallised material curve. While the modulus is hardly changed, the yield stress and the yield strain have been significantly increased. These effects are similar to those given by Allison and Ward (1967), for PET tested in uniaxial tension.

Compression with tension tests were carried out for four different crystallinities in the range 0 - 30%. It has been shown that the percentage crystallinity in a typical sheet specimen can vary by $\pm$ 3%, and this error together with experimental errors limited the accuracy to which the crystallinity of a group of specimens could be quoted to $\pm$ 4%. This large error explains in part the unusual scatter of points found in measuring the variation of the compressive yield stress with applied tension. The best straight lines through the experimental points are shown in Figure 33 and the μ and k_o values calculated from these lines are summarised in Table 5.

Despite the errors, these results show that increasing the percentage crystallinity increased the value of both μ and k_o. Attempts were made to determine the effect of spherulite size by crystallising at higher temperatures ($\approx 220^oC$) but the resulting specimens were so brittle that they fractured under small loads.

The increase in k_o with crystallinity is to be expected as the crystalline regions embedded in an amorphous matrix will tend to reinforce the structure and increase the yield stress. However, the increase in μ with crystallinity is more surprising as a more ordered structure might be expected to be less influenced by pressure both in its compressibility and volume changes associated with yield. Sardar, Radcliffe and Baer (1968) have studied the yield behaviour of semi-crystalline polyoxymethylene under hydrostatic pressure, and found a marked effect of pressure on the yield behaviour. They found that the crystalline regions of the polymer played a significant role in determining the yield stress over the entire pressure range, and ascribed this to volume increases associated with the break up of crystalline lamallae during yield. Peterlin (1966) has suggested a similar mechanism for the deformation of polyethylene rather than any intrinsically crystalline mode of deformation such as twinning or slip. In the light of these comments it would seem possible that the increasing pressure dependence shown by crystalline PET may also be due primarily to the break up of the crystalline regions at yield with larger volume changes than are required for deformation of the amorphous material.

2.4.7 The effect of plasticiser on the yield behaviour of epoxy resin

Results in Section 3.1 are given for the epoxy resin D (CIBA MY750) and the composition of this resin was given in Section 2.1. A second epoxy resin, C was tested which was of the same compsition as D but contained a smaller amount of plasticiser (see Section 2.1.1.4). The cast sheets of both C and D were approximately 1.6 mm thick, and were tested using 6.4 mm dies at a crosshead speed of 0.2 mm/min. Table 6 compares the μ and k_o values determined for these materials.

The value of k_o appears to decrease with increase of plasticiser content, while the effect of pressure and the value μ increases. As the influence of plasticiser on the molecular structure of a polymer is, as yet, uncertain this result can only be a qualitative indication of the general effect. However, it would not seem unreasonable that plasticiser should have the shown effect for if it acts to increase the overall volume of the structure movement of the polymer molecules under stress will be facilitated thus decreasing the yield stress, while the compressibility of the structure may be increased thereby causing μ to increase. Studies of birefringence effects in plasticised and unplasticised PVC (Andrews and Kazama (1968)) appear to confirm the above results. These workers have shown that plasticiser allows more orientation of the chain backbone during deformation, while the effect of the plasticiser molecules themselves is probably small.

3 DISCUSSION OF RESULTS AND THEORY

3.1 The Yield Criterion

3.1.1. Definition of a yield criterion

In the previous sections the stress-strain curves for a range of rigid polymers were presented, and it was shown that in each case there was a characteristic stress which could be defined as a yield point. It was shown that this stress does not correspond to the limit of Hookean elasticity, as recoverable viscoelastic strains could be produced before the yield point. However, the yield stress does correspond to the onset of large scale plastic strains within the material, and as such it is an important parameter in defining the response of a material to various states of stress. It is the purpose of this section to attempt to define the general states of stress under which the polymers considered here may be brought to the yield point, and thereby to define one of the possible limiting conditions of mechanical strength for these materials. To begin with only the results obtained for PMMA will be considered, and viable extensions of the conclusions to other polymers will be discussed later.

An important assumption in producing any yield criterion is that yielding depends only on the magnitudes of the three principal applied stresses for an istropic material. For many polymeric materials the validity of this assumption is not immediately apparent as it is well known that some polymers yield under a sufficiently high constant tensile load some time after applying the load (Ender (1968), Ender and Andrews (1965)). Time effects therefore have a major influence on the yield behaviour of certain polymeric materials. In the tests used here however, the yield stress has been determined in the equivalent to a constant strain rate test, and provided one is aware that the yield condition may differ when determined under conditions of constant load for example, a useful interpretation of the yield condition may be made. Temperature and strain rate are important variables affecting the yield stress, and hence the yield criterion, as well as parameters of a molecular nature such as crystallinity and amount of plasticiser. The effect of these variables is discussed in Section 2.4.

For an isotropic material plastic yielding will only depend on the magnitudes of the three principal applied stresses and not on their directions, and any yield criterion can be expressed by

$$f(J_1\ J_2\ J_3) = 0 \qquad \text{(Hill (1950))}$$

where J_1, J_2, and J_3 are the first three invariants of the applied stress tensor. They are defined in terms of the principal components of stress σ_1, σ_2, σ_3 by the relations

$$J_1 = \sigma_1 + \sigma_2 + \sigma_3 \qquad J_2 = -(\sigma_1 \sigma_2 + \sigma_2 \sigma_3 + \sigma_3 \sigma_1)$$

$$J_3 = \sigma_1 \sigma_2 \sigma_3$$

Hence any stress state is specified either by the three principal stresses, or by the three tensor invariants, and only functions symmetrical in the three principal stresses are permissible as yield criteria, as the material is assumed isotropic.

3.1.2 Stress space and the yield surface.

Any state of stress can be completely specified by the values of the principal stress components σ_1, σ_2, and σ_3, and such a state may be represented by a vector in a three dimensional space, where the principal stresses are taken as Cartesian co-ordinates (Haigh (1920)). The yield criterion is expressed mathematically by the function $f(J_1\ J_2\ J_3) = 0$ or $f'(\sigma_1,\ \sigma_2\ \sigma_3) = 0$ and this is the equation of a surface in stress space.

In the plane strain compression test with additional tension used here, various triaxial states of stress (Appendix 1) have been applied to the material to produce yield, and some section of the yield surface in stress space has therefore been mapped. Only the two applied principal stresses σ_1 and σ_2 have been measured, and to determine the position of the section of the yield surface with respect to the co-ordinates of stress space the relation between the third principal stress σ_3 and the other two principal stresses must be found. Ford and Williams (1964) found a relation between the principal stresses for a similar type of plane strain compression test by using plasticity theory to analyse the non-linear elastic strains appearing before the yield point. Reasonable agreement between theory and experiment was found. However, to use this analysis it was necessary to assume that deformation took place at constant volume, which is known to be untrue for several polymers (Krause et al. (1966), Whitney and Andrews (1967)), and it was also necessary to neglect strain rate effects.

For the stresses used here, however, it is not imperative to describe the complete deformation as it is only the relation between the principal stresses at the yield point that is required. At the moment of yield, as described in section 2.2., the stress is constant with time while the strain is increasing at a constant rate. That is, the yield point has the appearance of a momentary condition of pure viscous flow. A more detailed discussion of this condition in relation to the molecular processes taking place will be given in the next section but here it is sufficient to note that for viscous flow the strain rate will be some function of the applied shear stresses. To be more specific, if the applied stresses are as shown in Figure 35 then the three principal strain rates $\dot{\varepsilon}_1$ $\dot{\varepsilon}_2$ and $\dot{\varepsilon}_3$ will be functions of the three principal components of the deviatoric stress tensor (Nadai (1950)). The deviatoric stress tensor for the stresses applied in plane strain compression with tension (Figure 35) is given by

$$D = \begin{vmatrix} -\sigma_1 - \sigma & & \\ & \sigma_2 - \sigma & \\ & & -\sigma_3 - \sigma \end{vmatrix} \quad \text{where } \sigma = \frac{-\sigma_1 + \sigma_2 - \sigma_3}{3}$$

so that the principal strain rate in the z direction (Figure 36) is given by $\dot{\varepsilon}_3 = F(-\sigma_3 - \sigma)$, where F is the function relating strain rate and shear stress at the yield point. For the plane strain tests used here it has been shown that $\varepsilon_3 = 0$ (Appendix 1), hence at the moment of yield $\dot{\varepsilon}_3 = 0$ or $-\sigma_3 - \sigma = 0$.

Therefore $$\frac{2}{3}\left[-\sigma_3 + \frac{(\sigma_1 - \sigma_2)}{2}\right] = 0$$

and $$\sigma_3 = \tfrac{1}{2}(\sigma_1 - \sigma_2). \qquad (3)$$

This is the same relation found by Ford and Williams as described above. However strain rate effects have not been excluded as these are included in the function F, and no assumption has been made about volume changes which, if they occur at the yield point, will also appear in the function F. The only assumption made here is that if the shear stress or deviatoric stress component is zero the strain rate at the yield point will also be zero.

Equation 3 determines the value of σ_3 for given values of σ_1 and σ_2 and thereby determines the section of the yield surface $f'(\sigma_1\ \sigma_2\ \sigma_3) = 0$ for which the various stress states σ_1 σ_2 were measured. The lines shown in Figures 24 and 25 are sections of the yield locus, given by Equation 3, for the various materials.

3.1.3. The equation of the yield locus

The considerations of the previous section have indicated that flow at the yield point is determined by the shear or deviatoric components of the applied stress tensor. The function $f'(\sigma_1, \sigma_2, \sigma_3)$ for the yield criterion will therefore in general involve any applied shear stresses of the form τ_{xy}, τ_{yz}, τ_{zx} etc, and the normal stress differences $(\sigma_x - \sigma_y)$, $(\sigma_y - \sigma_z)$, and $(\sigma_z - \sigma_x)$. The yield criteria of Tresca and von Mises are functions which contain these terms, and these criteria have been widely used for metals with reasonable success. More recently the von Mises yield criterion has also been used to describe the yielding of certain polymers.

The results presented in section 2.3. however, indicate that yielding in the polymers studied here, unlike metals, is also influenced by the hydrostatic component of stress since the compressive yield stress decreased with applied tension more rapidly than would be expected if the shear yield stress of the material were independent of pressure. The function $f'(\sigma_1, \sigma_2, \sigma_3)$ must therefore also include the effect of pressure on yielding. There are several function f' which could be used within the limitations described above but in view of the success of the von Mises and Tresca yield criteria in explaining shear yielding in metals, and the relative simplicity of these functions, more detailed consideration was given to these criteria.

3.1.4. von Mises yield criterion

The yield condition proposed by von Mises in 1913, may be written in terms of principal stresses:-

$$(\sigma_1 - \sigma_2)^2 + (\sigma_2 - \sigma_3)^2 + (\sigma_3 - \sigma_1)^2 = 6k^2 \qquad (4)$$

where k is a constant identified with the shear yield stress in a state of pure shear. This may also be interpreted as meaning that a material will yield when the elastic strain energy of distortion reaches a critical value. It may be written as $f(J_2') = 0$, where J_2' is the second invariant of the deviatoric stress tensor (Hill (1950)) and in this form illustrates an important assumption of von Mises that the hydrostatic stress component does not appear in the yield criterion. Results presented by Thorkildson (1964)

on tension and torsion of PMMA tubes, and similar experiments by Ely (1967), indicated that von Mises yield criterion may be applicable. Rider and Hargreaves (1969) and Bridle, Buckley and Scanlan (1968) used a modification of von Mises as a yield criterion for anisotropic polymers, together with an internal stress term to explain their results on drawn PVC and PET respectively. This criterion reduced to the form given in Equation 4 for an isotropic material. Ford and Williams (1964) also assumed applicability of von Mises yield criterion to discuss the general stress-strain behaviour of thermoplastics in terms of plasticity theory.

Using the condition that $\sigma_3 = \frac{1}{2}(\sigma_1 - \sigma_2)$ in Equation 4, von Mises yield criterion for the compression with tension tests used here reduces to:

$$\sigma_1 + \sigma_2 = \pm 2k \qquad (5)$$

which is the equation of two parallel lines in σ_1 σ_2 stress space. The intercepts of these lines on the co-ordinate axes are equal, and therefore Equation 5 predicts the yield stresses in tension and compression to be equal, contrary to the results given in section 2.3.

To explain the different tensile and compressive yield stresses observed experimentally, the effect of the hydrostatic component of stress must be included, and in its simplest form this may be achieved by assuming k to be a linear function of the hydrostatic stress P. It has been well reported that the yield stress of many polymers is sensitive to hydrostatic pressure Whitney and Andrews (1967), Bridgman (1953), Ainbinder, Laka, and Maiors (1965) and Sardar, Radcliffe, and Baer (1968) and Holliday (1967) have reported the yield stress of polyoxymethylene and polystyrene respectively to be linearly dependent on pressure for hydrostatic pressures up to 200N/mm^2. Therefore assuming k to be a linear function of the hydrostatic stress component P we have:-

$$k = k_o - \mu P \qquad (6)$$

where k_o and μ are constants. This type of relation has been extensively used in soil mechanics, where the constants k_o and μ have been called the cohesion and coefficient of internal friction, respectively. For convenience this nomenclature will be retained here. The analysis of the applied stresses in Appendix 1 shows that the hydrostatic stress component can be written as

$$P = \frac{(-\sigma_1 + \sigma_2 - \sigma_3)}{3}$$

and applying the condition that $\sigma_3 = \frac{1}{2}(\sigma_1 - \sigma_2)$, this becomes

$$P = -\tfrac{1}{2}(\sigma_1 - \sigma_2)$$

and in (6) we have $$k = k_o + \mu \frac{(\sigma_1 - \sigma_2)}{2} \qquad (7)$$

Substituting Equation (7), together with the condition $\sigma_3 = \frac{1}{2}(\sigma_1 - \sigma_2)$ into von Mises yield condition 4, we have

$$(\sigma_1 + \sigma_2)^2 = 4\left[k_o + \mu \frac{(\sigma_1 - \sigma_2)}{2}\right]^2$$

$$\text{or} \quad \sigma_1 + \sigma_2 = \pm 2 \left[k_o + \mu \frac{(\sigma_1 + \sigma_2)}{2} \right] \qquad (8)$$

This relation gives a linear variation of σ_1 with σ_2 in σ_1 σ_2 stress space (see Figure 4), and the intercepts on the co-ordinate axes are unequal. The intercepts are given by

$$-\sigma_1 = \frac{2k_o}{(1-\mu)} \qquad (9)$$

$$\text{and} \qquad +\sigma_2 = \frac{2k_o}{(1+\mu)} \qquad (10)$$

The relation in (6) is such that the shear yield stress k is increased under hydrostatic pressure or compression (P negative), and in (8) this gives the yield stress in compression greater than the yield stress in tension in accord with the experimental observations.

Other functions of the hydrostatic stress component could be taken, for example a parabolic relation of the form $k^2 = k_o - \mu P$, as suggested by Schleicher (1926) to explain data on sandstone and marble. This type of relationship would predict a non linear variation of σ_1 with σ_2, where deviations from linearity will depend upon the value of μ, and will be most pronounced in the $+\sigma_1$ $+\sigma_2$ quadrant. A complete investigation of the stress states in the $-\sigma_1$, $-\sigma_2$ and $+\sigma_1$, $+\sigma_2$ quadrants is necessary to determine the validity of equation 6 (Sternstein and Ongchin (1969)).

3.1.5. Tresca's yield criterion

Tresca's yield criterion proposes that a material will yield when the maximum shear stress reaches a certain critical value. In terms of the principal stresses this may be written:-

The material will yield when $\frac{\sigma_1 - \sigma_3}{2} = \text{constant}$ $\sigma_1 > \sigma_2 > \sigma_3$

or $\frac{\sigma_1 - \sigma_2}{2} = \text{constant}$ $\sigma_1 > \sigma_3 > \sigma_2$

$\frac{\sigma_2 - \sigma_3}{2} = \text{constant}$ $\sigma_2 > \sigma_1 > \sigma_3$

In this criterion the intermediate principal stress is considered as having no influence upon the yield behaviour. The criterion may also be written in the form $f(J_2', J_3') = 0$, where J_2' and J_3' are the second and third invariants of the deviatoric stress tensor, but the result is complicated and not very useful. The hydrostatic component of stress does not appear in this criterion and like von Mises yield criterion this criterion has been widely used to explain the yield behaviour of several metals with reasonable success. In the form presented above Tresca's yield condition has not been used for polymers, although Whitney and Andrews (1967) have used a modified version including the effect of hydrostatic pressure to explain their results on PS.

Tresca's yield condition will not produce a smooth surface in stress space as the yield surface will be bounded by three sets of parallel planes of the form $\frac{\sigma_1 - \sigma_3}{2}$ = constant. These six planes define a regular hexagonal prism in stress space, whose axis coincides with the space diagonal of the positive and negative quadrants of the $\sigma_1\ \sigma_2\ \sigma_3$ axes. With suitable adjustments of the constants, it can be shown that Tresca's hexagonal prism is inscribed in the straight circular cylinder representing von Mises yield criterion (Hill (1950)).

For the compression-with-tension tests used here the relation $\sigma_3 = \frac{1}{2}(\sigma_1 - \sigma_2)$ has been shown to apply, and no matter what the magnitude or sign of σ_1 and σ_2, σ_3 will always be the intermediate stress. Accordingly Tresca's yield locus will be given by

$$\frac{\sigma_2 - \sigma_1}{2} = \pm k$$

where k is the shear yield stress in a state of pure shear. This is a locus identical to that given by von Mises yield condition (Equation 5), and predicts the same yield stresses for tension and compression which makes it inapplicable to the results in section 2.3.

The introduction of pressure dependence into this yield criterion can be carried out in two ways. Since yielding in shear is assumed to be independent of the intermediate principal stress σ, it can be suggested that the pressure or normal stress across the shear plane determines k, and not the hydrostatic stress.

This gives a relation of the form:-

$$k = k_o - \mu\sigma_n, \qquad (11)$$

where σ_n is the normal stress across the shear plane. On the other hand, if k is determined by the hydrostatic component of stress a relation of the form

$$k = k_o - \mu P \qquad (12)$$

will be obtained, where P is the hydrostatic stress as before.

Equation 11 is the yield condition formulated by Coulomb in 1773 to describe the fracture of building stone and the yielding of soils. This type of yield criterion has been widely used to describe the yield behaviour of loose granular materials which flow in compression with marked changes in volume Terzaghi and Peck (1948), Rowe (1962). It has also been discussed in relation to the yield behaviour of oriented polyethylene by Keller and Rider (1966) and Hinton and Rider (1968).

The yield criterion in Equation 11 was interpreted by Mohr in 1900 using a construction from which it is possible to find the state of stress on any plane in the material for given applied stresses. The construction is essentially a plot of shear stress against normal stress. Considering the case of plane strain compression with tension the principal stresses σ_1 and σ_2 are plotted on the normal stress axis, and a circle of diameter $(\sigma_2 - \sigma_1)$ is drawn through these points. A point on this circle making an angle 2α

with the normal stress axis represents the state of stress in terms of shear stress and normal stress, on a plane in the material inclined at an angle α see Figure 39. Equation 11 appears as a straight line in the diagram, and stress circles to which this line is tangent represent states of stress in the material at the yield point.

It can be seen that the slope of the line (Equation 11) given by the parameter μ determines the angle of the shear plane. If the angle ϕ is defined as in figure 39, then we can write $\mu = \tan \phi$ and $2\alpha = \phi + 90^\circ$. By considering the geometry of the figure it can be shown that

$$\frac{\sigma_1}{2} (1 - \sin \phi) + \frac{\sigma_2}{2} (1 + \sin \phi) = k_o \cos \phi \qquad (13)$$

This is the equation of the yield locus in the σ_1 σ_2 diagram predicted by the Mohr-Coulomb yield criterion for the stress condition of plane strain compression with applied tension. The principal stress σ_3 remains the intermediate stress for all values of σ_1 and σ_2, and the straight line represented by (13) gives the shape of the yield locus across the whole σ_1 σ_2 diagram. This line makes unequal intercepts on the co-ordinate axes given by

$$-\sigma_1 = \frac{2k_o \cos \phi}{(1 - \sin \phi)} \qquad (14)$$

$$+\sigma_2 = \frac{2k_o \cos \phi}{(1 + \sin \phi)} \qquad (15)$$

Alternatively, considering the relation in Equation 12, the hydrostatic stress $P = -\frac{1}{2} (\sigma_1 - \sigma_2)$ for the compression-with-tension tests considered here. Since $\sigma_3 = \frac{1}{2} (\sigma_1 - \sigma_2)$ will always be the intermediate stress, Tresca's yield condition modified for the effect of hydrostatic stress may be written:-

$$\frac{\sigma_2 - \sigma_1}{2} = \pm \left[k_o + \mu \frac{(\sigma_1 - \sigma_2)}{2} \right] \qquad (16)$$

This is the equation to a pair of straight lines in σ_1 σ_2 stress space making unequal intercepts on the co-ordinate axes, given by:-

$$-\sigma_1 = \frac{2k_o}{(1 - \mu)} \qquad (17)$$

and

$$+\sigma_2 = \frac{2k_o}{(1 + \mu)} \qquad (18)$$

Therefore Tresca's yield condition modified for pressure dependence predicts a yield stress in tension less than the yield stress in compression in accord with the experimental observations.

3.1.6. Experimental Evidence for the yield criterion

It has been shown that by introducing the effect of hydrostatic pressure into the yield criteria of von Mises and Tresca a linear relation between σ_1 and σ_2 for the compression-with-tension tests can be found, in agreement with the experimentally observed benaviour. The linear relation predicted by these modified criteria has also been confirmed experimentally in the quadrant of stress space where both σ_1 and σ_2 are compressive (Figure 26).

In an attempt to distinguish between the effects of hydrostatic pressure or pressure normal to the shear plane, ie between pressure dependent Tresca or the Mohr-Coulomb criterion, the yield stress in uniaxial compression has been measured in comparison to the yield stress in plane strain compression.

Von Mises yield criterion modified for pressure dependence can be written in general:-

$$(\sigma_1 - \sigma_2)^2 + (\sigma_2 - \sigma_3)^2 + (\sigma_3 - \sigma_1)^2 = 6(k_o - \mu P)^2$$

which for uniaxial compression becomes:-

$$2\sigma_1^2 = 6\left[k_o + \frac{\mu\sigma_1}{3}\right]^2$$

or $$\sigma_1 = -\frac{3k_o}{(\sqrt{3} - \mu)}$$

which is the yield stress in uniaxial compression.

Tresca's yield criterion modified for pressure dependence can be written in general as:-

$$\frac{\sigma_2 - \sigma_1}{2} = k_o - \mu P \qquad \sigma_2 > \sigma_3 > \sigma_1$$

which for uniaxial compression becomes:-

$$-\frac{\sigma_1}{2} = -\left(k_o + \frac{\mu\sigma_1}{3}\right)$$

or $$\sigma_1 = -\frac{2k_o}{\left(1 - \frac{2\mu}{3}\right)}$$ which is the yield stress in uniaxial compression.

The Mohr-Coulomb yield criterion is given by:-

$$k = k_o - \mu\sigma_n$$

where k is the shear stress, and σ_n the normal stress acting on a plane inclined at $(90 - \alpha)^\circ$ to the compression axis. With the relations $2\alpha = \phi + 90^\circ$ and $\mu = \tan\phi$, the yield stress in uniaxial compression is given by:-

$$\sigma_1 = -\frac{2k_o \cos\phi}{(1 - \sin\phi)}$$

From the analyses in sections 3.1.4. and 3.1.5., the yield stresses in plane strain compression predicted by the three criteria are:-

von Mises $$\sigma_1 = -\frac{2k_o}{(1 - \mu)} \qquad (9)$$

Tresca $$\sigma_1 = -\frac{2k_o}{(1 - \mu)} \qquad (17)$$

Mohr-Coulomb $$\sigma_1 = -\frac{2k_o \cos \phi}{(1 - \sin \phi)} \qquad (14)$$

Therefore the ratio $\frac{\text{plane strain yield stress}}{\text{uniaxial yield stress}} = \frac{\sigma^P}{\sigma^u}$ is given by

von Mises $$\frac{\sigma^P}{\sigma^u} = \frac{2(\sqrt{3} - \mu)}{3(1 - \mu)}$$

Tresca $$\frac{\sigma^P}{\sigma^u} = \frac{(3 - 2\mu)}{3(1 - \mu)}$$

Mohr-Coulomb $$\frac{\sigma^P}{\sigma^u} = 1$$

The experimental value of $\frac{\sigma^P}{\sigma^\mu}$ for PMMA given in section 2.3 was 1.28 ± 0.16.

This last result shows that the Mohr-Coulomb yield criterion is not applicable to the measured data on PMMA, and it can be concluded that for PMMA the normal stress across the shear plane is not an important factor influencing the yield process.

3.1.7 The yield criteria and plasticity theory

In order to describe the development of plastic strains within a deforming material it is necessary to consider rules of flow beyond the limit of plasticity defined by the yield criterion. In the general theory of plasticity, Hill (1950), Nadai (1950), it is assumed that there exists a scalar function of stress called the plastic potential such that the plastic strain increment in a particular direction can be obtained from the partial derivative of the plastic potential in this direction (Hill (1948)). The plastic potential is further assumed to be a surface in stress space of the same shape as the yield criterion. This assumption leads to St Venant's principle that the principal axes of stress and plastic strain increment must coincide and, since the plastic potential is everywhere parallel to the yield surface, to the result that yielding will always occur in a direction normal to the yield surface.

In the previous sections it has been shown that the yielding of PMMA can be explained in terms of a relation $k = k_o - \mu P$ where the shear yield stress k is dependent upon the hydrostatic stress component P. In terms of the plasticity theory described above, this means that any plastic shear deformation will be associated with a volume expansion since a plastic strain increment normal to the yield surface will include a component of volume strain as well as the usual pure shear strain. However it has been shown by Whitney and Andrews (1967) that flow of PMMA beyond the yield point takes place at essentially constant volume, and some difficulty is therefore encountered in applying plasticity theory to materials which exhibit pressure dependent yielding and yet flow at constant volume. This difficulty can be overcome, if it is assumed that the hydrostatic stress component determines the particular state of the material at the yield point, in a way similar to the use of the concept of a critical state in soil mechanics (Schofield and Wroth (1968)). With this idea it is envisaged that the hydrostatic stress component specifies the critical value k required to produce flow which then takes place in accord with

plasticity theory at constant volume. The supposition that the state of the polymer at the yield point depends on the hydrostatic stress does not seem unreasonable in view of the large volume changes prior to yield reported by Whitney and Andrews (1967), and Krause, Segreto, Przirembel, and Mach (1966) for several polymeric materials. Yielding determined by the pressure dependent criteria of Tresca or von Mises, described above, should then take place on planes inclined at 45° to the principal stress axes. For PMMA results given earlier showed that at the instant of yield the inclination of the shear directions was very close to 45° although after unloading the elastic relaxation decreased the inclination to the compression axis to 37°. For PS however, the inclination of the shear directions at yield was shown to differ significantly from 45°, and this is discussed in a later section in terms of a possible volume change on initial yielding as opposed to the continuous volume increase with plastic strain demanded by plasticity theory applied to pressure dependent materials.

3.1.8 The Values of the cohesion and coefficient of internal friction for PMMA

The effect of the hydrostatic pressure on the critical shear stress for yield has been introduced in the form $k = k_o - \mu P$ where k is the shear stress in pure shear, and P is the hydrostatic component of stress (positive in tension). It has been shown that for this relation both von Mises and Tresca's yield criteria predict the same linear relation across the whole of the σ_1 σ_2 diagram. By comparison of the slope of the lines determined experimentally (see Figures 24 and 25) with the slope predicted by the two criteria, values of the constants k_o and μ can be determined.

For both von Mises and Tresca the slope of the line in the $-\sigma_1$, $+\sigma_2$ quadrant, is given by

$$\frac{\sigma_2}{\sigma_1} = \frac{(1 - \mu)}{(1 + \mu)} \qquad (19)$$

From Table 4 the slope $\frac{\sigma_2}{\sigma}$ for PMMA was found to be 0.619 ($\pm$ 0.011), and in Equation (19) this gives a value

$$\mu = 0.225 \pm 0.008$$

The value of the plane strain compressive yield stress without tension predicted by both Tresca and von Mises yield criteria is the same and is given by $\sigma_1 = \frac{2k_o}{(1 - \mu)}$. The experimentally determined value of σ_1 can be found from Table 3 which for PMMA is 119.4 ± 1.6 N/mm^2, and hence the value of k_o can be calculated using the value of μ determined above.

$$\text{ie} \quad k_o = 46.2 \pm 1.1 \text{ N/mm}^2$$

Therefore ratio of plane strain to uniaxial yield stress (see Section 3.1.6) is found to be

(a) von Mises $\frac{\sigma_p}{\sigma_\mu} = 1.29 \pm 0.02$

(b) Tresca $\frac{\sigma_p}{\sigma_\mu} = 1.10 \pm 0.02$

The experimentally determined value of $\frac{\sigma_p}{\sigma_\mu}$ was found to be 1.28 ± 0.16 for PMMA, and in view of this result it appears that von Mises yield criterion modified for pressure dependence is more applicable although the results given by each criterion are very similar, and more sensitive tests are required to distinguish precisely between them. Sternstein and Ongchin (1969) have studied the yielding of PMMA tubes under axial tension and internal pressure, and found that for the states of biaxial tension produced, a von Mises type yield criterion, modified for a linear pressure dependence (Equation 6) was applicable. Tests on acrylic tubes under axial tension or compression and internal pressure have been reported by Ely (1967), and a similar type of pressure modified von Mises yield criterion was found to be appropriate.

3.2 Interpretation of the yield criterion

3.2.1 Introduction

In the previous sections the importance of both the hydrostatic and shear components of stress on the rate sensitive yielding of PMMA has been indicated, and a satisfactory explanation of yielding must account in a consistent way for these different effects. It is important therefore to relate the phenomena observed with the bulk polymer to the molecular mechanisms responsible for yielding.

There has been considerable discussion concerning the mechanism of yielding in polymers below their glass transition temperature (T_g) with particular reference to the phenomenon of cold drawing in tension. One of the earlier theories proposed that localised heating of the sample, due to the mechanical work of extension, raised the polymer above its glass transition temperature (Marshall and Thompson (1954), Müller and Jäckel (1952)). Although significant temperature rises during flow have been reported (Nakamura and Skinner (1955), Vincent (1960)) yielding has been observed at low temperature where the heating of the sample during deformation was insufficient to raise the polymer above its glass transition temperature. It is apparent therefore that localised heating effects cannot be a complete explanation of plastic yielding.

A second theory proposes that yielding in tension is due to the increase of a free volume (Doolittle and Doolittle (1957)) associated with deforming units in the polymer structure (Litt and Koch (1967), Ender (1968)). The large volume changes due to the high ratio of yield stress to Young's modulus found in polymers are considered as contributing to the free volume which under tensile stresses would increase until it reaches its value at the glass transition temperature. At this point flow would occur. In compressive states of stress however, a conflict arises if the complete volume reduction is at the expense of the free volume because the fractional free volume could become negative if the hydrostatic pressure is large enough. Ender (1968) proposes that in this case both the free volume and the occupied volume must be compressed. Whitney and Andrews (1967) have measured volume changes during uniaxial compression of several polymers and found a nett contraction which decreased up to the yield point and thereafter remained constant. This was interpreted as a volume contraction due to the hydrostatic stress (Poisson's ratio effect), and a volume expansion associated with the mechanism of yielding. It is apparent that this result goes some way to explaining the free volume anomaly described above but a consistent analysis must involve a more detailed understanding of the relation between the total and free volume.

Another approach is to consider that the applied stress induces molecular flow and the internal viscosity of the polymer decreases with increasing stress to the point where appreciable molecular flow becomes possible. This idea can be discussed in terms of the Eyring viscosity equation (Glasstone, Laidler, Eyring (1941)) in which a stress-dependent thermally activated rate process determines flow. Robertson (1963) has shown that the yield behaviour of

polycarbonate can be explained using the Eyring viscosity equation, and Roetling (1965) and Crowet and Homes (1964) have discussed the tensile behaviour of PMMA at various strain rates and temperatures using this equation. Ishai (1967) also found a deviatoric stress biased diffusional mechanism as the predominant factor in the yielding of glassy epoxy resins. In the following sections the Eyring viscosity equation will be discussed in more detail in relation to the yield behaviour observed here but it is apparent that a combination of the effects mentioned above could be present in any given experimental case since these different interpretations are not mutually exclusive.

3.2.2 A molecular mechanism for yielding

Unlike metals in which deformation can take place by shearing on well defined lattice planes, in polymers deformation must proceed by a more homogeneous shear process in which the whole structure plays a part. Studies of solution viscosities (Bueche (1962)) have shown that the segment lengths involved in flow are small compared with the molecular length, in agreement with the view that the unit of flow is a segment of the polymer chain. The flow of the polymer chains in the structure can be thought of as the resultant motion of segments that jump from one equilibrium position to another at a given rate, and it is necessary that there should be some co-ordination of the movement of the segments if the chain as a whole is to progress. When no stress is applied to a unit there will be a certain amount of thermal energy available, and the unit will spontaneously jump to and fro at a natural frequency f. If the energy barrier to this motion is E_o, then according to Boltzmann's relation the probability that a unit will acquire enough energy to move to a new position is $\exp(-E_o/k_BT)$ where k_B is Boltzmann's constant, and T the absolute temperature. At equilibrium therefore, the natural frequency with which units oscillate back and forth will be given by a relation

$$f = f_o \exp\left[\frac{-E_o}{k_BT}\right] \qquad (20)$$

where f_o is a basic frequency. A segment will be able to jump to a new equilibrium position provided: (a) there is enough volume available for the segment to move into and (b) the segment has enough energy to break loose from its neighbours and move into the hole. The volume mentioned in (a) leads to the concept of free volume, which is discussed in detail by Bueche (1962), in relation to the motion of molecular segments of polymers above the glass transition temperature. At these temperatures the energy required by (b) becomes unimportant.

For glassy polymers below the glass transition temperature, the effect of both (a) and (b) must be considered. If we consider for the moment a shear stress S applied to the bulk sample then assuming that this has no effect on the total volume the contribution to E_o from factor (a) will be unchanged. Each deforming unit will experience an average force F in the direction of the applied stress, and the energy barrier to motion in this direction will be lowered by an amount $F\lambda$. This is because the force F does work $F\lambda$ on the unit, as it moves from one equilibrium position to the next through a distance λ see figure 40. Under this bias the nett frequency of jumps in the direction of the applied force will become

$$f_{nett} = f_o \left[\exp - \frac{(E_o - \frac{F\lambda}{2})}{k_B T} - \exp - \frac{(E_o + \frac{F\lambda}{2})}{k_B T} \right]$$

$$\therefore \quad f_{nett} = f_o \exp - \left(\frac{E_o}{k_B T}\right) \left[\exp \left(\frac{F\lambda}{2k_B T} \right) - \exp - \left(\frac{F\lambda}{2k_B T} \right) \right]$$

$$\text{or} \quad f_{nett} = 2 f \sinh \frac{F\lambda}{2k_B T} \qquad \text{(Glasstone et al.(1941))} \qquad (21)$$

If we now assign an effective cross sectional area A to the deforming unit, the stress acting upon this unit will be $\frac{F}{A}$, which can be taken as the applied stress S. Equation (21) then becomes:-

$$f_{nett} = 2 f \sinh \frac{S \lambda A}{2k_B T} \qquad (22)$$

The quantity λA has the dimensions of volume, and is referred to as the activation volume (V_a) for the process. The idea of an activation volume is difficult to interpret in terms of the polymer structure since an arbitrary area A was ascribed to a molecular segment under stress. However, it would seem reasonable that a molecular segment can be assigned a particular volume since segments vibrating about their equilibrium positions will exclude other molecules from taking up positions too close to them. In the above analysis the simple model of one type of deforming unit with volume V_a has been considered. A full description of the molecular processes is likely to involve a number of activation volumes for which the V_a value above will be a statistical average (see for example Roetling (1965)).

The bulk shear strain rate measured on a sample will be related to the frequency with which individual units shear, and therefore the shear strain rate ($\dot{G}$) will be given by

$$\dot{G} = 2A' f \sinh \frac{S V_a}{2k_B T} \qquad (23)$$

where A' is a constant. For small values of the applied shear stress, or at relatively high temperatures, so that $\left[\frac{SV_a}{2k_B T} \right]^2$ is small compared with $\frac{SV_a}{2k_B T}$, Equation 23 becomes:-

$$\dot{G} = BS \quad (B \text{ constant}) \qquad (24)$$

which is the usual expression for the viscosity of a Newtonian fluid. On the other hand if S is large we have:-

$$\dot{G} = C f \exp\left[\frac{S V_a}{2k_B T}\right] \quad (C \text{ constant}) \qquad (25)$$

which is the viscosity equation due to Eyring (1936). This equation gives the relation between the applied shear stress and the resultant shear strain rate for a polymer showing viscous flow, and as such allows a definition of the yield stress. If a polymer is made to deform at a constant strain rate then the applied shear stress will continue to increase until it is sufficient to cause the material to deform at this strain rate at which point the material will flow. The yield stress therefore becomes the stress necessary to make the material flow at the imposed strain rate. According to Equation 25 the shear yield stress will increase linearly with the logarithm of the strain rate. This was the type of variation found experimentally for PMMA at room temperature (see section 2.2.7), and the slope of this line will give a value for the activation volume V_a. For the data in Figure 9, $V_a = 1.44 \times 10^{-18}$ mm^3 which is a cube of side approximately 11 Å, and is not unreasonable in terms of the polymer structure. Similar values have been reported (Bueche (1962)) for polystyrene and polyethyl methacrylate (~ 13 Å) from measurements of time to fracture under constant load. Haward and Thackray (1968) have also given activation volumes of a number of polymers determined in tension and compression and at various temperatures. Roetling (1965) used a modification of Equation 25 involving two processes with different V_a values to describe the yielding of PMMA in tension, and he discusses these values in relation to the α and β relaxations found in PMMA. It is possible that the linear variation of yield stress with logarithm of the strain rate shown in Figure 9 also involves more than one process but measurements covering a range of temperatures up to the glass transition temperature are necessary in order to confirm this.

3.2.3 The effect of hydrostatic pressure

In the previous section it was shown that the strain rate behaviour of PMMA in tension and compression may be explained in terms of a stress biased segmental motion. The stress used for the derivation of the Eyring viscosity equation was a pure shear stress, and no allowance was made for any effects of the hydrostatic component of stress. It has been well reported in the literature that for many polymers the yield stress, and hence the yield mechanism, is noticeably influenced by hydrostatic pressure (see section 3.1). Therefore to extend the Eyring rate process model to other stress systems in which there is a hydrostatic component as well as a shear component of stress some modification is necessary.

In the presence of a hydrostatic component of stress, there will be a large elastic volume change which will alter the volume available for a molecular segment to move into, and thereby change the natural jump frequency f (Equation 20). Under a hydrostatic pressure, the available volume will decrease and the natural frequency of the polymer segment will also decrease. Consequently a higher shear stress will be needed to produce flow. Sasabe and Saito (1968) measured dielectric relaxation peaks in a series of poly alkyl methacrylates under high hydrostatic pressures and found that for all the relaxation processes studied the logarithm of the jump frequency decreased linearly with pressure so that

$$\ln f = \ln F_o - x P$$

$$\text{or} \qquad f = F_o \exp(-xP) \qquad (26)$$

where F_o is a natural jump frequency under zero hydrostatic pressure P, and

x is a constant and a type of bulk modulus expressing the compressibility of the available volume.

Substituting (26) in (25) we have:-

$$\dot{G} = C.F_o \exp(-xP) \exp\left(\frac{SV_a}{2k_BT}\right) \quad (27)$$

For a constant strain rate Equation 27 gives the shear yield stress in the form:-

$$S = \frac{2k_BT}{V_a} \ln\frac{\dot{G}}{CF_o} + \left(\frac{2k_BTx}{V_a}\right) P \quad (28)$$

$$\text{or} \quad S = k_o + \mu P \quad (29)$$

which is the relation suggested in section 3.1 for the variation of the shear yield stress with hydrostatic pressure. Equation 28 therefore allows an interpretation of the yield criteria discussed in section 3.1 in terms of the molecular processes associated with yielding, and gives the correct shear stress variation both with strain rate and pressure. The only other variable parameter in Equation 28 is the temperature, and temperature effects in relation to this equation are discussed in Section 2.4. Although Equation 28 gives a useful physical interpretation of the yield criterion in terms of pressure and strain rate effects observed here its application over a wider range of testing conditions must be considered with caution. As already mentioned V_a will be a statistical average of a large number of possible activation volumes, and this average is likely to change with the pressure, temperature, or strain rate as different segments of the molecular chains become active in the flow process. A better understanding of the relation between activation volume and the molecular processes taking place during deformation would lead to a wider application of the Equation 28.

3.2.4 The coefficient of internal friction in PMMA

Using Equation 28 it is possible to estimate a value for μ in terms of the parameters $\frac{2k_BT}{V_a}$ and x. In the previous section it was shown that if the shear yield stress is given by Equation 29, then the plane strain compressive yield stress is

$$\sigma_1 = \frac{2k_o}{(1-\mu)}$$

In terms of Equation 28 this gives

$$\sigma_1 = \frac{\frac{4k_BT}{V_a} \ln\frac{\dot{G}}{CF_o}}{1 - \frac{2k_BTx}{V_a}}$$

$$\text{or} \quad \sigma_1\left[\frac{V_a}{4k_BT} - \frac{x}{2}\right] = \ln\frac{\dot{G}}{CF_o} \quad (30)$$

The slope of the linear variation between the plane strain yield stress and the logarithm of the strain rate ($\dot{G}$) therefore permits an estimate of the quantity $\frac{2k_B T}{V_a x}$ (see Section 3.2.2.).

Values of x are given by Sasabe and Saito (1968) for two relaxation processes in PMMA. They consider a single relaxation process α' at temperatures well above the Tg which splits into two processes α and β at lower temperatures or higher pressures. From their data the value of x for the α' process was $1.7(N/mm^2)^{-1}$ while for the β process x was $0.7(N/mm^2)^{-1}$. These values give μ in the region of 0.1 to 0.04 which is a factor of 2-5 times too small but it is nevertheless encouraging to find agreement to an order of magnitude and of the correct form. There are many possible reasons for the discrepancy among which is the possibility that the dielectric relaxation peak measured by Sasabe and Saito does not correspond to the same relaxation process that leads to yielding in "Perspex" at high strains. In the following section a further contribution to the value of μ from a possible volume expansion on shearing is considered which will tend to increase the value calculated above.

3.2.5 Volume changes associated with yielding

In Section 3.2.3 the hydrostatic pressure was introduced into the yield condition by consideration of its effect on the amount of volume available for a molecular segment to move into under stress. This approach is consistent with the suggestion in Section 3.1 that the hydrostatic stress determines the state of the material for which yielding will then take place under the shear or deviatoric component of stress. Since the maximum shear stresses in any applied stress state are across planes inclined at 45° to the principal stress axes, plastic yielding would be expected to take place in these directions. Measurement of the angle of the shear zones observed in the polymers studied here has shown that this is in fact very nearly true in all cases (Table 3). However there is the notable exception of PS in which yielding was observed to take place on planes inclined at approximately 42° to the compression axis, and it is apparent that some additional effect to those already mentioned is controlling the shear direction in this material. A possible explanation is that there is a volume expansion associated with the shear process in each deforming unit which will lead to shear deformation on planes differing from 45° (see Section 3.2.6.).

Whitney and Andrews (1967) have studied the volume changes during compression of a series of polymers including PMMA and PS. By extrapolating the value of the bulk modulus at low strains they have shown that there is a relative volume expansion in opposition to the normal volume contraction, which increases up to the yield point, and thereafter further yielding takes place at constant volume. To explain this effect they suggest a stress-dependent thermally activated rate process for yielding with an incorporated "structure change" factor, which allows for changes in concentration of the basic deforming units in the polymer structure. It is also suggested that the effective unit involved in the structure change should have associated with it a local region of decreased density. Argon et al (1968) have also reported a steady state positive dilation in PS regardless of the sign of the hydrostatic stress which decayed in relatively short times when straining was interrupted. These workers used the model of a PS molecule acting like a bumpy line being drawn through gaps between other molecules to explain the volume dilatation and shear band behaviour of polystyrene. This model implies a transient volume expansion as a "bump" passes through a gap. A similar volume expansion associated with deformation is also considered appropriate to semi-crystalline polyoxymethylene by Sardar et al (1968). Bauwens (1967) has considered the propagation of plastic deformation in PVC in terms of the Eyring rate theory generalised for shear and hydrostatic stress components. The effect of

hydrostatic pressure was introduced by considering the change in free volume for the molecular segment to move into, and with this approach he found good agreement between the predicted and measured inclinations of Luders bands in flat tensile bars.

In Section 3.2.2 the shearing of a small deformation unit from one equilibrium position to the next was considered in terms of the work done to overcome the energy barrier to flow. As a single deformation unit or molecular segment cannot be considered in isolation from the rest of the structure, it is possible that during its passage over the energy barrier the deformation unit under consideration will disturb the surrounding structure to the extent that a local volume expansion will be necessary. If this is the case work will be done against the hydrostatic pressure and the apparent height of the energy barrier will be increased. If we assign an effective cross sectional area A to the deforming unit as before, the work done by the shear stress S in moving the unit through distance λ will be $S \lambda A$ as explained previously. The work done against the hydrostatic pressure P will be $P \lambda' A$, where λ' is the component of volume expansion normal to the shear direction. Equation 21 for the nett jump frequency then becomes

$$f_{nett} = 2f \sinh \frac{(S \lambda A - P \lambda' A)}{2k_B T} \qquad (31)$$

If we further assume that the normal displacement λ' is proportional to the shear displacement λ in the form $\lambda' = c\lambda$ where c is a constant we have:-

$$f_{nett} = 2f \sinh \frac{\lambda A}{2k_B T} (S - cP) \qquad (32)$$

or
$$\dot{G} = C f \exp \frac{V_a}{2k_B T} (S - cP) \text{ as before} \qquad (33)$$

and introducing the effect of hydrostatic pressure on the natural frequency f as before we have:-

$$\dot{G} = CF_o \exp(-xP) \frac{V_a}{2k_B T} (S - cP) \qquad (34)$$

For a constant strain rate this equation gives the shear yield stress in the form:-

$$S = \frac{2k_B T}{V_a} \ln \frac{\dot{G}}{CF_o} + \left[\frac{2k_B Tx}{V_a} + c \right] P \qquad (35)$$

which again is an equation of the form of (29)

$$\text{ie} \quad S = k_o + \mu P$$

In this case however the pressure dependence of the shear stress is envisaged as arising from two causes which involve the compressibility of the available volume on the one hand and a volume expansion arising from the shear process on the other.

3.2.6 The angle of a shear zone

The constant c described above was used to define the ratio of the shear displacement λ, to the displacement normal to the shear direction λ'; using this approach it is possible to account for the direction in which yielding was observed to take place in the various glassy polymers. The treatment given above due to Eyring considers deformation by simple shear so that extensions and displacements occurred only in two of the three principal directions. This type of treatment is consistent with plane strain deformation, and is therefore applicable to the deformation observed here. Consider a small element of material at some point in the deforming specimen at the yield point where a shear zone has just formed. If the direction of propagation of this zone is along a line inclined at $(90 - \beta)$ to the direction of the greatest principal stress σ_1 in simple plane strain compression, then the normal and shear stresses acting on the element will be as shown in Figure 41. There will be two equal shear stresses of the type considered by Eyring, and according to the supposition above there will be normal strains along the x and y directions proportional to the shear strains γ_{xy}, through the constant c. There will be no strains in the z direction (out of the paper), since the deformation is considered plane.

To begin with it will be assumed that strains ε_y, in the y direction, are small because the adjoining portions of non-yielding material do not participate in the deformation. In PS this is likely to be a good assumption as it has been shown that the deformation bands in this material are well defined with a sharp boundary between elastic and plastic material, and contain a uniform shear of up to 2.0 (Argon et al (1968)). In PMMA however, the shear zones at the yield point are more diffuse and appear to contain a shear strain of approximately 0.10 at the centre of the zone. If $\varepsilon_y = 0$ then the only component of expansion due to shearing will be along the x direction, and work will be done by the normal stress σ_x against this expansion.

It can be shown that

$$\sigma_x = -\sigma_1 \cos^2\beta$$

$$\sigma_y = -\sigma_1 \sin^2\beta$$

$$T_{xy} = \sigma_1 \sin\beta \cos\beta$$

$$\sigma_z = \sigma_3 \qquad (36)$$

The work done by the shearing stress T_{xy} in producing a simple shear strain γ_{xy} at the yield point is:

$$W_T = \tau_{xy} \gamma_{xy}$$

While the work done against the normal stress σ_x due to the volume expansion ε'_x is:-

$$W_\sigma = \sigma_x \varepsilon'_x$$

Therefore the total work absorbed by the material is:-

$$W = T_{xy} \gamma_{xy} + \sigma_x \varepsilon'_x \qquad (37)$$

Taking the ratio of the strains $\varepsilon'_x / \gamma_{xy}$ as equal to the ratio of the displacements λ / λ described earlier, we have $\varepsilon'_x = c\,\gamma_{xy}$ where c is the constant in Equation 35, used to define the relation between volume strain and shear strain.

Hence $W = T_{xy}\,\gamma_{xy} + \sigma_x\, c\gamma_{xy}$,

and using Equation 36.

$$W = \sigma_1 \sin\beta\alpha\cos\beta\gamma_{xy} - \sigma_1 \cos^2\beta\, c\gamma_{xy}$$

$$\therefore \frac{dW}{d\beta} = \sigma_1 \cos 2\beta\gamma_{xy} + 2\sigma_1 \cos\beta \sin\beta\, c\gamma_{xy}$$

$$= 0 \text{ for a maximum,}$$

$$\therefore \cos 2\beta = -c \sin 2\beta$$

$$\text{and } c = -\cot 2\beta \qquad (33)$$

For a volume expansion c will always be positive, and β will therefore be greater than 45°. If the stress σ_x is tensile, Equation 38 becomes $c = +\cot 2\beta$, and β will be less than 45° for a volume expansion. This type of behaviour has been observed with PS by Argon et al (1968).

It has already been mentioned that the above analysis is not likely to be a good representation of the shear zone behaviour of PMMA as strains in the y direction (ε_y) are possibly of the same order of magnitude as strains in the x direction (ε_x). The result is that for this material volume expansions will be isotropic and therefore will not affect the direction of a shear zone. However, it is useful to estimate an order of magnitude for the volume expansion in PMMA using Equation 38. In Section 2.3 it was shown that the angle β for PMMA was approximately 46°, and in Equation 38 we find $c = 0.035$. The shear strain in the zones was estimated as approximately 0.10 which gives $\varepsilon'_x = 0.0035$ or a volume expansion of 0.35% if the zones fill the whole specimen. This figure is in agreement with the volume expansion quoted by Whitney and Andrews (1967) from dilatometric measurements during uniaxial compression of PMMA.

Equation 35 gives $\mu = \frac{2k_B T x}{V_a} + c$

and using the value of $\frac{2k_B T x}{V_a}$ calculated in Section 3.2.4, the value of μ for PMMA is estimated to be $\mu = 0.135$. The effect of introducing a volume expansion term therefore is to improve the agreement between the value of μ estimated from theoretical considerations and the value found experimentally (Section 3.1.).

3.2.7 The extension of the yield criterion to other polymers

To produce a yield criterion for the other polymers investigated here, the analysis given in the preceding sections for PMMA should be extended to each material in turn. However, the similarity of the experimental data presented in Section 3.1, in part at least, justifies extension of the conclusions reached for PMMA to other polymers. The description of yielding as a rate process is likely to have general application to all the glassy polymers considered here, and the equation $k = k_o - \mu P$ (Section 3.1) will therefore be considered appropriate in each case. Values of μ and k_o have also been calculated for LDPE and HDPE using this equation although it is possible that other mechanisms such as slip and twinning of the crystal structure (see for example Frank, Keller and O'Connor (1958)) may be involved in the yield process.

For a material which shows a relatively large volume expansion on shearing, and deforms in well defined bands similar to those seen in PS, the pressure normal to the shear plane will have a major effect and Equation 35 will be similar to the Mohr-Coulomb criterion described in Section 3.1. If the deformation is more homogeneous as in PMMA then the hydrostatic pressure will dominate the yield behaviour either through the compressibility term x or the volume expansion associated with shearing. It is apparent that a combination of these effects will be present in any given case. The criteria of Tresca and von Mises predict the same variation of the plane strain compressive yield stress (σ_1) with applied tension (σ_2) as described in Section 3.1. The Mohr-Coulomb criterion predicts the ratio σ_2/σ_1 as

$$\sigma_2/\sigma_1 = \frac{(1 - \sin \phi)}{(1 + \sin \phi)} \quad \text{where } \tan \phi = \mu \ .$$

While for Von Mises and Tresca this ratio is

$$\sigma_2/\sigma_1 = \frac{(1 - \mu)}{(1 + \mu)} \ .$$

If μ values are small the difference between sin ϕ and tan ϕ is small, and μ values have therefore been calculated using this latter relationship. The cohesion k_o for each material has been found using the equation

$\sigma_1 = \frac{2k_o}{(1 - \mu)}$ where σ_1 is the plane strain compressive yield stress (Section 3.1.). The ratio of the volume strain to the shear strain has also been estimated for each material using the zone angles given in Section 2.3 and all these values are summarised in Table 7.

These figures can be used as an indication of structural effects associated with yielding in each of the polymers. The values for the cohesion k_o for all the glassy polymers are similar, and this reflects the basic glassy nature of these materials. It was shown in Equation 35 that the term k_o contains the natural equilibrium frequency (F_o) of the deforming units, and k_o will therefore reflect the particular relaxation process associated with yielding at the testing temperature. Values of the cohesion with varying temperature have been investigated for PMMA and this is discussed in section 2.4. The k_o

and μ results for the polyethylenes suggest a possible effect of the crystallinity either through degree of crystallinity or the nature of the crystalline structure and is discussed further in Section 2.4.

The effect of the polymer structure on the values of the parameters μ, k_o, and c is perhaps best illustrated by the results for PMMA and PS which exhibit markedly different modes of deformation but very similar pressure dependence. For PMMA the pressure dependence of the yield process is mainly due to the elastic compressibility of the structure, and only a small volume expansion is required to move the deforming units. For PS however where the structure is initially more compact and the benzene rings in the side groups more bulky the compressibility term (μ - c) is smaller than for PMMA and a larger volume expansion is required to move the deforming units. The shear strain in the bands for PS is the order of 2.0 which together with the value of c in Table 7 gives an associated volume expansion of approximately 25%. However the bands occupy little more than 1% of the total volume at the yield point so that the apparent volume expansion would be 0.25% which is in agreement with the value given by Whitney and Andrews (1967).

4 CONCLUSIONS AND SUGGESTIONS FOR FURTHER WORK

4.1 Summary and conclusions

The variation of the plane strain compressive yield stress with applied tension indicated a significant effect of the hydrostatic component of stress on the yield behaviour of all the polymers studied here. This has been considered in terms of the Tresca and von Mises yield criteria when it was found that a relation of the form $k = k_o - \mu P$ could be used to explain the observed pressure dependence of yielding for the stress states studied, where k is the critical shear stress for yield, P is the hydrostatic stress component, and μ and k_o material constants. It has also been shown that the yield point in PMMA, and similar polymers, corresponds to a condition of pure viscous flow, and that it is possible to consider yielding as an equilibrium between the applied strain rate and the rate at which units of the structure move. With this approach an equation of the same form as that given above has been derived which allows an interpretation of the yield condition in terms of the molecular processes associated with yield or flow in polymeric materials.

It has been shown that the cohesion k_o, which may also be defined as the shear yield stress in a state of pure shear, is related to the activation volume of the molecular segments involved in flow at the yield point and is also, therefore, related to the polymer structure and the conditions of testing. For PMMA it was found that over approximately three decades of strain rate at room temperature, k_o increased linearly with the logarithm of the strain rate, confirming the interpretation of yield as a rate process. The cohesion was found to decrease linearly with increasing temperature in the range 20-70°C but this result is difficult to interpret without a better knowledge of the relation between the activation volume and the units of the structure taking part in yielding at various temperatures. It has also been shown that increasing the percentage crystallinity of PET causes an increase in k^o values, and addition of plasticiser to epoxy resins produced a decrease in the value of k_o. These effects, together with the range of values observed with the different polymers studied, gave a qualitative indication of the effect of different polymer structure on yield behaviour.

The coefficient of internal friction μ is a parameter which expresses the sensitivity of a polymer to the hydrostatic stress component. It has been suggested that there are two separate contributions giving rise to the pressure dependence of yield in polymeric materials. One contribution is associated with the large elastic volume changes found in polymers for which the ratio of the yield stress to Young's modulus is significantly higher than in metals; such volume changes were considered as affecting the amount of free volume available for molecular segments involved in the yield process to move into. A second contribution was considered as arising from a volume expansion, related to the unit shear process, due to the co-operative movement necessary within the polymer structure for a particular segment to move from one equilibrium position to the next. The volume expansions, estimated from measurement of shear zone angles within deforming specimens, could be given reasonable interpretations in terms of the various polymer structures although these values can only be regarded as indication of the order of magnitude of such volume expansions. Further work is necessary to elucidate the precise volume changes resulting from yield. These two contributions to the pressure dependence of yielding are also likely to be present to varying degrees for a given polymer structure, as different units of the structure become involved in the flow process

under different conditions of testing. The value of μ has been measured for PMMA in the temperature range 20-70°C and was found to be constant. This is an interesting result suggesting that the various effects giving rise to pressure dependent yielding are unaffected by temperature changes. This seems unlikely to be true, and it may be that as the temperature increases the volume expansion on yielding decreases while the compressibility of the free volume increases, giving the overall effect of μ constant with temperature. The influence of the basic polymer structure on the pressure dependence of yielding has been illustrated by the range of μ values obtained for the various polymers studied, and by the significant changes observed with increasing crystallinity in PET and increasing plasticiser content in the epoxy resins.

It has been shown therefore, that yielding in rigid polymers is a complex process in which both the shear and hydrostatic components of stress play an important part. In view of the sensitivity of these materials to the testing conditions used, it is apparent that relatively simple yield criteria such as the pressure dependent criteria of von Mises and Tresca can only have application for a specified polymer structure and set of testing conditions. A more general yield criterion will involve such variables as strain rate and temperature. However, the yield condition given here in the form $k = k_o - \mu P$ permits a useful description of the response of the polymers studied to various applied stresses in terms of just two parameters which relate to the basic polymer structure.

4.2 Suggestions for further work

The description of the yield criterion and the various trends reported in μ and k_o values have all been centred upon results obtained from testing in plane strain. Results from other types of test have been discussed where possible but an investigation of the proposed yield criterion for other more general types of deformation would prove useful in indicating the general validity of the conclusions reached. Volume changes associated with the yield process are of importance in view of the influence of the hydrostatic stress component, and investigations of density changes during straining would be valuable in determining the magnitude of these effects. From this viewpoint it may also be possible to determine the factors causing the markedly different modes of deformation seen in PMMA and PS. An indication has been given of the effects of strain rate and temperature on the value of k_o but apart from investigating these effects further, it is clear that the temperature and strain rate dependence of μ should be given further consideration with a view to establishing more precisely the origins of pressure dependence.

In these experiments it has been shown that the parameters μ and k_o give a useful indication of the molecular processes associated with yield, and measurement of these parameters in conjunction with dynamic mechanical tests for example, would prove useful in relating bulk properties to structure. In this context determination of values of μ and k_o for a series of polymers with precisely controlled changes in structure, such as different side groups attached to the main polymer chain, would give further information on the relation between structure and mechanical properties. Indications of the influence of crystalline structure can be found from comparison of yield stress data on crystalline and amorphous polymers but variation of the degree of crystallinity in more precise experiments than those described here for PET would indicate the relative importance of the amorphous and crystalline regions in the deformation of crystalline polymers.

REFERENCES

AINBINDER, S B, LAKA, M A, MAIORS, T Y (1965) Polym. Mech. 1 50.

ALLISON, S W, WARD, I M (1967) Brit. J App. Phys. 18, 1151.

ANDREWS, R D, KAZAMA, Y (1968) J App. Phys. 39, 4891.

ARGON, A S, ANDREWS, R D, GODRICK, J A, WHITNEY, W (1968) J App. Phys. 39, 1899.

ASTBURY, W T, BROWN, C J (1946) Nature 158, 871.

BAER, E (1964) Engineering Design for Plastics (Reinhold NY).

BAUWENS, J (1967) J Poly. Sci. A2, 5, 1145.

BEARDMORE, P (1969) Phil. Mag. 19, 389.

BISHOP, J F W (1958) J Mech. Phys. Solids 6, 132.

BOWDEN, P B (1968) Polymer, 9, 449.

BOYER, R F, SPENCER, R, WILEY, R M (1946) J Poly, Sci 1, 249.

BRIDGMAN, P W (1946) J App. Phys. 17, 225.

BRIDGMAN, P W (1953) J App. Phys. 24, 560.

BRIDLE, C, BUCKLEY, A, SCANLAN, J (1968) J Mat. Sci. 3, 622.

BROWN, N, WARD, I M (1968) J Poly. Sci. A2, 6, 607.

BROWN, N, WARD, I M (1968) Phil. Mag. 17.2, 961.

BUECHE, F (1962) Physical Properties of Polymers. (Interscience).

CROWET, C, HOMES, G A (1964) App. Mat. Res. 3, 1.

DAUBENNY, R P, BUNN, C W, BROWN, C J (1954) Proc. Roy. Soc. A226, 531.

DOOLITTLE, A K, DOOLITTLE, D B (1957) J App. Phys. 28, 901.

ELY, R E (1967) Poly. Eng. and Sci. 7, 40.

ENDER, D H, ANDREWS, R D (1965) J App. Phys. 36, 3057.

ENDER, D H (1968) J Appl. Phys. 39, 4877.

EYRING, H (1936) J Chem. Phys. 4, 283.

FORD, H, WILLIAMS, J G (1964) J Mech. Eng. Sci 6, 405.

FORD, H (1948) Proc. Inst. Mech. Eng. 159, 115.

FRANK, F C, KELLER, A, O'CONNOR, A (1958) Phil. Mag. 3, 64.

GLASSTONE, S, LAIDLER, K J, EYRING, H (1941) The Theory of Rate Processes (McGraw Hill).

GREEN, A P (1951) Phil. Mag. 42.2, 900.

HAIGH, B P (1920) Engineering 109, 158.

HARTLEY, F D, LORD, F W, MORGAN, L B (1954) Phil. Trans. Roy. Soc. A247, 23.

HAWARD, R N, THACKRAY, G (1968) Proc. Roy. Soc. A302, 453.

HILL, R (1948) Proc. Roy. Soc. A193, 282.

HILL, R (1950) The Mathematical Theory of Plasticity (OUP Oxford).

HINTON, T. RIDER, J G (1968) J App. Phys. 39, 4932.

HOLLIDAY, L (1967) Chem. and Ind. June 973.

ISHAI, O (1967) J App Poly. Sci. 11, 1863.

KELLER, A, LESTER, G R, MORGAN, L B (1954) Phil. Trans. Roy. Soc. A247, 1.

KELLER, A, RIDER, J G (1966) J Mat. Sci. 1, 389.

KOLB, H J, IZARD, E F (1949) J App. Phys. 20, 571.

KRAUSE, I, SEGRETO, A J, PRZIREMBEL, H, MACH, R L (1966) J Mat. Sci. and Eng. 1, 239.

LITT, M H, KOCH, P (1967) J Poly. Sci. B5, 251.

MARSHALL, I, THOMPSON, A B (1954) Proc. Roy. Soc. A221, 541.

MILLER, R L, NIELSEN, L E (1961) J Poly. Sci. 55, 643.

MÜLLER, F H, JÄCKEL, K (1952) Koll. Zeit. 129, 145.

NADAI, A (1950) Theory of Flow and Fracture of Solids (McGraw Hill).

NAKAMURA, M, SKINNER, S M (1955) J Poly. Sci. 18, 423.

PETERLIN, A (1966) J Poly. Sci. C, 15, 427.

RIDER, J G, HARGREAVES, E (1969) J Poly. Sci. A2, 7, 829.

ROBERTSON, R E (1963) J App. Poly. Sci. 7, 443.

ROETLING, J A (1965) Polymer 6, 3:1.

ROWE, P W (1962) Proc. Roy. Soc. A269, 500.

SARDAR, D, RADCLIFFE, S V, BAER, E (1968) Poly. Eng. and Sci. 8, 290.

SASABE, H, SAITO, S (1968) J Poly. Sci. A2, 6, 1401.

SCHLEICHER, F (1926) Zeit. and. Math. Mech. 6, 199.

SCHOFIELD, A N, WROTH, C P (1968) Critical State Soil Mechanics (McGraw Hill).

STERNSTEIN, S S, ONGCHIN, L (1969) Pre-print. Am. Chem. Soc. Meeting. New York.

TERZAGHI, K, PECK, R B (1948) Soil Mechanics in Engineering Practice (Chapman and Hall).

THOMPSON, A B, WOODS, D W (1956) Trans. Farad. Soc. 52, 1383.

THORKILDSEN, R L (1964) Engineering Design for Plastics. Editor E Baer. (Rheinhold, NY).

VINCENT, P I (1960) Polymer 1, 7.

WHITNEY, W, ANDREWS, R D (1964) Textile Division Report No TD-123-64, MIT.

WHITNEY, W, ANDREWS, R D (1967) J Poly. Sci. C, 16, 2981.

WILLIAMS, J G (1967) Trans. J Plast. Inst. 35, 505.

APPENDIX 1 THE PLANE STRAIN COMPRESSION TEST

1.1 Introduction

To analyse the deformation of glassy polymers, compression testing in plane strain as developed by Ford and Williams (1964) was chosen as this method has several advantages over the more commonly used uniaxial tensile and compression tests. The behaviour of polymers at large strains is difficult to determine in a uniaxial tensile test because the reduction in area produces necking and hence indeterminate strain conditions, while in uniaxial compression although fracture may be eliminated some barrelling of the specimen is unavoidable and the load bearing area of the specimen will vary throughout the test. The plane strain compression test overcomes these problems to a large extent, and a definable strain system and area under load are produced from which the stress-strain behaviour for large strains may be derived.

1.2 Simple plane strain compression

The specimen in the form of a flat plate with edges parallel to the axes of x, y, and z, is compressed in the x direction between two parallel, flat, highly polished dies as shown schematically in Figure 36. The dies are lubricated to give minimal friction, and the specimen then suffers negligible constraint to elongation in the y direction. The material under the tool is, however, restrained from moving in the z direction by the constrain of the undeformed material on either side of the deformed section. This test has the advantage that the area under load remains constant, and no instability due to reduction in area can occur. It is also possible to obtain ductile behaviour from materials such as polystyrene (PS) and polymethylmethacrylate (PMMA) which normally break in a brittle manner in tension. Stress and strain can be directly derived from simple measurements of load and displacement, and if one thickness of test piece is used material variations are minimised, as the test sections may be taken over a limited area of material.

1.3 Plane strain compression with tension or compression

In any investigation of a yield criterion it is necessary that the material should be subjected to a stress system which allows variation of the principal stress ratios, and in this way sections of the yield locus in stress space can be charted. Therefore the arrangement described above was modified so that small tensile or compressive loads could be applied in the plane of the sheet, in the y direction, as shown in Figure 37. In this way a range of stress ratios $\frac{\sigma 1}{\sigma 2}$ could be achieved.

1.4 The assumption of planar deformation

In practice it is important to be sure that at the yield point the plastically deforming material under the dies is elastically constrained by the undeformed region outside the dies because only if this is true will it be possible to define the stress system. For there to be no movement of material in the z direction, the specimen must ideally be confined between effectively rigid blocks with faces parallel to the planes of flow, and the deminsions of the specimen and forces or displacements applied to it must be independent of the z co-ordinate. This experimental arrangement has been employed by Bridgman (1945). However, the simpler test arrangement described in Appendix 1.2 has been widely used for the plane strain testing of metals in compression, and the assumption that deformation is constrained to be

planar has been carefully justified for these materials by Ford (1948). It was found that, provided the percentage lateral spread was small in comparison with the percentage reduction in thickness, compression of a wide sheet approximated to plane strain deformation with the exception of narrow zones near the ends of the compressed section.

Ford and Williams (1964) have checked this last point using polyethylene sheet, and their tests have been repeated here using PMMA (see Section 2.3.6). In both cases it was found that if the specimen width (w) was greater than four times the die breadth (b), deformation was effectively constrained. Further proof of planar flow in this type of test has been noted from observations of deformed sections of glassy polymers viewed in polarised light which showed a birefringence pattern consistent with constrained flow along the dies except for small regions at the ends of the deformed section. (Private communication - S Raha). If small values of the additional stress σ_2 are applied to a strip where the width (w) is greater than or equal to the length and much greater than the thickness (h_o) then the assumption that the percentage lateral spread is small in comparison with the percentage reduction in thickness will still be true, and approximate planar deformation will be maintained.

1.5 The state of stress

Considering first the case of simple plane strain compression without applied tension or compression. The dies are assumed to be so well lubricated that no shear stresses arise across the die surface, and the applied stress σ_1 will therefore be a principal stress. It is also assumed that there is no strain in the z direction along the dies, and a principal stress σ_3 is therefore necessary to account for the constraint. There will be no stress, σ_2 in the y direction (Green (1951)). Provided the stresses are uniform and the material isotropic, the stresses acting on an elemental cube of material in the deforming section will be as shown in Figure 34 and a biaxial state of stress will exist.

For the case of plane strain compression with applied tension or compression, a third principal stress σ_2 is added, and the stresses acting on an elemental cube will be as shown in Figure 35 and a triaxial state of stress will be produced.

Both of the stresses σ_1 and σ_2 are known from measurements of the applied load and the area of the specimen while the stress σ_3 is unknown. With a knowledge of the relation between stress and strain for the material under test, the principal stress σ_3 can be found in terms of the other two stresses provided it can be assumed that the strain in the z direction (ε_3) is zero. It has been shown for metals, for which well known stress-strain laws exist, that at the yield point $\sigma_3 = v\,\sigma_1$ for simple plane strain (Hill 1950)), and consequently $\sigma_3 = v(\sigma_1 - \sigma_2)$ * for plane strain compression with applied tension. Whether such simple relations between the stresses can be found for polymeric materials is doubtful but it is sufficient to note that σ_3 will be some function of the other two applied stresses, which can therefore be used to give various states of triaxial stress for an investigation of the yield condition.

The principal stresses σ_1, σ_2, and σ_3 form the components of the applied stress tensor which can be split in the usual way into deviatoric and hydrostatic components. Calling tensile stresses positive and compressive stresses negative the stress tensor may be written:-

---

*v is Poisson's ratio, typically 0.3 for metals.

$$\begin{vmatrix} -\sigma_1 & & \\ & \sigma_2 & \\ & & -\sigma_3 \end{vmatrix} = \begin{vmatrix} (\sigma_1 + \sigma_2 - \sigma_3)/3 & & \\ & (-\sigma_1 + \sigma_2 - \sigma_3)/3 & \\ & & (-\sigma_1 + \sigma_2 - \sigma_3)/3 \end{vmatrix} + \begin{vmatrix} -(\sigma_1 + \sigma_2)/3 & & \\ & (\sigma_1 + \sigma_2)/3 & \\ & & 0 \end{vmatrix}$$

A B

$$+ \begin{vmatrix} -(\sigma_1 - \sigma_3)/3 & & \\ & 0 & \\ & & (\sigma_1 - \sigma_3)/3 \end{vmatrix} + \begin{vmatrix} 0 & & \\ & (\sigma_2 + \sigma_3)/3 & \\ & & -(\sigma_2 + \sigma_3)/3 \end{vmatrix}$$

where A is the hydrostatic stress component, and B is a shear stress in the plane defined by σ_1 and σ_2. Both the sign and magnitude of A will depend upon the relative magnitude of σ_1 and σ_2. For example by applying a sufficiently large tensile value of σ_2 a state of hydrostatic tension could be achieved, or on the other hand applying a compressive value of σ_2 a state of hydrostatic compression could be achieved. This test arrangement can therefore be used for studying the effect of the hydrostatic component of stress over a limited range.

1.6 The mode of deformation and test geometry

In the simple analysis of the stress system for plane strain compression mentioned above, it was assumed that the stress and strain were homogeneous throughout the test section. However, it is well known for this kind of double indentation test that the corners of the dies produce singular points in the stress distribution (Nadai (1950)). This leads to definite inhomogeneous distributions of stress and strain as plastic flow begins. This inhomogeneous deformation has been closely investigated by Green (1951) and Hill (1950) and their theoretical predictions have been confirmed for some metals. By considering slip line field theory Green shows that two modes of deformation can occur in this type of test depending upon the ratio of die breadth (b) to the specimen thickness (h) at yield. For $1 < \frac{b}{h} < \sqrt{2}$ the deformation is mainly confined to regions of intense shear radiating from the die edges, while for $\frac{b}{h} > \sqrt{2}$ deformation takes place as a number of independent rigid wedges sliding along a criss-cross of slip lines inclined at 45° to the compression axis. These two possibilities are shown schematically in Figure 42. Using these modes of deformation Green goes on to calculate the increase in pressure on the dies over that for homogeneous compression, and the variation he found is shown in Figure 43.

The material conditions assumed by Green seem unlikely to apply to a polymeric material but in the paper by Ford and Williams (1964) the same form of variation as predicted by Green is shown for polyethylene, although the maxima were shifted along the $\frac{h}{b}$ axis. This shift could occur if they did not use the specimen thickness at yield; but also as they suggest it may be due to the fact that polyethylene work hardens and is therefore unlike the ideal material assumed by Green in his analysis. The agreement between the results of Ford and Williams and the theoretical predictions of Green are nevertheless surprising, and a check for this geometrical effect was made here for PMMA. No significant variation of the yield stress with the ratio $\frac{h}{b}$ was found within the experimental error (Section 2.3). However, it is apparent from Green's analysis that any error in yield stress measurements from this geometrical effect is minimised by using the smallest possible ratio of the specimen thickness to die breadth ($\frac{h}{b}$).

Although no agreement with Green's analysis was found here from the PMMA yield stress data, striking confirmation of his proposed modes of deformation was found.

1.7 Other factors affecting the measurement of stress

Detailed analysis of a set of experimental results with a discussion of the necessary corrections is given in the section on experimental results. For the sake of completeness, however, the factors affecting measurements from the plane strain compression test will be briefly mentioned here.

1.7.1 Friction

Although the dies were well lubricated, it is possible that the friction between the specimen and dies was sufficiently large to exert an appreciable restraint on the specimen. This will lead to an increase in pressure under the central region of the dies. The magnitude of the effect can be estimated, and it can be shown that it is likely to lead to only a small correction.

1.7.2 Shoulder restraint

The region of undeformed specimen just outside the dies will exert a restraining force in opposition to the principal stress σ_1. It has been shown that this restraining force is independent of the die breadth (Williams (1967)) and can be corrected for by making measurements using dies of different breadths.

1.7.3 Nominal and true stress

In Appendix 1.4 it was noted that in narrow zones at the end of the compressed section there is no effective constraint. This leads to flow along the dies within these zones, and a corresponding increase in load bearing area. The magnitude of this effect has been estimated and found to be small at the yield point so that the error in taking σ_1 as a nominal stress (load divided by the area of specimen under load as calculated from the original specimen width w and the die breadth b) instead of a true stress (load divided by the current area of specimen under load), will be small.

The effective area over which the additional stress σ_2 acts will however decrease in proportion to the compressive strain (ε_1). Since the compressive strains ε_1 measured at yield are relatively large (~ 0.13) the true stress value of σ_2 at yield will be noticeably larger than its nominal stress value, and a correction will be necessary to give σ_2 in terms of true stress.

APPENDIX 2 THE APPARATUS

2.1 Requirements for design

The factors controlling the conditions of plane strain in the double indentation test have already been outlined in Appendix 1, and it was these factors which also controlled the dimensions of the compression apparatus. The specimen width had to be greater than four times the die breadth while the die breadth had to be at least twice the specimen thickness. With these limitations in mind, an optimum die breadth of 6.4 mm was chosen together with a specimen width of 38 mm. Other requirements were that the dies had to remain accurately parallel and in line throughout the test while being able to move freely vertically. The surfaces in contract with the specimen had to be highly polished to minimise friction and as flat as possible to ensure uniform stress distribution. Since loads of up to 50 kN could be applied to the compression rig, it was also necessary that the component parts of the rig could withstand these loads with only a negligible amount of distortion. An accurate method of measuring large strains without the complicating effect of machine elasticity was also required.

Within the dimensions of the compression rig and the limitations imposed for plane strain conditions, it was also necessary to construct a tensile rig in order to apply a tensile stress to the specimen whilst under compression. A completely independent loading system was required which would apply a uniform stress to the sheet specimen, and which would allow various values of load to be applied and maintained constant. A simple but effective arrangement to meet these requirements is given in Appendix 2.3.

Later in the project, the apparatus was used in conjunction with a 100 kN Tensometer Type E testing machine but no changes in design were necessary. A refined piece of apparatus for this type of plane strain compression test has been developed by Ford and Williams (1964) in which a sub-press provides the compression, and resistance transducers measure specimen strain. However the apparatus described here is considerably cheaper, and is relatively simple to construct and operate.

2.2 Design of the compression rig

A diagram of the compression rig is shown in Figure 44. The rig was constructed throughout of mild steel, and a set of four interchangeable dies in the range of breadths 2.4 mm - 9.5 mm and of standard width 57.2 mm were made.

To ensure rigidity, the dies were made by machining to size 12.7 mm square mild steel blocks. These were subsequently cyanide hardened to a depth of 0.25 mm so that the polished die faces would be undamaged by small flaws on the specimens. Each pair of dies was made so that the edges were parallel to $\pm$ 0.01 mm and the faces flat and parallel to $\pm$ 0.01 mm. A high polish was given to the die faces using emery papers and diamond powder, and during this polishing the edges of the die were given a small radius, as sharp corners were known to restrict material from flowing perpendicular to the dies (Ford and Williams (1964)).

Each of the dies was rigidly mounted on a 25.4 mm square section block of mild steel. The relative movement of the dies was maintained accurately in line by four carefully machined plates attached to the bottom die block. Ample lubrication ensured minimal friction between the die block and the plate faces. The assembled rig was built so that the top was parallel to the bottom to within $\pm$ 0.05 mm.

In this type of arrangement measurement of specimen strain is relatively simple in that it is only necessary to measure the relative displacement of the top and bottom dies. This was accomplished by rigidly mounting two dial gauges at each end of the top die block such that their stems made contact with small plates attached to the bottom die block. The gauges had a full scale deflection of 1.02 mm and were scaled to read 0.0025 mm. The zero reading of these gauges could be adjusted by means of screws under the contact plates. Since the separation of the dial gauges (approximately 150 mm) was much greater than the width of specimen being compressed (approximately 38.1 mm) any tilt occurring during the compression was magnified. Such tilting of the top die with respect to the bottom could be virtually eliminated by using metal shims between the top of the rig and the compression anvil of the testing machine. Generally a tilt of less than 0.025 mm over a tool section of 38.1 mm was considered acceptable. However, the deflection finally recorded was the mean of the two dial gauge readings, which automatically corrected for any tilt of the dies. Dial gauges are known to be subject to dynamic errors likely in such spring and lever systems but the rates of testing here were generally sufficiently slow for these errors to be small. Figure 45 shows the complete compression rig.

2.3 Design of tensile rig

A tensile stress was applied to the sheet specimen, while under compression, using an independent tensile rig. Tension was provided by means of a small hydraulic ram constructed out of the components of a $1\frac{1}{2}$ ton (15 kN) 'Evershure' hydraulic car jack, and mounted in a stirrup arrangement. The remainder of the car jack was used as an oil reservoir and pumping unit connected to the ram by means of flexible hydraulic hosing. The pressure of the hydraulic fluid in the system was monitored by means of the Budenberg hydraulic pressure gauge, with a full scale deflection of 1200 lb/in^2 (8.3 MN/m^2), and scaled to read in steps of 20 lb/in^2 (0.17 MN/m^2). The pressure of the hydraulic ram was converted into a tension on the specimen by means of the stirrup arrangement shown in Figure 46 and a pair of wide grips in which the specimen was mounted. The grips which fitted close up to the compression dies were of the self-locking type, and pivoted so that any misalignment of the specimen was compensated for as loading proceeded. The dimensions of the grips and stirrup arrangement were such that a standard specimen 102 mm x 38 mm x 1.6 mm was gripped over 32 mm at each end, leaving a section of specimen actually under test approximately 38 mm x 38 mm x 1.6 mm.

The whole of the tensile rig was hung by soft springs from a supporting frame around the compression apparatus. This arrangement was necessary so that small deviations of the specimen from the plane perpendicular to the dies were automatically rectified as the compression dies began to load the specimen. The supporting frame for the tensile loading system was also mounted on levelling screws so that the system could be approximately aligned before loading. A photograph of the complete biaxial loading system is shown in Figure 47. To check that the rig was pulling uniformly, a PMMA specimen of dimensions 38 mm x 38 mm x 1.6 mm was mounted in the tensile rig, and loaded whilst being observed in polarised light. The pattern of birefringence was uniform across the whole width of the specimen showing that with careful mounting a uniform stress distribution could be accomplished.

To load the sheet in compression in the plane of the sheet, the tensile rig was replaced by a similar rig suspended in the same way but this time the pressure of the ram was applied directly to the ends of the specimen, by means of small holders. These specimen holders consisted of mild steel blocks in which an accurately machined slot had been made to take the specimen with a

tight fit. The holders were mounted rigidly in the rig and butted up to within 3 mm of the main compression dies to ensure no buckling of the specimen could occur. This arrangement is shown in Figure 46.

2.4 Correction for rig deflection

Although the compression rig was constructed so that its deflection under load would be small some elastic distortion as well as the usual "settling" of component parts occurred under loading, and it was necessary to correct for this effect. As the dial gauges are mounted to measure the displacement between the top and bottom dies only, any deflection of the testing machine or load cell during loading is not involved in the gauge readings.

The rig was set up for compression in the usual way (see Section 2.1) with the usual amount of lubricant but no specimen was included. Figure 48 shows the resulting plot of rig deflection, as recorded by the dial gauges, against the applied load. The rapid initial rise of rig deflection was due to the lubricant being squeezed out, and to settling of the components. At higher loads a linear relation between deflection and load was seen due to the elastic distortion of the rig. The curve in Figure 48 together with similar curves taken at intervals during the period of this project were used to correct the dial gauge readings for rig deflection.

2.5 Calibration of the hydraulic ram in the tensile rig

The force exerted by the small hydraulic ram in the tensile rig was measured experimentally from the pressure of the fluid in the pumping system, and it was necessary to relate the reading of the pressure gauge to the load applied to the specimen. This calibration was achieved by mounting the ram between the crosshead and load cell of the Instron testing machine, and thereby measuring the load on the ram for a given pressure.

Keeping the crosshead stationary, the pressure in the ram was slowly increased, and readings of pressure were taken against load recorded by the Instron. Corresponding load readings were taken while slowly releasing the pressure. The results of these tests are shown in Figure 49 and although it is apparent that some sticking in the ram has occurred, the error due to sticking was within the error of reading ($\pm$ 34 kN/m^2) and a useful linear relation between pressure and load is obtained. It was also noted during these tests that any creep in load recorded by the Instron load cell was reflected by a corresponding creep in the reading of the pressure gauge. These experiments indicated that the hydraulic ram was a sufficiently sensitive and accurate means of loading.

APPENDIX 3 FRICTION BETWEEN THE DIES AND THE SPECIMEN DURING COMPRESSION

In Sections 2.3.6.2 and 2.3.7 expressions were given for the increase in pressure under the dies due to the effect of surface friction between the specimen and the dies. The derivation of these expressions is given here in terms of the pressure dependent yield criteria described earlier.

3.1 Plane strain compression

In Figure 50 the forces acting on an element of material between the dies of thickness dx at a distance x from the centre line, are shown. The pressure on the element is σ_y and ϕ_s is the coefficient of surface friction between the specimen and the die surfaces.

Resolving horizontally $2\phi_s \sigma_y dx = h\, d\sigma_x$ (39)

According to pressure dependent Tresca's yield criterion, yield will occur when

$$(\sigma_y - \sigma_x) = 2\left[k_o + \mu \frac{(\sigma_x + \sigma_y + \sigma_z)}{3}\right]$$

and for plane strain $\sigma_z = \frac{1}{2}(\sigma_x + \sigma_y)$

$$\therefore (\sigma_y - \sigma_x) = 2k_o + \mu(\sigma_x + \sigma_y) \quad (40)$$

Pressure dependent von Mises yield criterion written as

$$(\sigma_y - \sigma_x)^2 + (\sigma_x - \sigma_z)^2 + (\sigma_z - \sigma_y)^2 = 6\left[k_o + \mu \frac{(\sigma_x + \sigma_y + \sigma_z)}{3}\right]^2$$

also gives equation (40) for plane strain conditions.

Differentiating equation (40)

$$(1 - \mu)\, d\sigma_y = (1 + \mu)\, d\sigma_x$$

and in equation (39) we have

$$2\phi_s \sigma_y dx = \frac{(1 - \mu)}{(1 + \mu)} d\sigma_y h$$

Using the condition that when $x = \frac{b}{2}$, $\sigma_x = 0$ and $\sigma_y = \frac{2k_o}{(1 - \mu)}$

we have

$$\sigma_y = \frac{2k_o}{(1 - \mu)} \exp \frac{2\phi_s}{h} \frac{(1 + \mu)}{(1 - \mu)} x$$

Integrating over the surface of the die, we find the mean pressure acting:

$$\frac{b}{2} \frac{}{p} = \frac{2k_o}{(1 - \mu)} \int_0^{b/2} \exp \frac{2\phi_s}{h} \frac{(1 + \mu)}{(1 - \mu)} x \; dx$$

$$\therefore \quad \bar{p} = \frac{2k_o h}{b\phi_s (1+\mu)} \left[\exp \frac{b\phi_s}{h} \frac{(1+\mu)}{(1-\mu)} - 1 \right]$$

$$\text{or} \quad \bar{p} \doteq \frac{2k_o}{(1-\mu)} \left[1 + \frac{b\phi_s}{2h} \frac{(1+\mu)}{(1-\mu)} \right] \quad \text{assuming } \phi_s \text{ is small}$$

which is the expression used in Section 2.3.6.2.

3.2 Uniaxial compression

In Figure 51 the forces acting on an elemental cylinder of height h and thickness dr are shown. In cylindrical co-ordinates, a pressure p acts on the ends of the cylinder such that $T_{zr} = \phi_s p$ where ϕ_s is the coefficient of surface friction. The stress σ_z is assumed constant throughout h and σ_θ is set equal to σ_r.

For equilibrium we have $h \frac{d\sigma_r}{dr} - 2\phi_s p = 0$ (41)

According to pressure dependent Tresca's yield criterion, yield will occur when

$$(\sigma_z - \sigma_r) = 2 \left[k_o - \mu \frac{(\sigma_z + \sigma_r + \sigma_\theta)}{3} \right]$$

or when

$$(p + \sigma_r) = 2 \left[k_o - \frac{\mu}{3} (2\sigma_r - p) \right]$$

$$\therefore \quad p(3 - 2\mu) + \sigma_r (3 + 4\mu) = 6k_o \qquad (42)$$

According to pressure dependent von Mises yield criterion, yield will occur when

$$(\sigma_r - \sigma_\theta)^2 + (\sigma_\theta - \sigma_z)^2 + (\sigma_z - \sigma_r)^2 + 6 T^2_{rz} = 6 \left[k_o - \frac{(\sigma_\theta + \sigma_r + \sigma_z)}{3} \right]^2$$

For small friction T^2_{rz} is negligible, and therefore

$$(\sigma_r + p)^2 + (p + \sigma_r)^2 = 6 \left[k_o - \frac{\mu}{3} (2\sigma_r - p) \right]^2$$

$$\text{or} \quad p(3 - \sqrt{3}\mu) + \sigma_r (3 + 2\sqrt{3}\mu) = 3\sqrt{3} k_o \qquad (43)$$

Differentiating (42) and (43), we have

Tresca $\frac{d\sigma_r}{dr} = -\frac{dp}{dr}\frac{(3-2\mu)}{(3+4\mu)}$ $\therefore$ in (41) $\frac{dp}{dr} = -\frac{2\phi_s}{h}\, p\, \frac{(3+4\mu)}{(3-2\mu)}$

von Mises $\frac{d\sigma_r}{dr} = -\frac{dp}{dr}\frac{(3-\sqrt{3}\mu)}{(3+2\sqrt{3}\mu)}$ $\therefore$ in (41) $\frac{dp}{dr} = -\frac{2\phi_s}{h}\, p\, \frac{(3+2\sqrt{3}\mu)}{(3-\sqrt{3}\mu)}$

These last two equations can be integrated with respect to r

so that

Tresca $p = \frac{6k_o}{(3-2\mu)} \exp\left[\frac{2\phi_s}{h}\frac{(3+4\mu)}{(3-2\mu)}(a-r)\right]$

von Mises $p = \frac{3\sqrt{3}\,k_o}{(3-\sqrt{3}\mu)} \exp\left[\frac{2\phi_s}{h}\frac{(3+2\sqrt{3}\mu)}{(3-\sqrt{3}\mu)}(a-r)\right]$

where a is the radius of the cylinder.

The mean pressure on the dies is therefore

$$\bar{p} = \int_0^a \frac{2\pi r\, p\, dr}{\pi a^2}$$

which gives

Tresca $\bar{p} = \frac{6k_o}{(3-2\mu)}\left[1 + \frac{2\phi_s}{3}\frac{(3+4\mu)}{(3-2\mu)}\frac{a}{h}\right]$ (44)

Von Mises $\bar{p} = \frac{3\sqrt{3}\,k_o}{(3-\sqrt{3}\mu)}\left[1 + \frac{2\phi_s}{3}\frac{(3+2\sqrt{3}\mu)}{(3-\sqrt{3}\mu)}\frac{a}{h}\right]$ (45)

In Section 2.3.7 these equations are represented by:-

$$\bar{p} = \sigma\,(1 + \phi_s \frac{a}{h}\, m)$$

where σ and m are constants found in Equations (44) and (45).

APPENDIX 4 DEFORMATION BANDS IN AMORPHOUS POLYSTYRENE AND THEIR RELATION TO THE SLIP LINE FIELD

Polystyrene deformed in plane strain compression shows inhomogeneous plastic shear deformation in the form of intense shear deformation bands. These bands are distinct from craze marks and must not be confused with the latter. Crazes occur in a direction perpendicular to the principal tensile stress, while the deformation bands are nearly parallel to the planes of maximum shear stress (see Section 2.3.).

A general theory, known as the slip line field theory, has been developed to analyse deformation in metals. The theory assumes a rigid, perfectly plastic, isotropic solid, with no strain hardening and no time or strain rate effects. It considers the loci of the directions of maximum shear stress and shear strain rate in the material to form two orthogonal families of curves known as slip lines. These lines not only provide a theoretical indication of the manner in which the material deforms but also through the plasticity equations and Hencky's relations (Hill (1950)) can be used to give good approximations to loads required to produce plastic deformation. No direct observation of slip line fields in deforming metals can be made but a proposed slip line field can be verified by comparing experimental and theoretical deformation loads, and by observing the form of the elastic-plastic boundaries within the deformed material.

Since the slip lines are loci of directions of maximum shear stress, and the deformation bands in polystyrene are approximately parallel to planes of maximum shear stress, the bands will give some indication of the shape of a slip line field.

Samples of unoriented compression moulded polystyrene sheet were compressed in plane strain at room temperature between polished dies. Two types of test were carried out and in each case the material was compressed just to the yield point. Sections cut from the centre of the deformed specimens were studied in transmitted light.

4.1 Plane strain lubricated compression (compression between smooth" parallel dies)

In this case the dies were well lubricated so that it could be assumed that the die-specimen interface was unable to support any shear stress. The theoretical slip line field consists of two sets of lines intersecting orthogonally and inclined at 45° to the compression axis. For comparison Figure 14 shows the deformation bands, viewed in polarised light, in a section of a polystyrene specimen deformed between lubricated dies. Although the shearing of one band by another causes some distortion, the bands in the centre of the specimen are straight and inclined at approximately 45° to the compression axis. The two sets of bands intersecting approximately orthogonally clearly show the slip line field described above.

In order to apply slip line field theory, the experimentally observed deviation of the bands from the direction of maximum shear stress will be neglected. For the above simple slip line field for compression between smooth parallel dies the pressure under the die is 2k at yield, where k is the shear yield stress of the material. The experimentally measured pressure to produce yield in the specimen shown in Figure 14 was 106 ± 5 N/mm^2 at an approximate strain rate of 0.0014 sec^{-1}. Hence the constant k is 53.4 N/mm^2.

4.2 Plane strain unlubricated compression (compression between "rough" parallel dies)

The dies and specimen were cleaned free of grease so that for theoretical

analysis the dies could be assumed to be so rough that the greatest possible frictional stress, namely the yield stress in shear, was induced at the die specimen interface in the regions where yield occurred. The slip line field solution for these conditions as developed by Hill (1950) is shown in Figure 52 for a ratio of die width to specimen height of 5.0 which was the ratio used experimentally. Because the die-specimen interface is ideally rough, slip lines of one family meet the surface tangentially while lines of the other family meet the surface normally. The undeformed regions are shaded in the figure.

Figure 53 shows a section of a polystyrene specimen, deformed under the unlubricated conditions described above, viewed in white light. Although heavy cracking has occurred the deformation bands are clearly visible. It is apparent that there are regions of undeformed material both outside the dies and at the centre of the specimen consistent with the slip line field solution. It can also be seen that the deformation bands show the curvatures suggested for the slip lines in Figure 52 and the orthogonal sets of bands meet the surfaces approximately normally and tangentially. The deviation of the band angle by about 10° from the ideal slip line field solution at the surface indicates that there has been a small amount of slippage and that the interface was not ideally rough.

Using the slip line field in Figure 52 the theoretical mean pressure under the dies is 4.08 k. The constant k has been determined from Appendix 4.1. Hence the predicted mean pressure is 217 N/mm^2. Experimentally the pressure required to produce yield in the specimen shown in Figure 53 was 226 ± 15 N/mm^2 at an approximate strain rate of 0.003 sec^{-1}.

This agreement is surprising in the light of the assumptions made about the material in order to construct the slip line fields, and in the deviations of the experimentally observed directions of the slip lines from the theoretically predicted ones. The fact that the unlubricated dies are not ideally rough should lead to a yield stress below the predicted one. However, there is evidence that the shear yield stress of a number of polymeric materials, including polystyrene, increases with applied pressure (see Sections 2.3, 3.1, and 3.2) and this effect may be leading to fortuitously good agreement. Nevertheless deformation bands in polystyrene when approximated to planes of maximum shear stress give a useful qualitative verification of the postulated slip line field.

TABLE 1

MODULUS, YIELD STRESS AND YIELD STRAIN FOR ALL POLYMERS EXAMINED

MATERIAL	MODULUS		YIELD STRESS		YIELD STRAIN
	kN/mm^2	STRAIN RATE SEC^{-1}	N/mm^2	STRAIN RATE SEC^{-1}	
PMMA	3.5 ± 0.3	0.20×10^{-3}	143.0 ± 2.1	2.12×10^{-3}	0.133 ± 0.015
PS	3.2 ± 0.3	0.16×10^{-3}	107.4 ± 1.9	1.49×10^{-3}	0.058 ± 0.015
PVC	4.4 ± 0.3	0.12×10^{-3}	93.3 ± 1.8	2.02×10^{-3}	0.047 ± 0.015
EPOXY D	2.4 ± 0.2	0.23×10^{-3}	100.6 ± 1.3	2.35×10^{-3}	0.068 ± 0.015
PET	1.4 ± 0.2	0.52×10^{-3}	64.3 ± 0.9	5.05×10^{-3}	0.068 ± 0.020
HDPE	1.0 ± 0.2	0.37×10^{-3}	41.3 ± 0.7	2.30×10^{-3}	0.016 ± 0.020
LDPE	0.12 ± 0.03	0.95×10^{-3}	10.3 ± 0.5	1.53×10^{-3}	0.012 ± 0.020

TABLE 2

SHEAR ZONE ANGLES FOR ALL POLYMERS EXAMINED

MATERIAL	$\alpha\,^{o}$ MEASURED	α'^{o} CORRECTED
PMMA	37.1 ± 2.1	44 ± 2
PS	37.3 ± 0.7	42 ± 1
PET	42.0 ± 1.5	47 ± 2
PVC	41.2 ± 1.9	46 ± 2
EPOXY D	39.6 ± 1.5	44 ± 2

TABLE 3

EQUATION OF PLANE STRAIN COMPRESSIVE STRESS AGAINST APPLIED TENSION CURVES FOR ALL POLYMERS EXAMINED

MATERIAL	EQUATION OF THE BEST STRAIGHT LINE IN σ_1 VS σ_2 DIAGRAM IN N/mm^2 ($\sigma_2 = b - a\sigma_1$)	STRAIN RATE SEC^{-1}
PMMA	$\sigma_2 = 73.8\ (\pm 0.98) - 0.619\ (\pm 0.011)\ \sigma_1$	2.13×10^{-3}
PS	$\sigma_2 = 62.1\ (\pm 6.2\ ) - 0.593\ (\pm 0.064)\ \sigma_1$	1.38×10^{-3}
PVC	$\sigma_2 = 73.4\ (\pm 2.3\ ) - 0.787\ (\pm 0.028)\ \sigma_1$	2.02×10^{-3}
EPOXY D	$\sigma_2 = 65.7\ (\pm 2.7\ ) - 0.652\ (\pm 0.035)\ \sigma_1$	2.22×10^{-3}
PET	$\sigma_2 = 51.6\ (\pm 1.8\ ) - 0.775\ (\pm 0.041)\ \sigma_1$	4.80×10^{-3}
HDPE	$\sigma_2 = 29.2\ (\pm 0.7\ ) - 0.711\ (\pm 0.024)\ \sigma_1$	2.30×10^{-3}
LDPE	$\sigma_2 = 8.0\ (\pm 0.2\ ) - 0.853\ (\pm 0.036)\ \sigma_1$	1.57×10^{-3}

TABLE 4

EQUATION OF PLANE STRAIN COMPRESSIVE STRESS AGAINST APPLIED COMPRESSION CURVES FOR PMMA AND PS

MATERIAL	EQUATION OF THE BEST STRAIGHT LINE IN σ_1 VS σ_2 DIAGRAM IN N/mm^2 ($\sigma_2 = b - a\sigma_1$)	STRAIN RATE SEC^{-1}
PMMA	$\sigma_2 = 98.6\ (\pm 3.3) - 0.637\ (\pm 0.019)\ \sigma_1$	2.34×10^{3}
PS	$\sigma_2 = 62.3\ (\pm 2.0) - 0.580\ (\pm 0.015)\ \sigma_1$	1.57×10^{3}

TABLE 5

VARIATION OF THE COEFFICIENT OF INTERNAL FRICTION AND THE COHESION WITH CRYSTALLINITY FOR PET

CRYSTALLINITY % ($\pm$ 4)	μ	k_o /Nmm^{-2}
AMORPHOUS	0.127 $\pm$ 0.026	29.0 $\pm$ 1.9
12	0.077 $\pm$ 0.027	31.2 $\pm$ 1.6
21	0.139 $\pm$ 0.012	34.8 $\pm$ 0.9
27	0.187 $\pm$ 0.042	37.6 $\pm$ 3.8
31	0.228 $\pm$ 0.022	41.1 $\pm$ 2.6

TABLE 6

VARIATION OF THE COEFFICIENT OF INTERNAL FRICTION AND THE COHESION WITH PLASTICISER CONTENT FOR THE TWO EPOXY RESINS

MATERIAL	k_o /Nmm^{-2}	μ
(C) 20 parts by weight plasticiser	46.3 $\pm$ 4.3	0.121 $\pm$ 0.025
(L) 40 parts by weight plasticiser	40.1 $\pm$ 1.8	0.210 $\pm$ 0.034

TABLE 7

COHESION, COEFFICIENT OF INTERNAL FRICTION AND RATIO OF VOLUME STRAIN TO SHEAR STRAIN FOR ALL POLYMERS EXAMINED

MATERIAL	THE COHESION k_o /Nmm^{-2}	THE COEFFICIENT OF INTERNAL FRICTION μ	THE RATIO OF VOLUME STRAIN TO SHEAR STRAIN c	$\frac{2k_BTx}{V_a} = (\mu - c)$
PMMA	46.2 $\pm$ 1.1	0.225 $\pm$ 0.008	0.035	0.190
PS	38.8 $\pm$ 3.3	0.256 $\pm$ 0.050	0.123	0.133
PVC	41.1 $\pm$ 1.5	0.119 $\pm$ 0.015	0	0.119
EPOXY D	40.1 $\pm$ 1.8	0.210 $\pm$ 0.025	0.035	0.175
PET	29.0 $\pm$ 1.9	0.127 $\pm$ 0.026	0	0.127
LDPE	4.3 $\pm$ 0.3	0.079 $\pm$ 0.021	NO RESULT	
HDPE	17.1 $\pm$ 0.6	0.169 $\pm$ 0.016	NO RESULT	

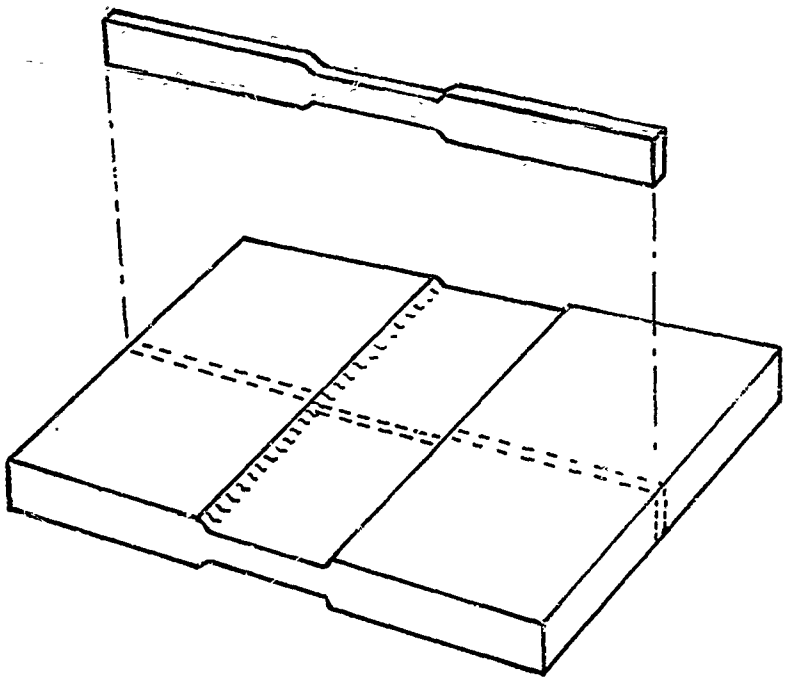

FIGURE 1. Diagram showing the position of a section cut from a deformed specimen in order to observe the mode of deformation.

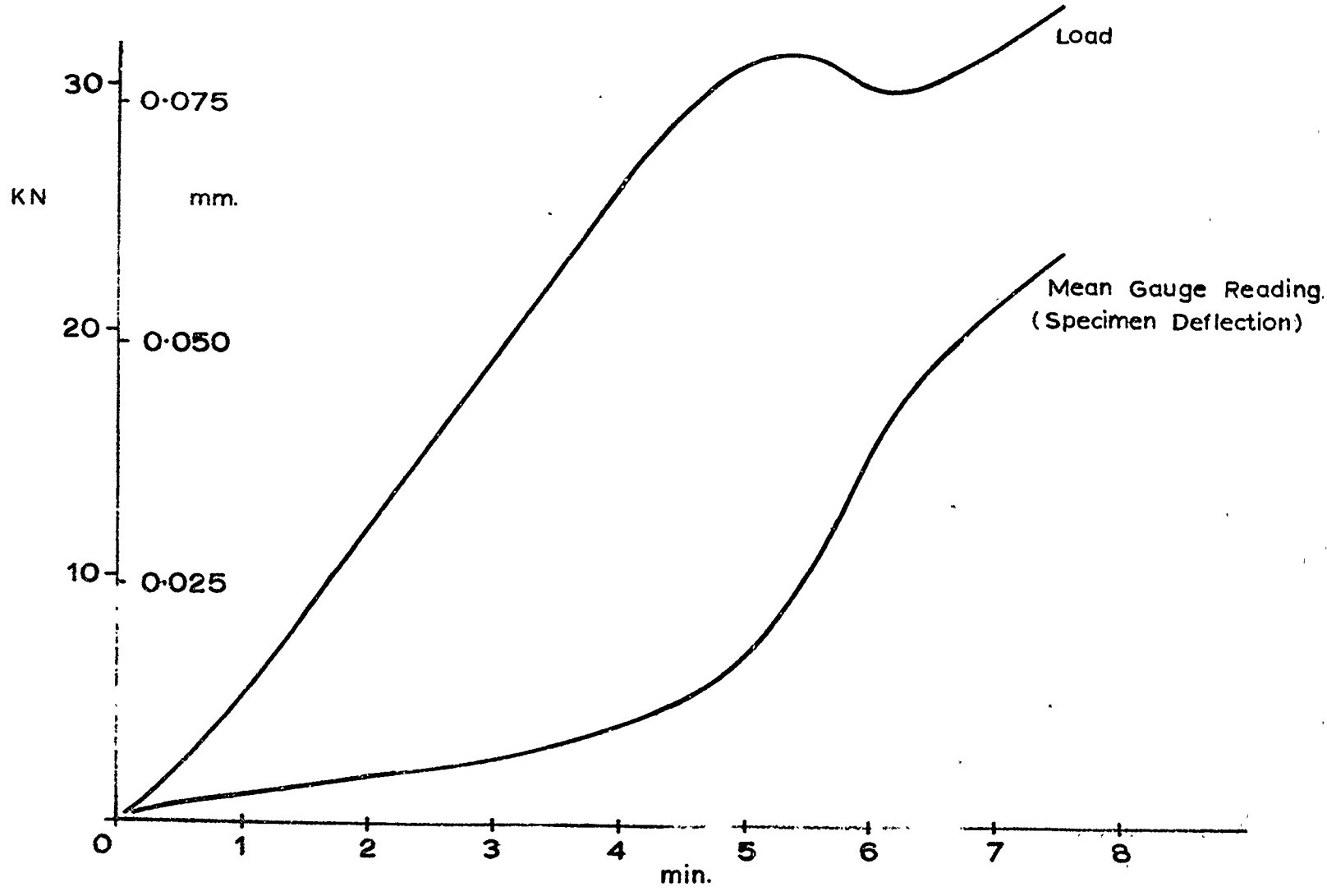

FIGURE 2. Variation of load, and mean dial gauge reading (specimen deflection) with time, for a P.M.M.A. specimen. (Compressed between 6.4 mm dies at room temperature, and at a constant crosshead speed of 0.2 mm/min).

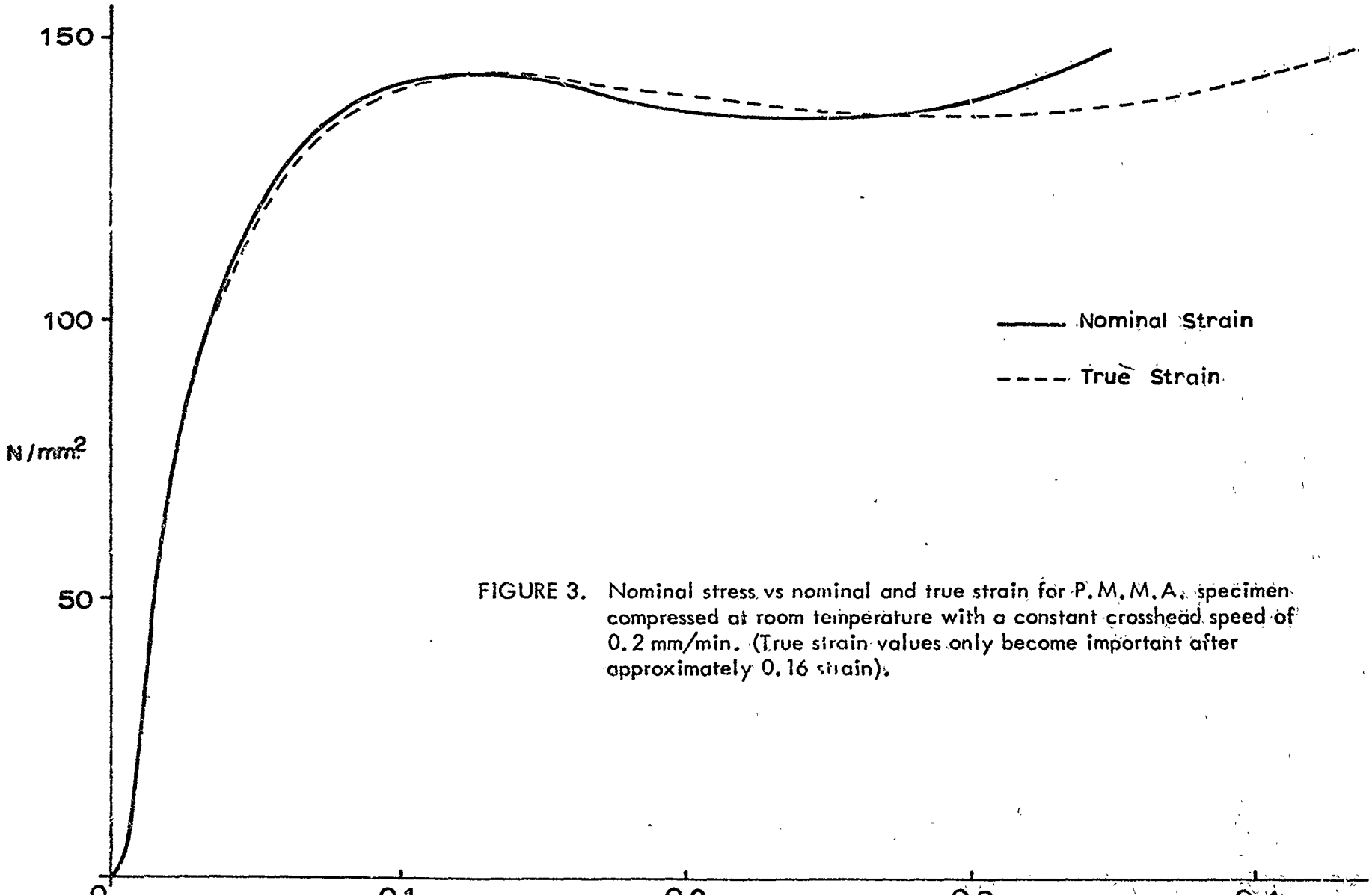

FIGURE 3. Nominal stress vs nominal and true strain for P.M.M.A. specimen compressed at room temperature with a constant crosshead speed of 0.2 mm/min. (True strain values only become important after approximately 0.16 strain).

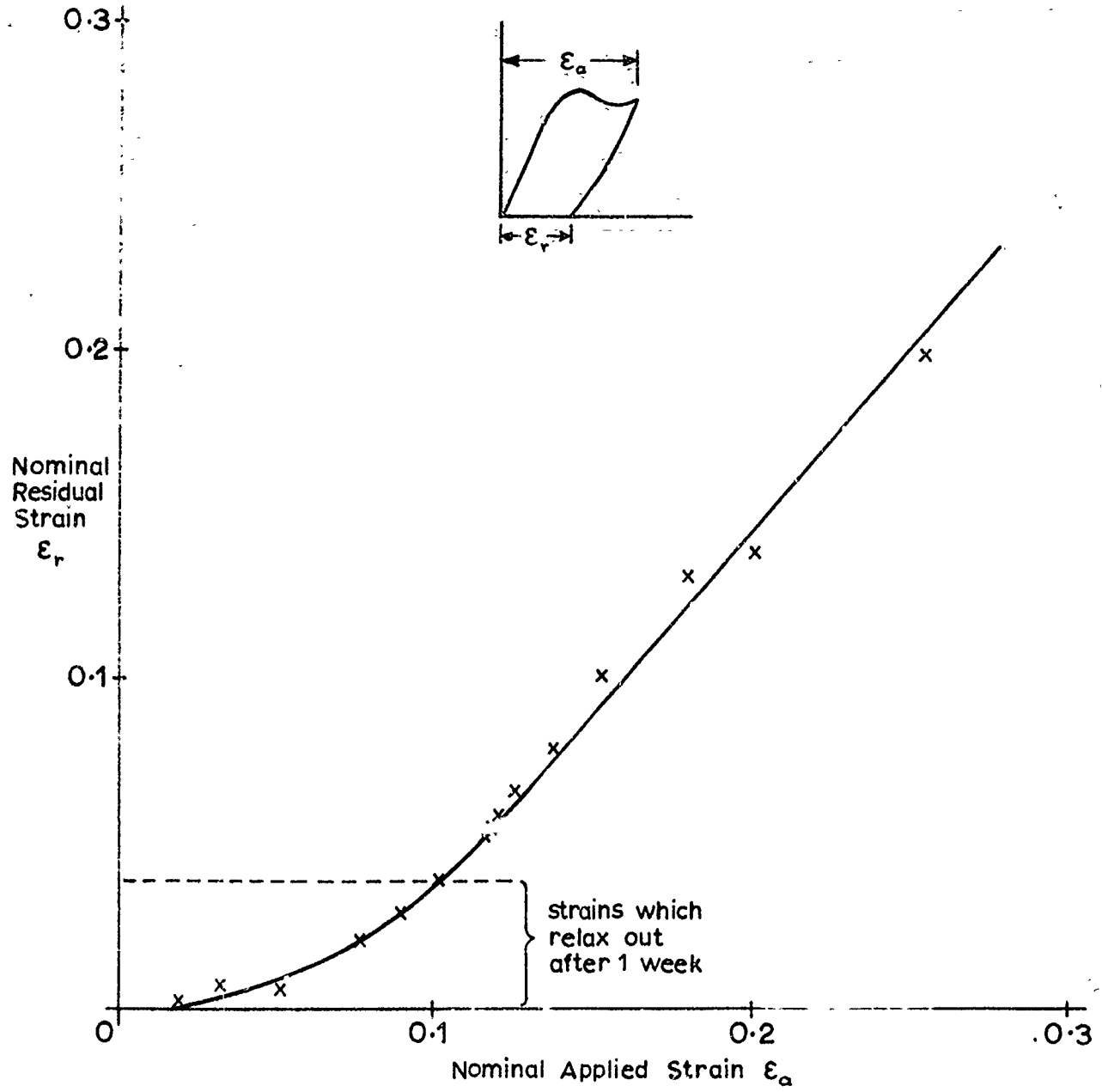

FIGURE 4. Residual strain measured immediately after unloading, against the applied strain. (P.M.M.A. specimens compressed at room temperature using 6.4 mm dies and constant crosshead speed of 0.2 mm/min. After 1 week at room temperature approximately 0.039 residual strain had relaxed out.)

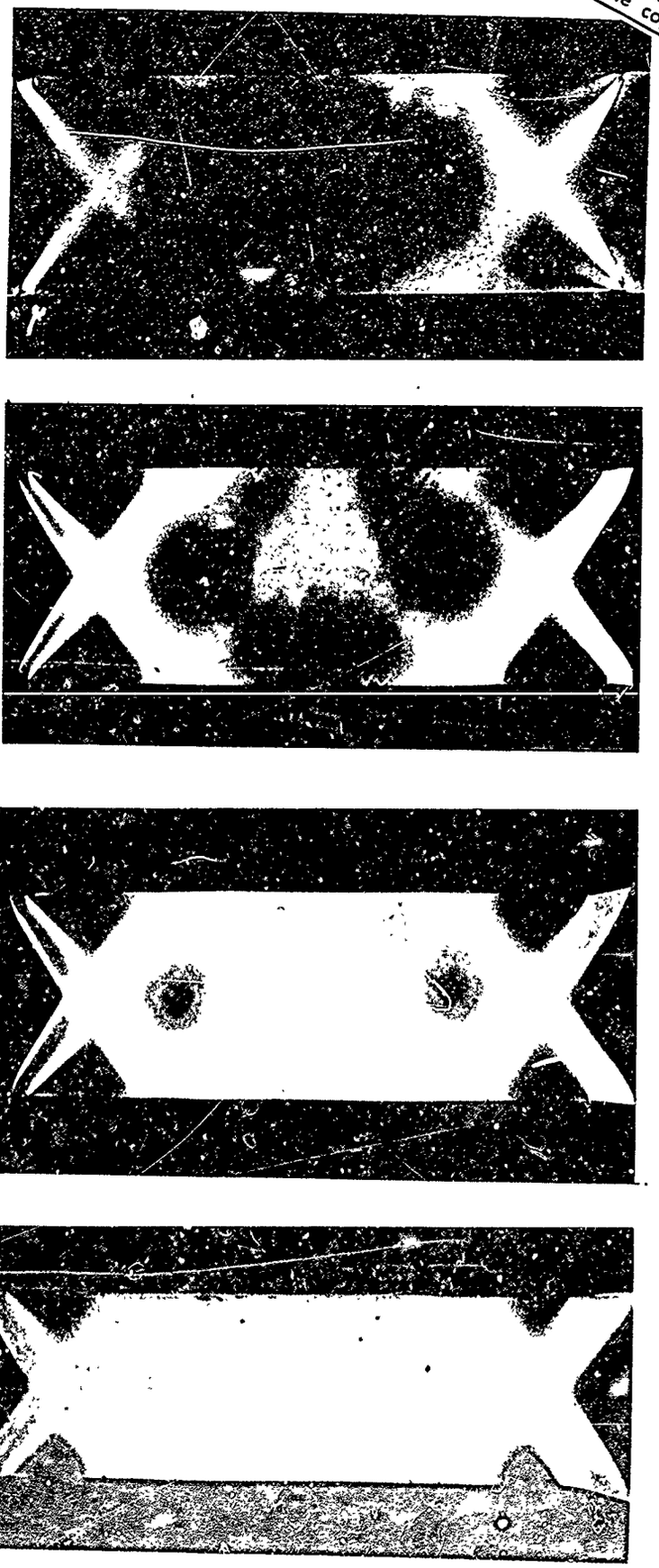

0.109 strain

0.119 strain

0.144 strain

0.219 strain

FIGURE 5. Sections of PMMA specimens taken to increasing compressive strains, viewed between crossed polars. The strains quoted are nominal strains and relate to the stress-strain curve in Figure 3.

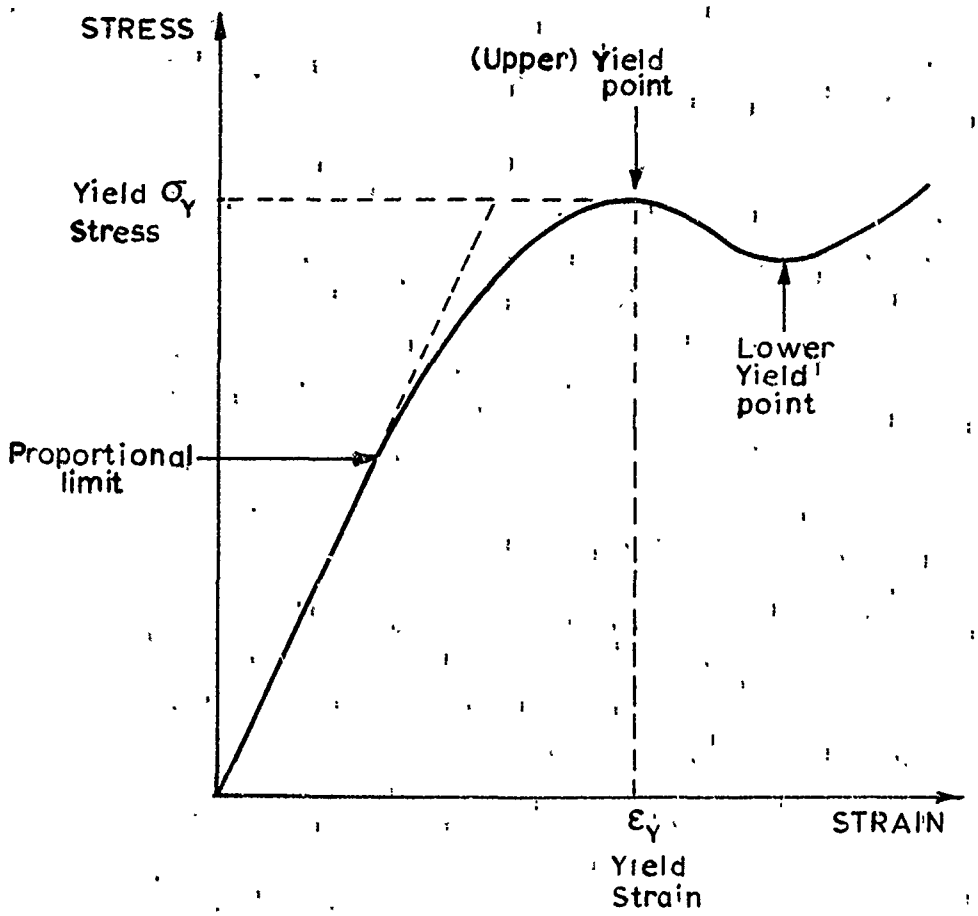

FIGURE 6. Schematic stress-strain curve defining terms used in the text.

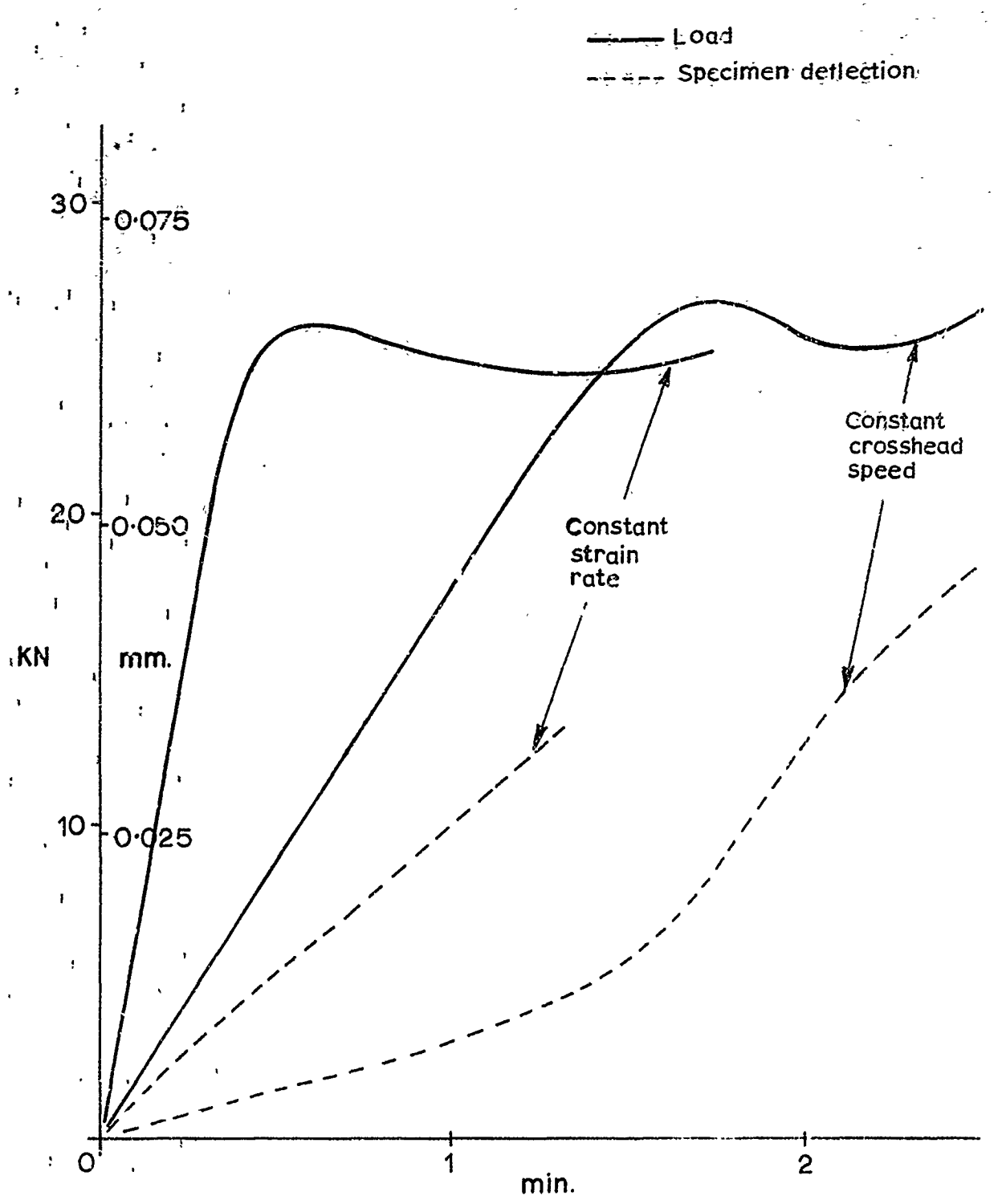

FIGURE 7. Load and specimen deflection against time for constant strain rate and constant crosshead speed tests
(Specimen deflection rate and crosshead speed 0.27 mm/min. In the constant crosshead speed test, the specimen deflection rate at the yield point was close to 0.27 mm/min).

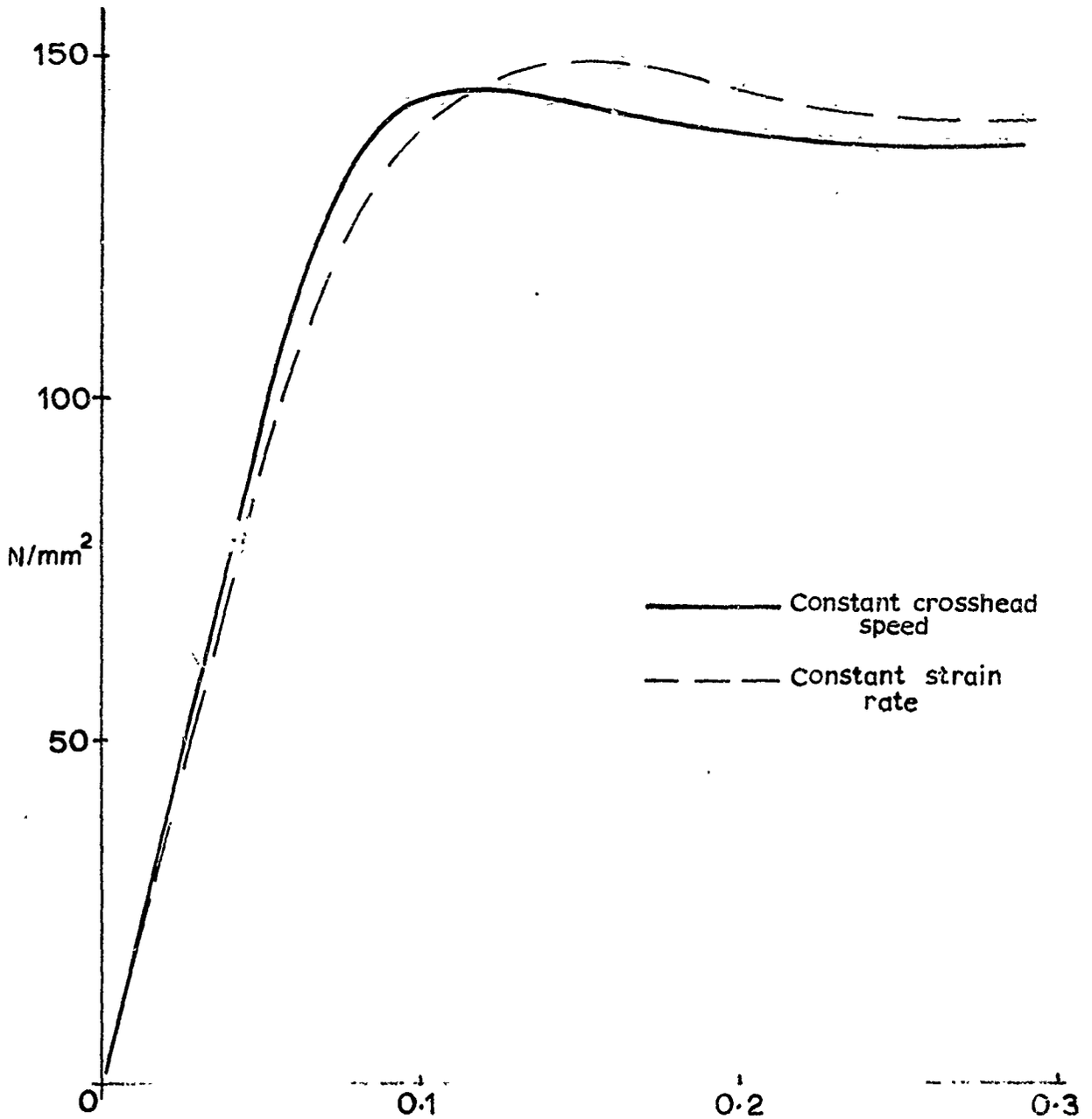

FIGURE 8. Nominal stress-nominal strain for P.M.M.A. at constant crosshead speed and constant strain rate. (Curves, derived from figure 7, illustrate that strain rate behaviour prior to yield does not significantly affect the yield stress).

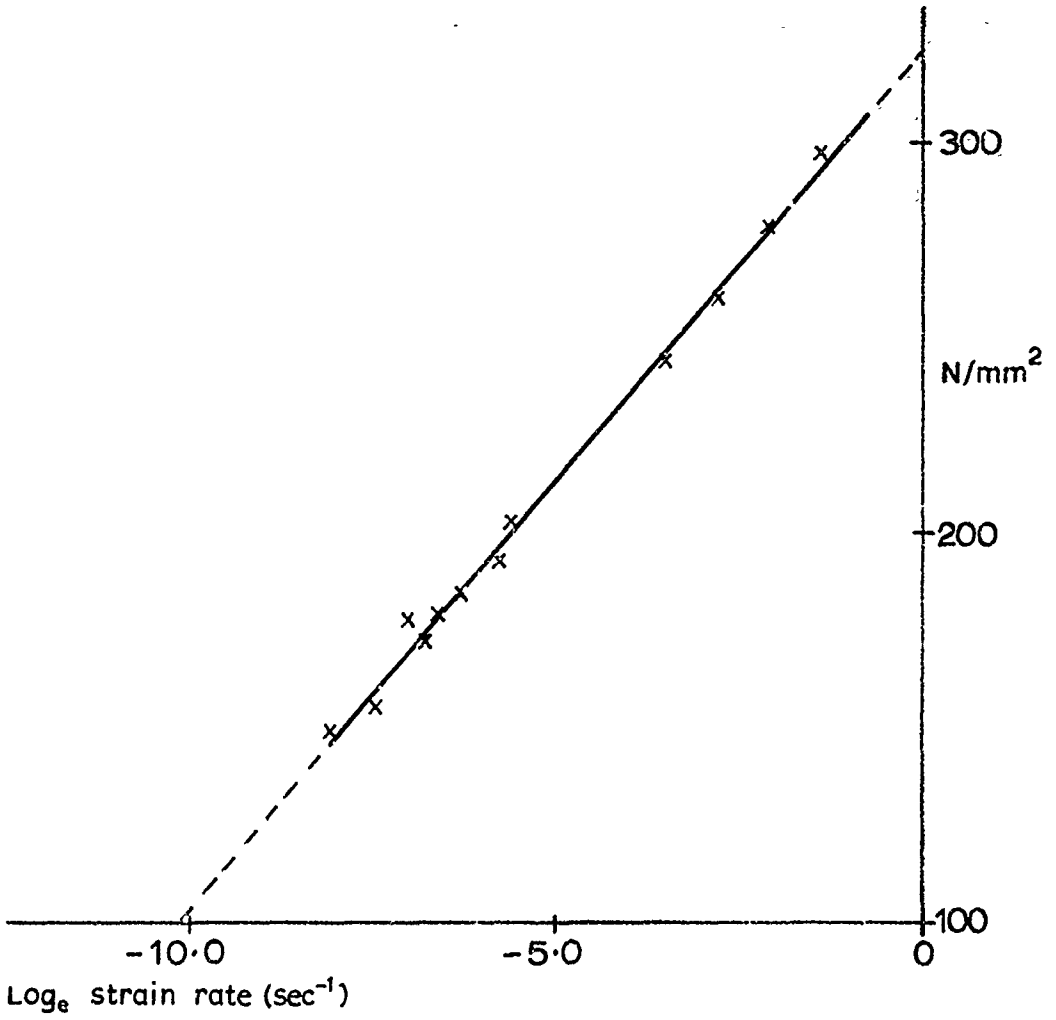

FIGURE 9. Variation of plane strain compressive yield stress of P.M.M.A. with strain rate as calculated from the crosshead speed. (Specimens compressed at constant crosshead speed using 6.4 mm dies at room temperature).

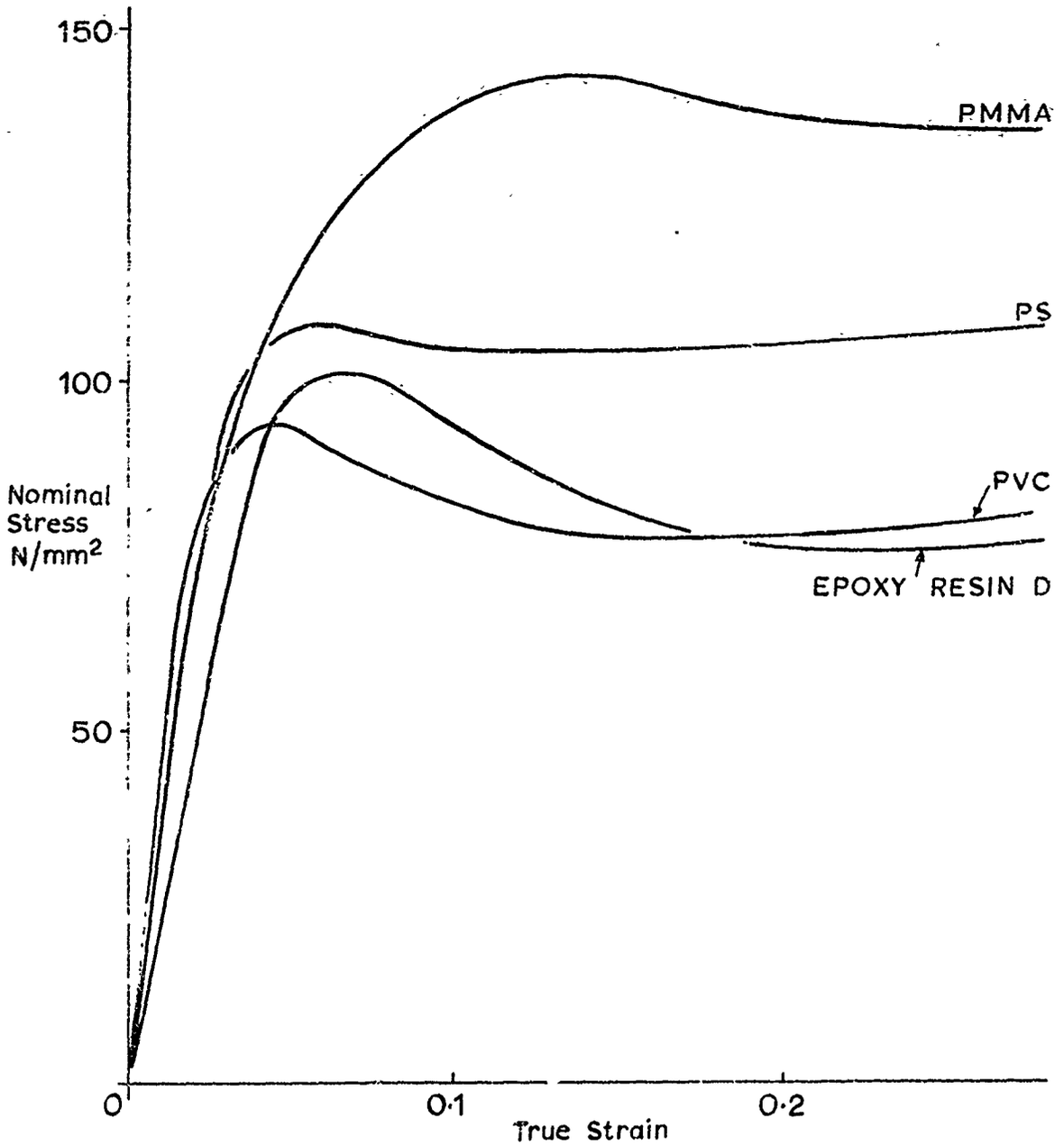

FIGURE 10. Stress-strain curves determined in plane strain compression for four glassy polymers. (A load drop is seen with each material and the yield point is defined as the maximum stress point. Materials compressed between 6.4 mm dies at room temperature, and at crosshead speed of 0.2 mm/min).

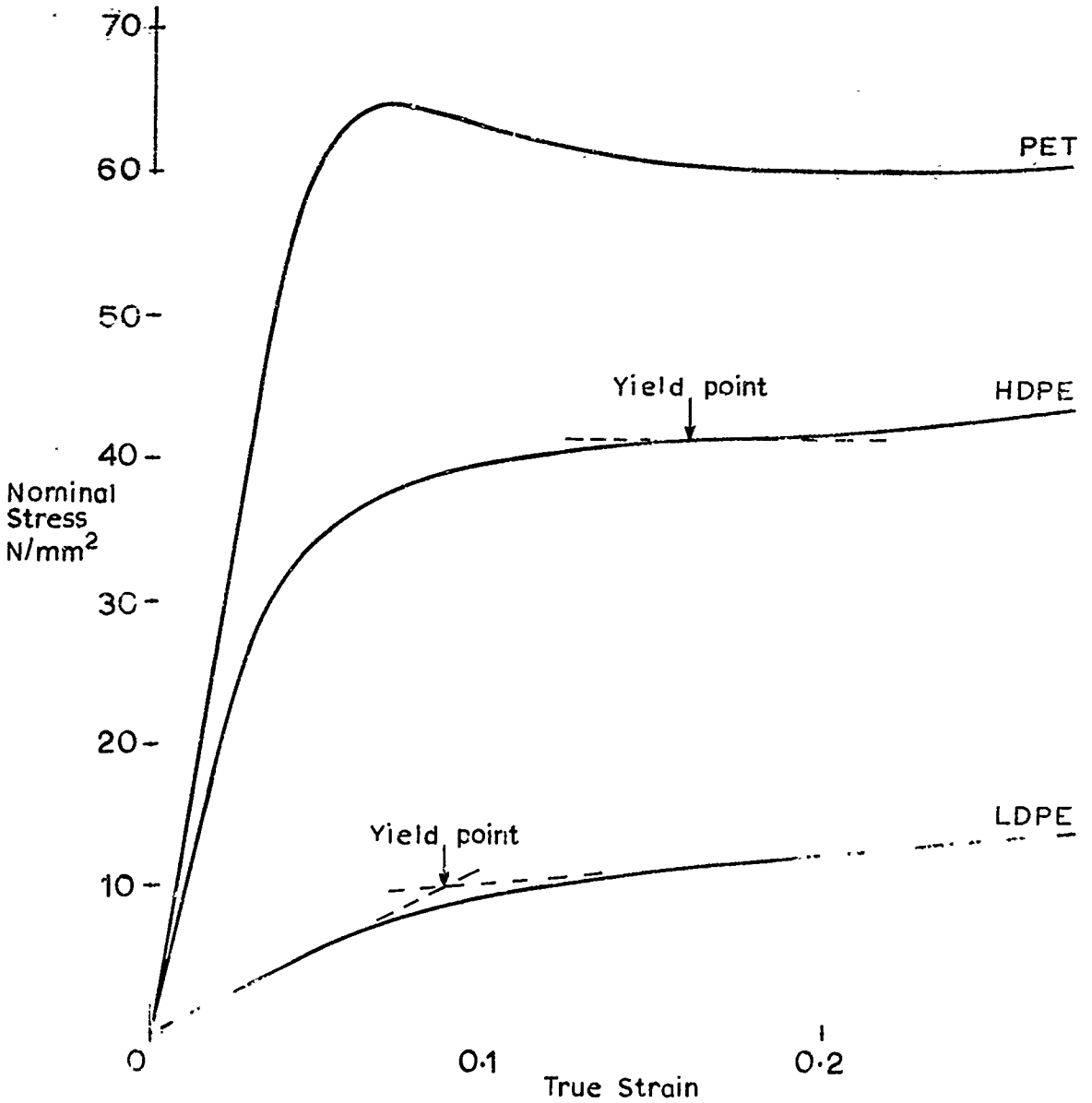

FIGURE 11. Stress-strain curves determined in plane strain compression for the polyethylenes and P.E.T. (Yield point taken as indicated for L.D.P.E. and H.D.P.E., while for P.E.T. the yield point is as before at the maximum stress point).

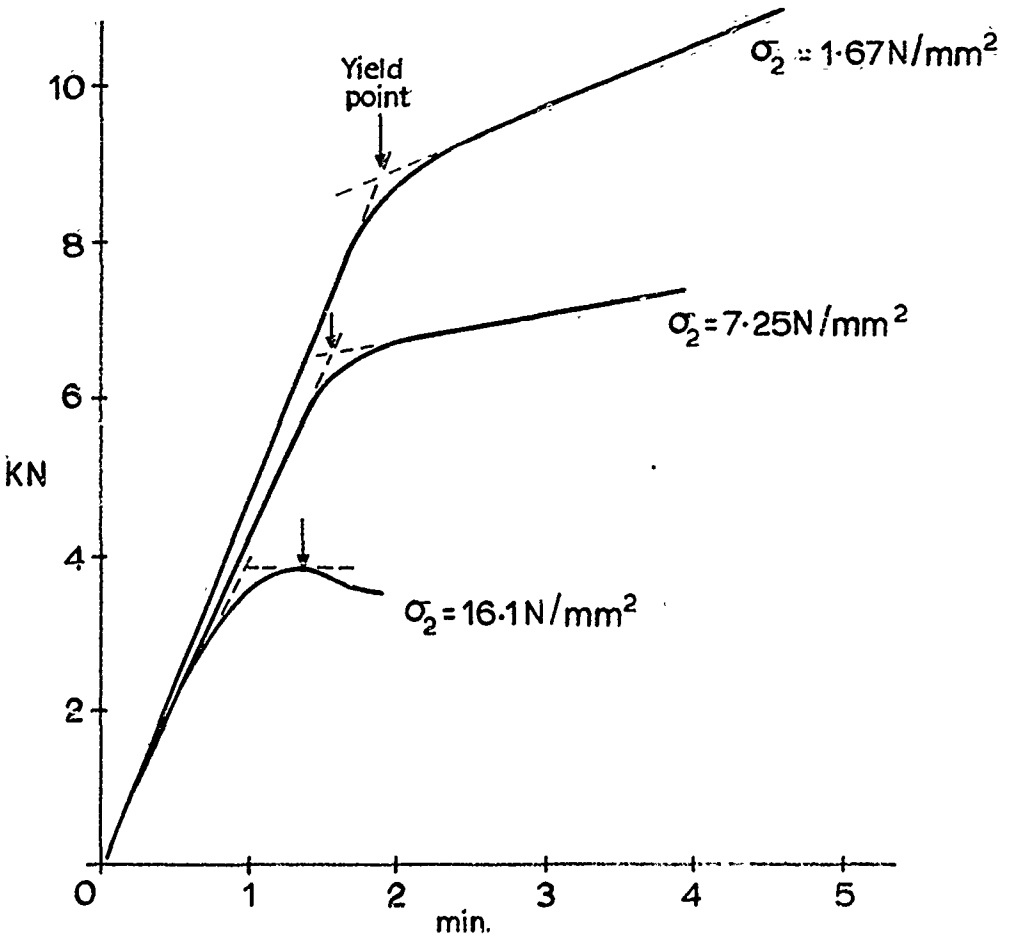

FIGURE 12. Curves of load against time, as produced by the Instron or Tensometer, for plane strain compression of H.D.P.E. with various values of additional tension σ_2. (Specimens compressed at room temperature using 6.4 mm dies and constant crosshead speed of 0.2 mm/min. NB at higher tensions a load drop is produced giving the yield point as the maximum load as for the glassy polymers).

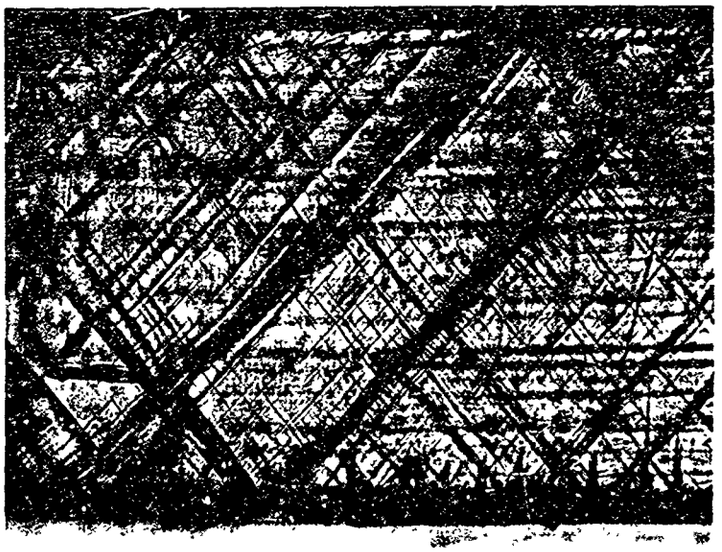

FIGURE 13. PMMA

1 mm

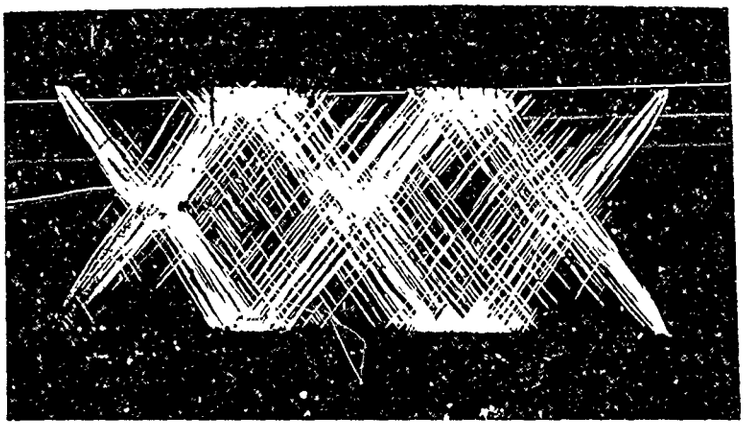

FIGURE 14. PS

1 mm

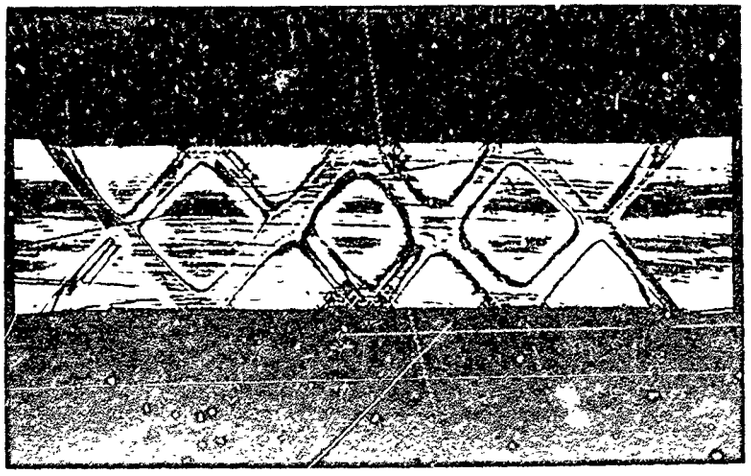

FIGURE 15. PVC

1 mm

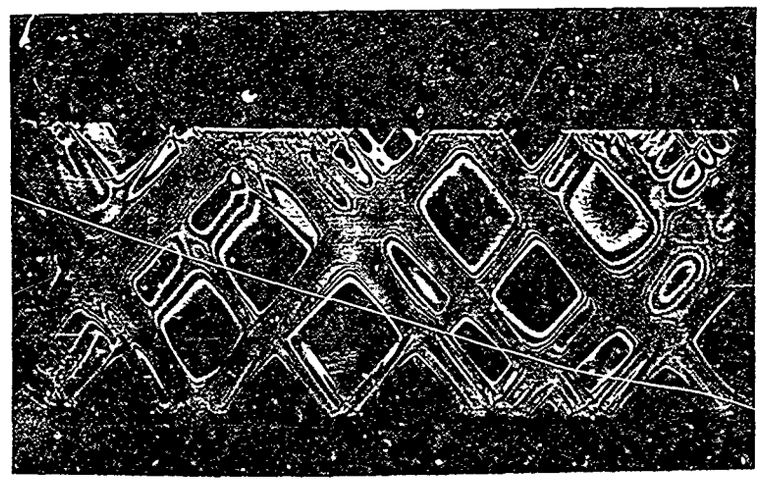

FIGURE 16. Epoxy Resin D

1 mm

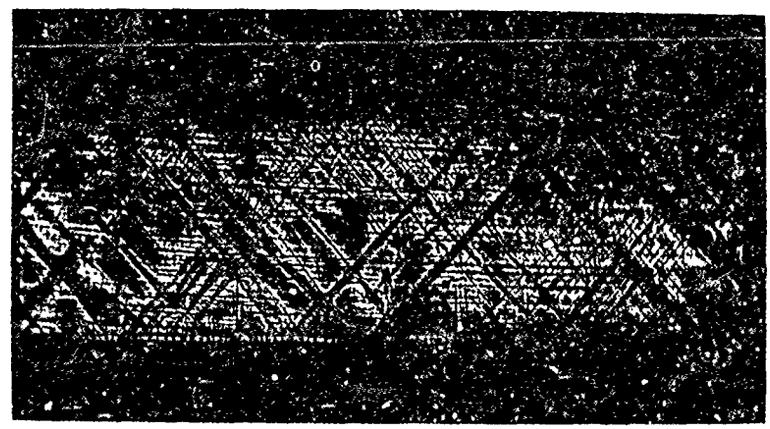

FIGURE 17. PET

1 mm

FIGURES 13-17. Sections viewed in plane polarised white light from specimens taken just to the yield point using 6.4 mm dies.

In the text the regions of yielded material such as those shown by PMMA are called shear zones, and the much narrower plastic regions shown by PS and PET are called shear or deformation bands.

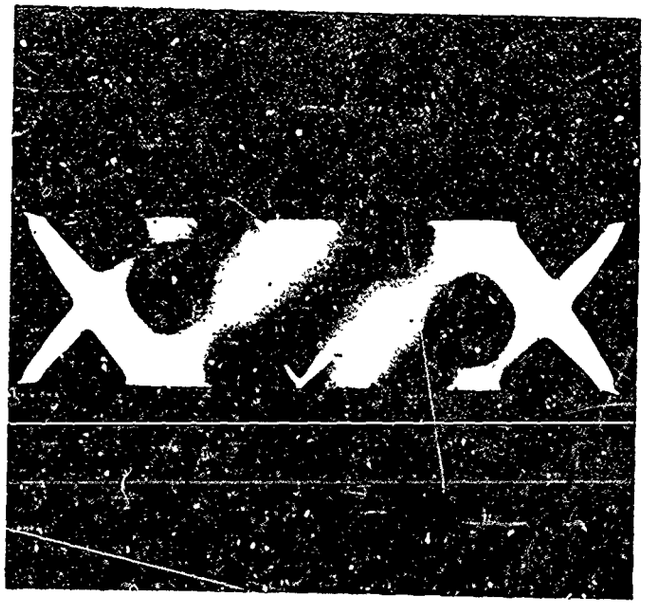

100 um

FIGURE 18. Englarged section of PET specimen showing two types of deformation with narrow deformation bands a few micrometres wide, and broader shear zones.

The large shear strains contained in these zones can be seen where they have cut the smaller deformation bands.

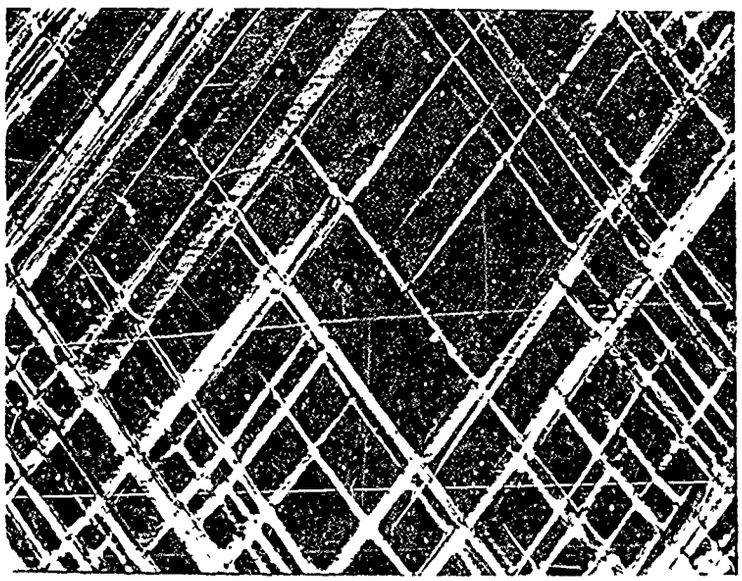

200 um

FIGURE 19. Englarged section of PS specimen viewed between crossed polars.

Some bands appear to be slightly blurred due to the thickness of the section used. However, the narrow well defined nature of these bands can be seen, which appear to propagate without distortion of the surrounding material.

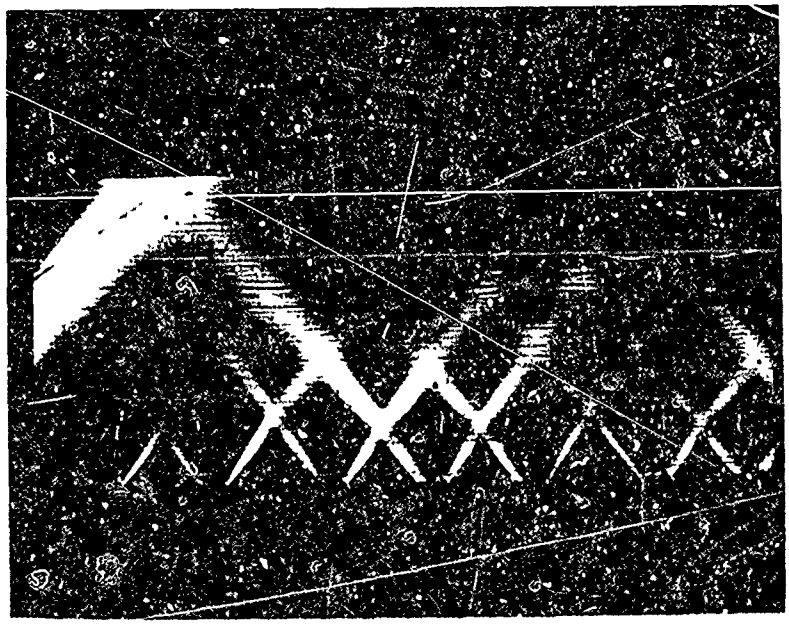

FIGURE 20. Section of PMMA specimen, viewed in polarised light, for which a number of fine scratches on one surface have localised the deformation into narrower shear zones.

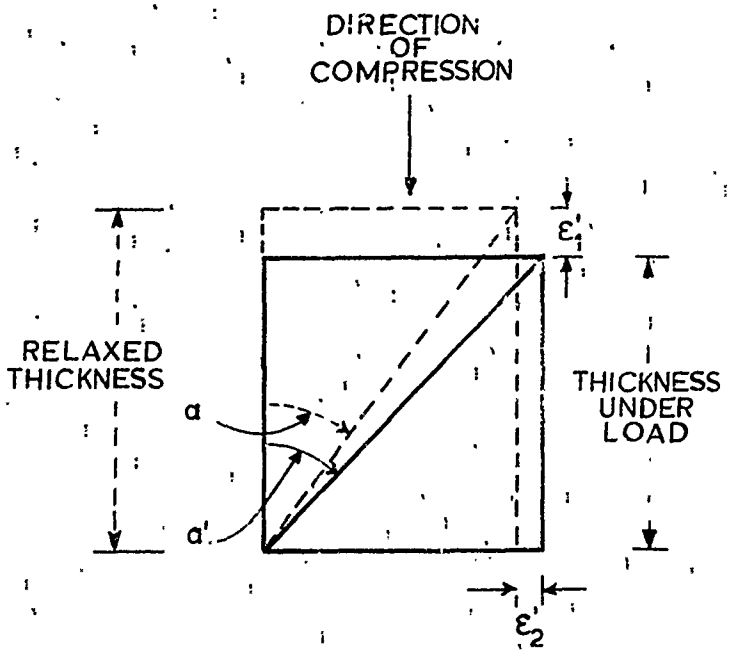

FIGURE 21. Diagram to show the effect of relaxation on the shear zone angle.

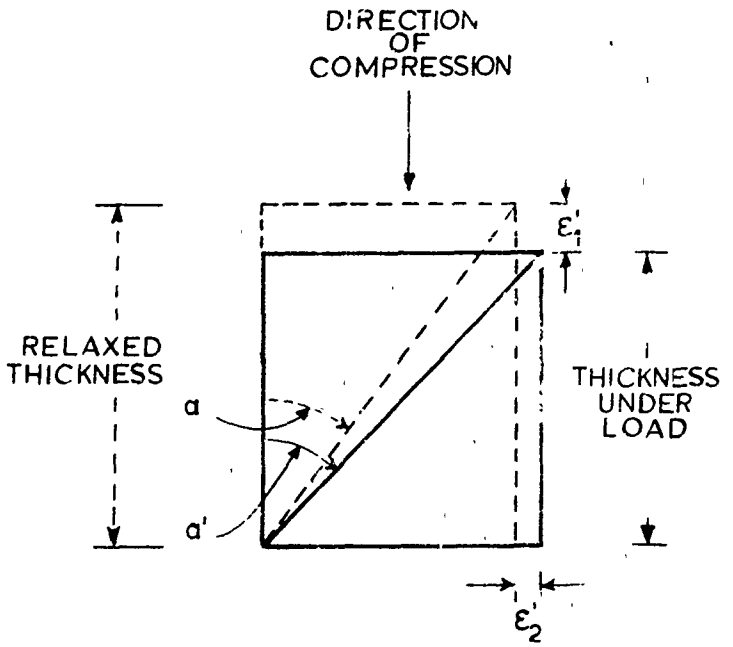

FIGURE 21. Diagram to show the effect of relaxation on the shear zone angle.

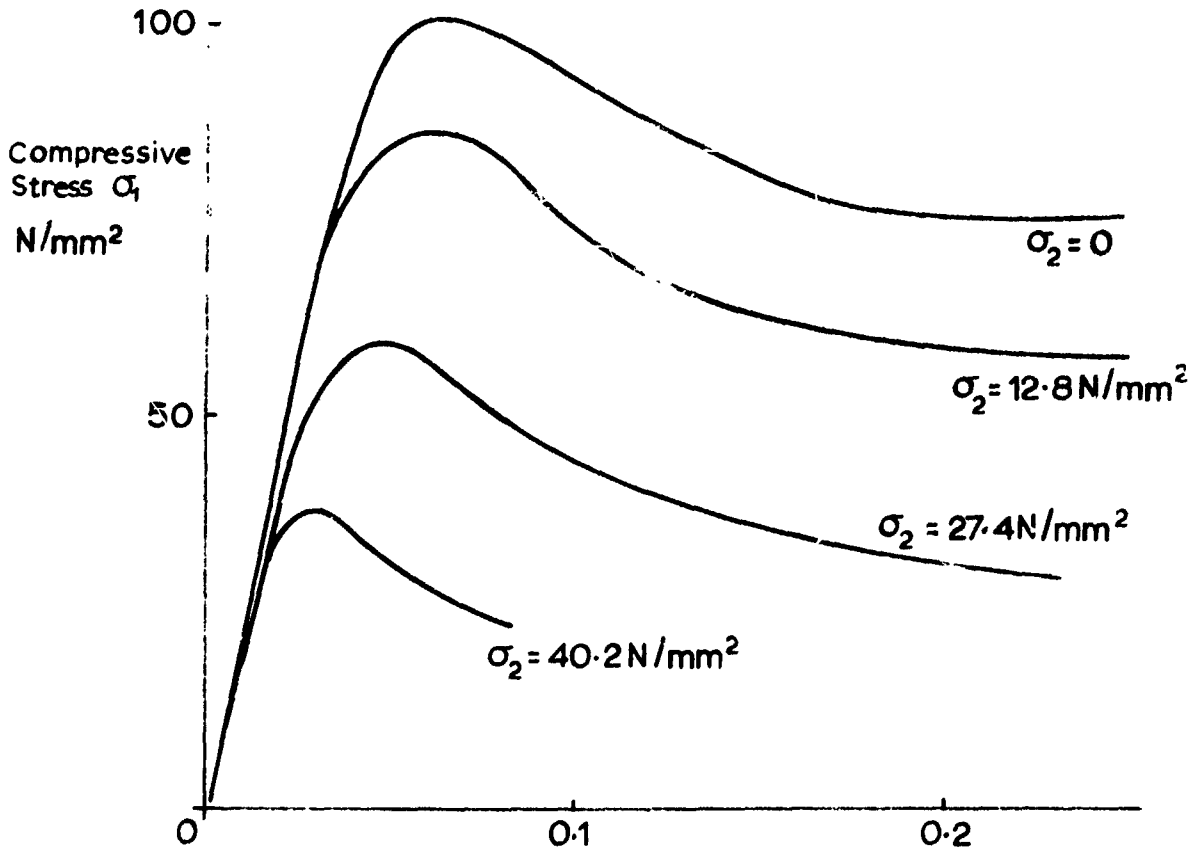

FIGURE 22. Stress-strain curves for Epoxy Resin D measured in plane strain compression for various values of additional tension σ_2. (Curves obtained at room temperature using 6.4 mm dies and constant crosshead speed of 0.2 mm/min).

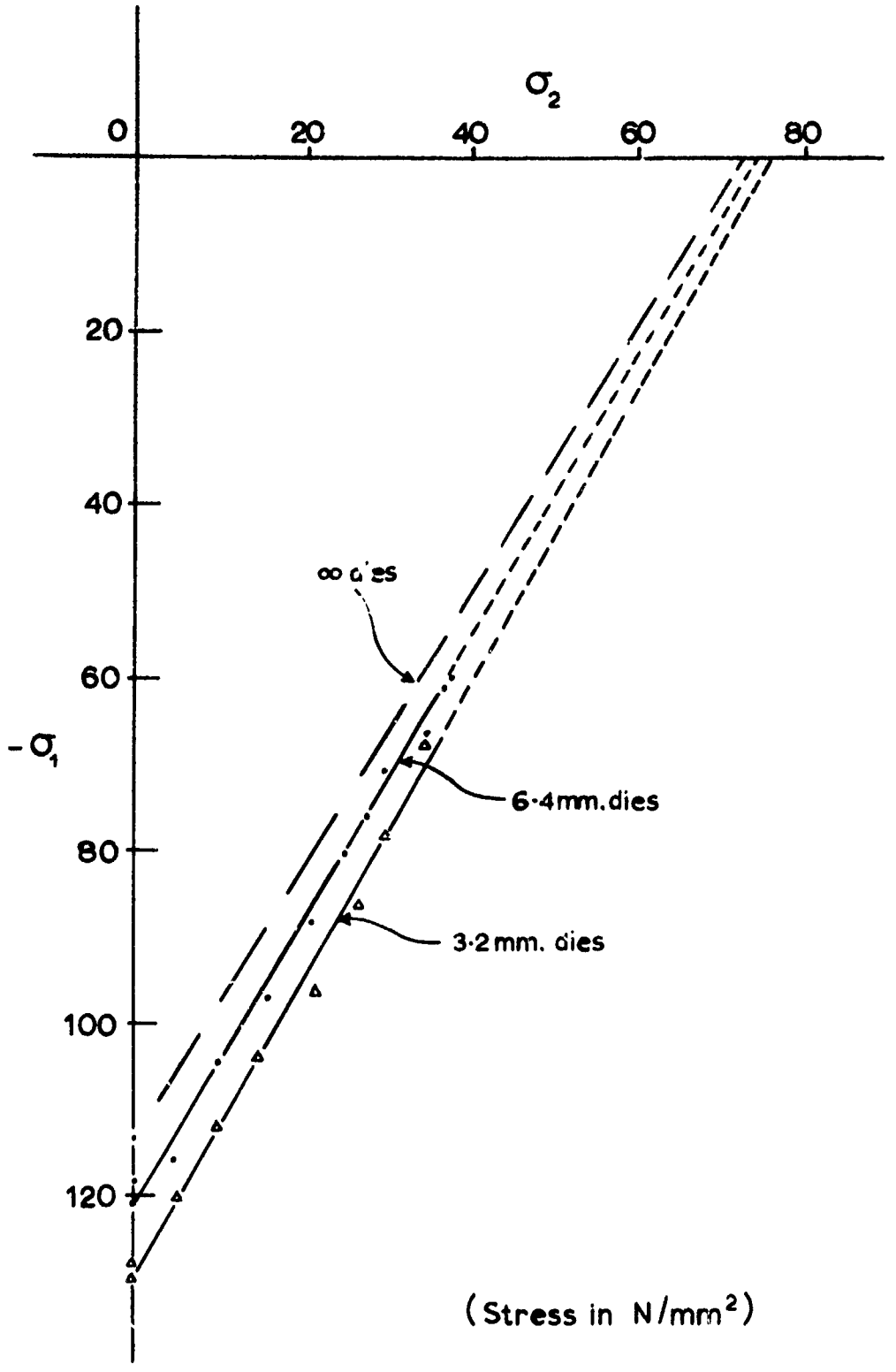

FIGURE 23. Variation of the plane strain compressive yield stress ($-\sigma_1$) with additional tension ($+\sigma_2$) for P.M.M.A. using 6.4 mm and 3.2 mm dies at room temperature and constant crosshead speed of 0.2 mm/min. (The line corrected for shoulder restraint (∞ dies) is also shown).

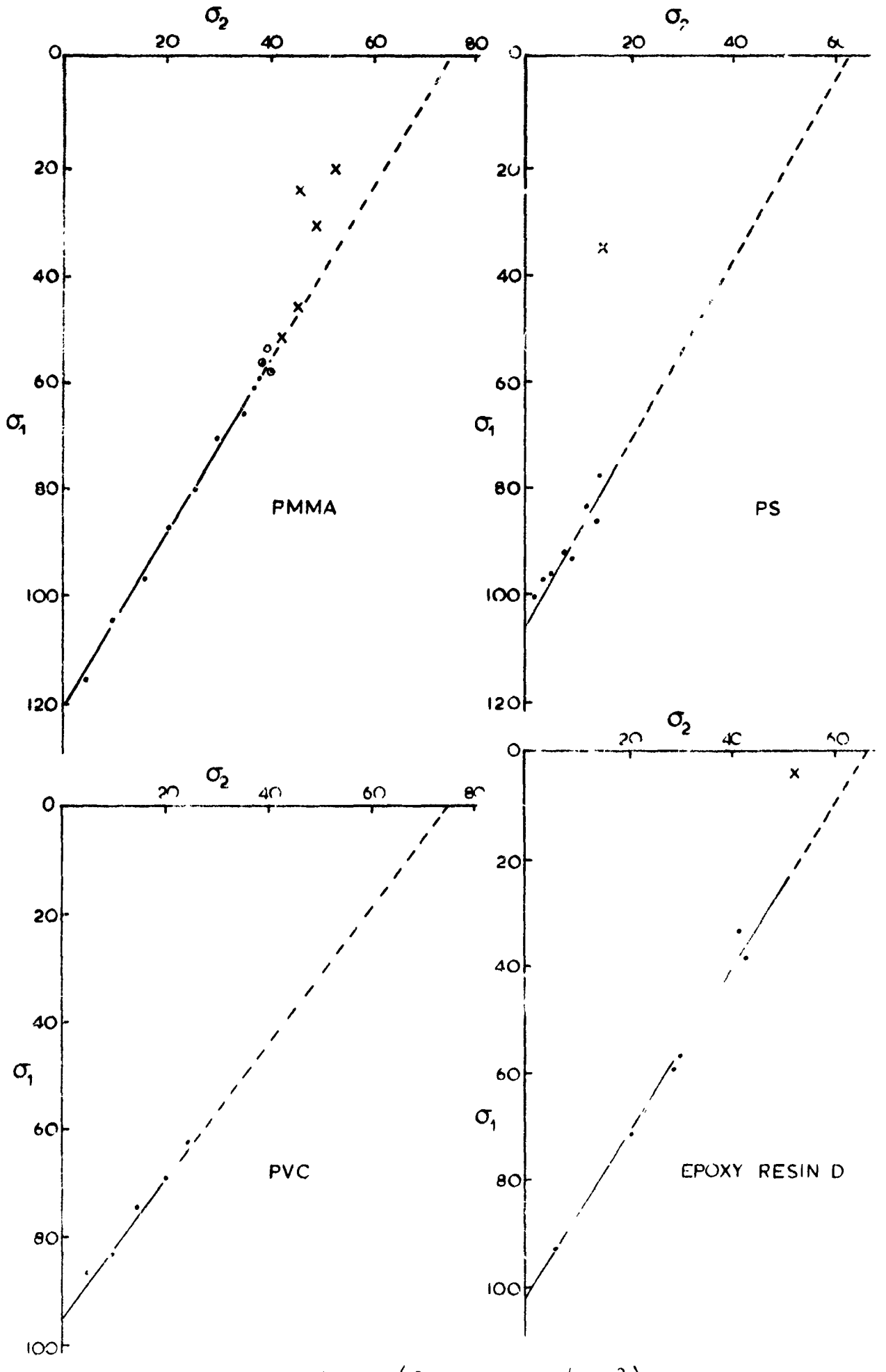

FIGURE 24. Variation of plane strain compressive yield stress σ_1, with applied tension σ_2. (See also Figure 25)

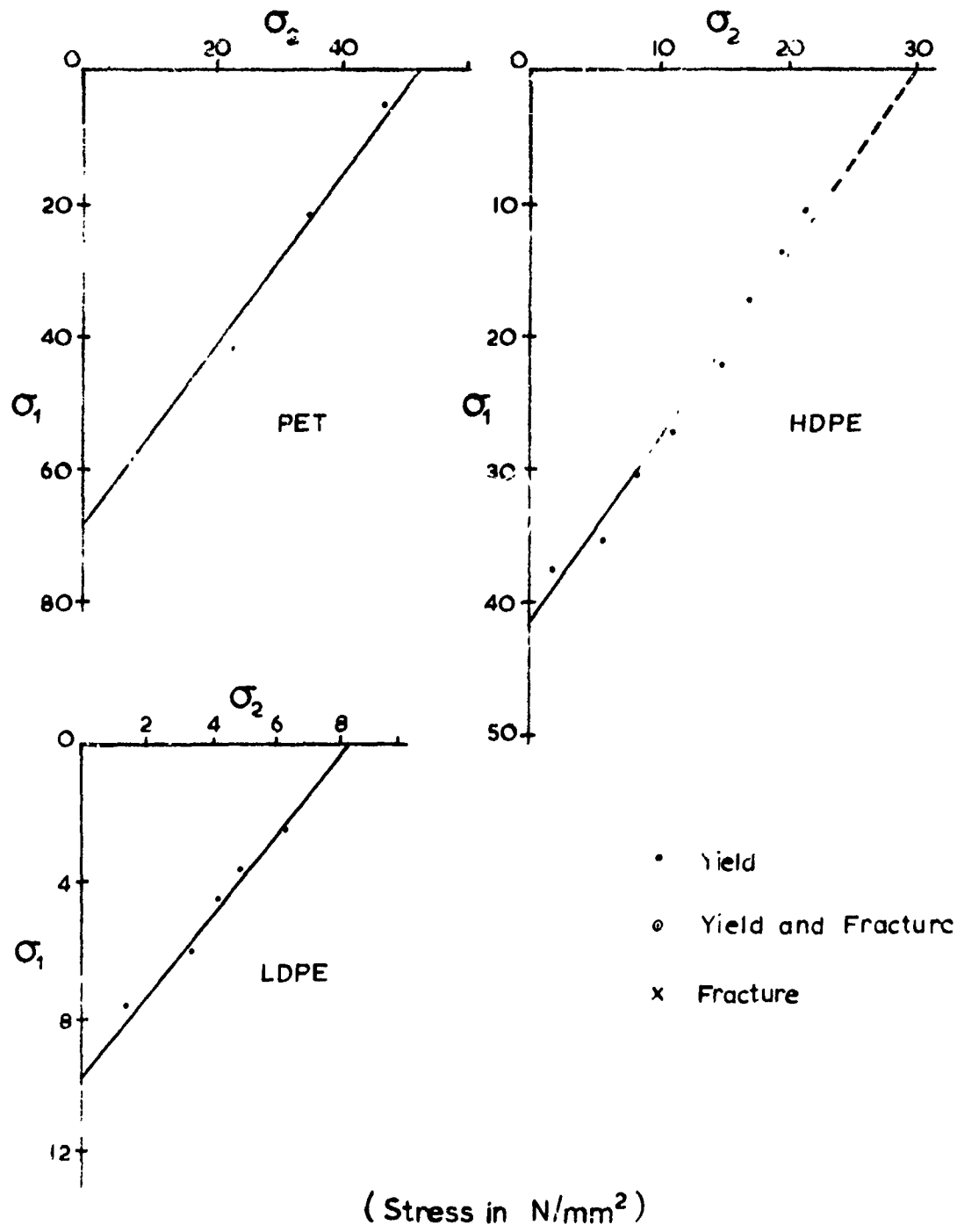

FIGURE 25. Variation of plane strain compressive yield stress σ_1, with applied tension σ_2 through experimental yield points. (Range of stresses investigated for glassy polymers limited by intervention of fracture).

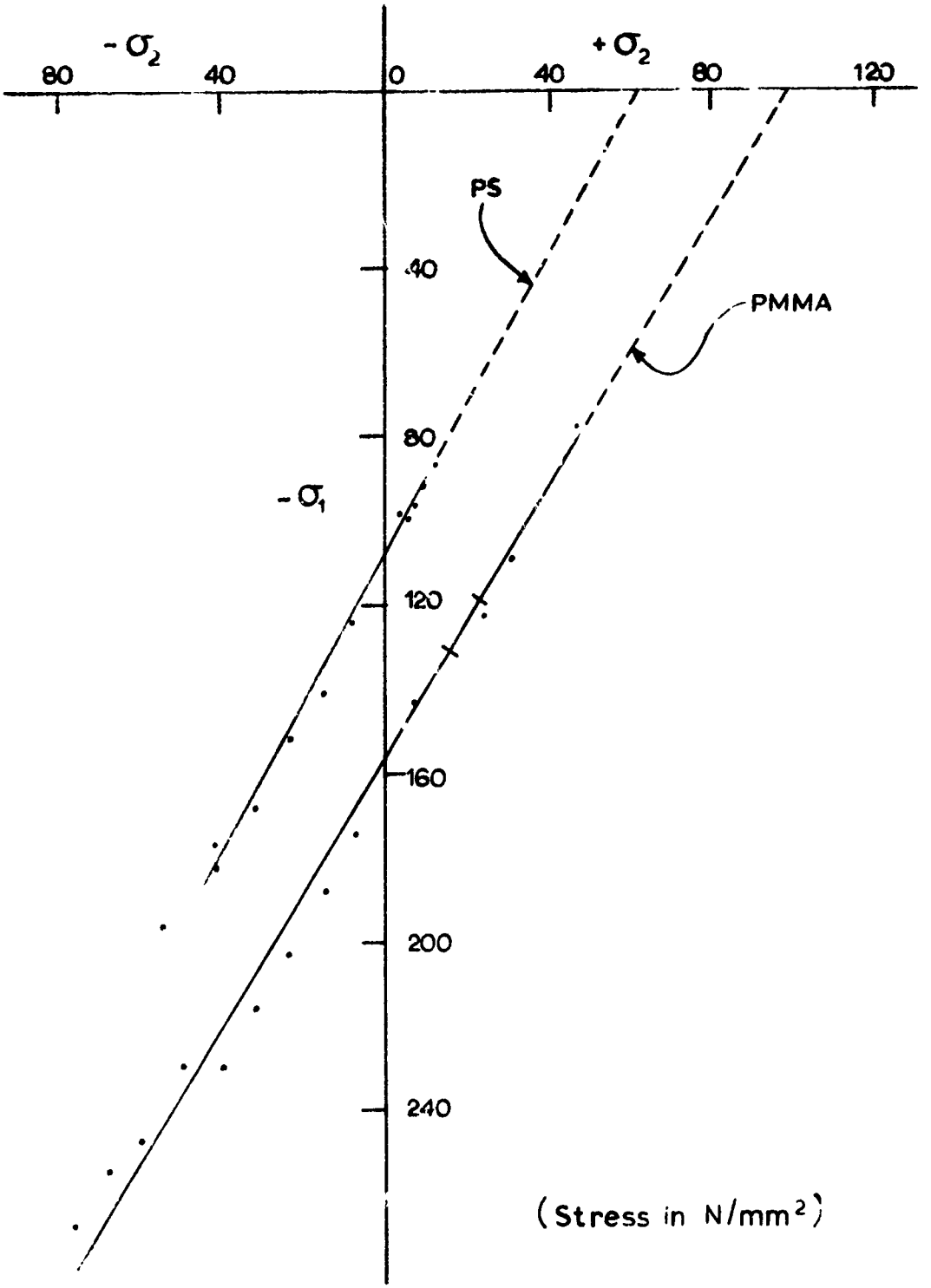

FIGURE 26. Variation of plane strain compressive yield stress of P.M.M.A. and P.S. with applied tension or compression. (Specimens compressed between 6.4 mm dies, at room temperature with constant crosshead speed of 0.2 mm/min).

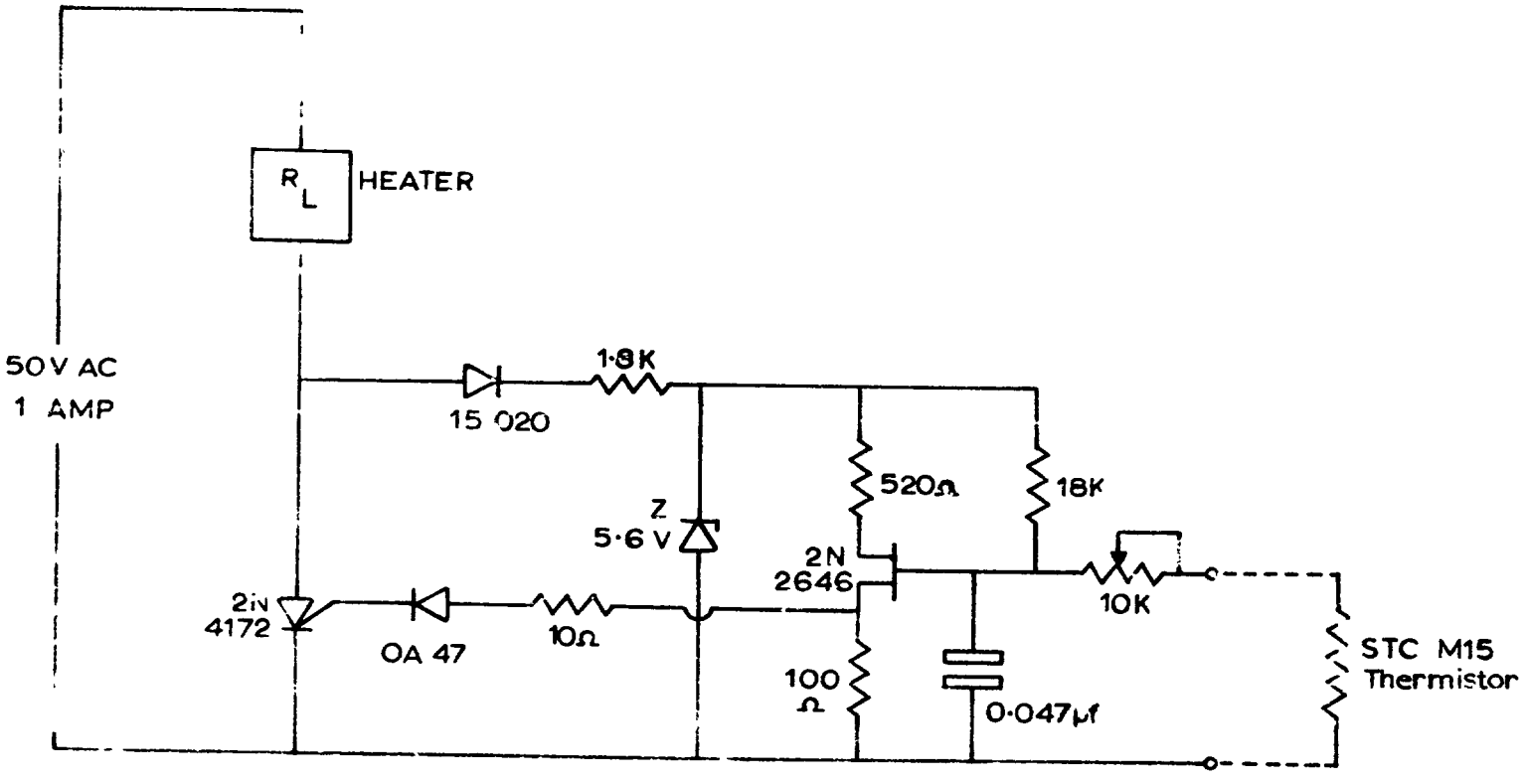

FIGURE 27. Temperature control circuit used for heating dies to tolerance of $\pm$ 0.5°C.

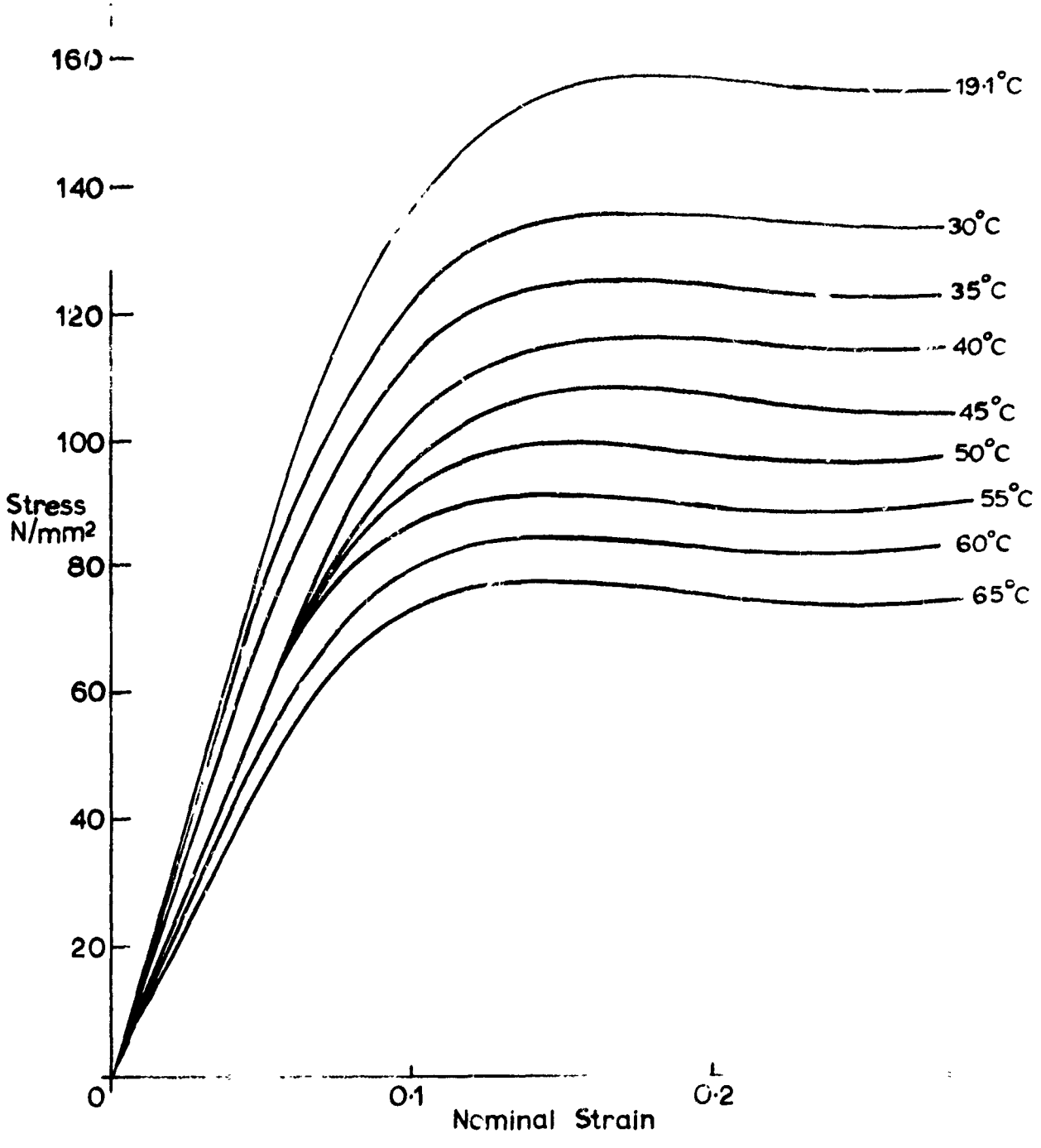

FIGURE 28. Plane strain compression of P.M.M.A. at various temperatures using 6.4 mm dies and constant crosshead speed of 0.2 mm/min.

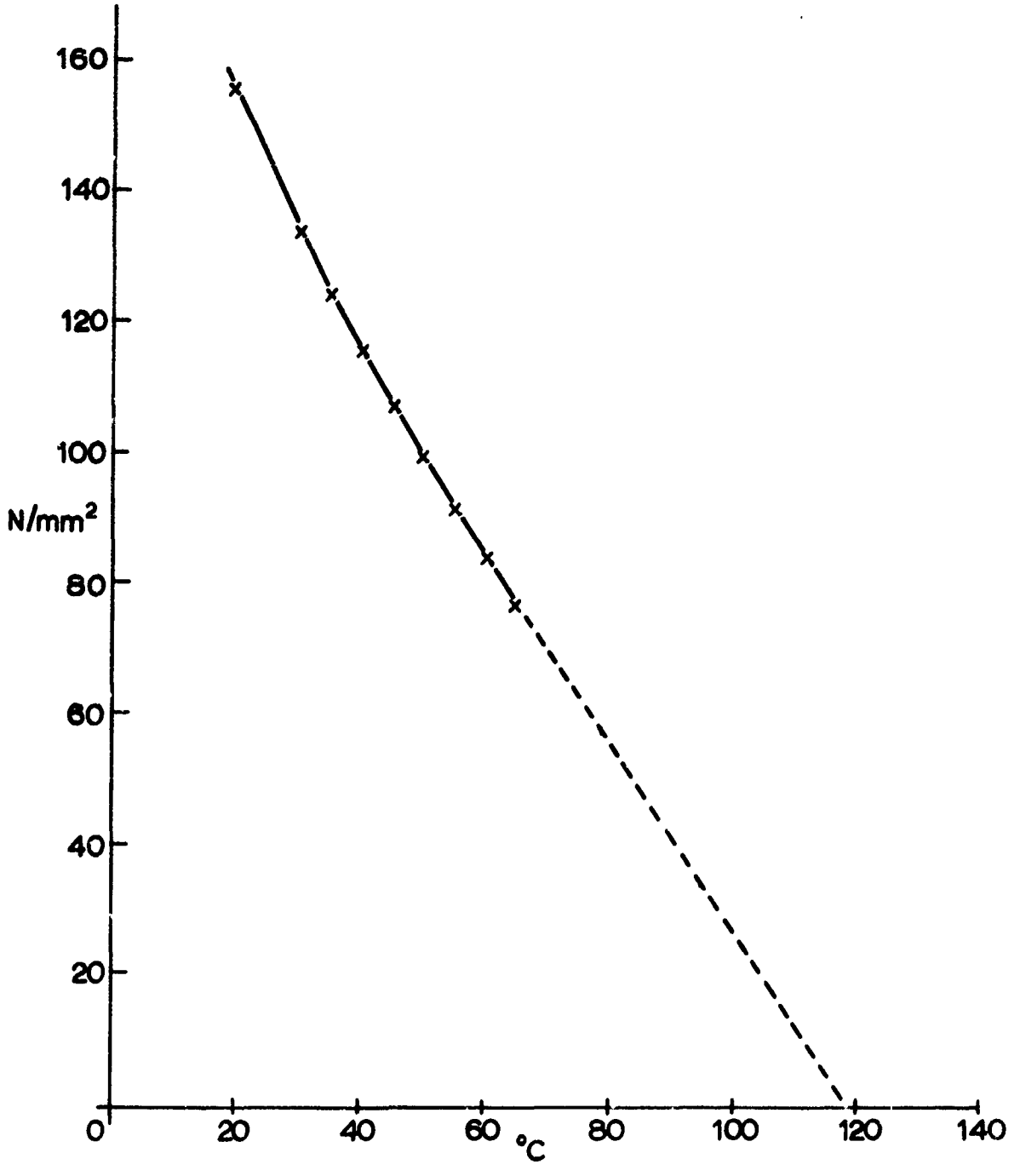

FIGURE 29. Variation of plane strain compressive yield stress of P.M.M.A. with temperature (derived from figure 28).

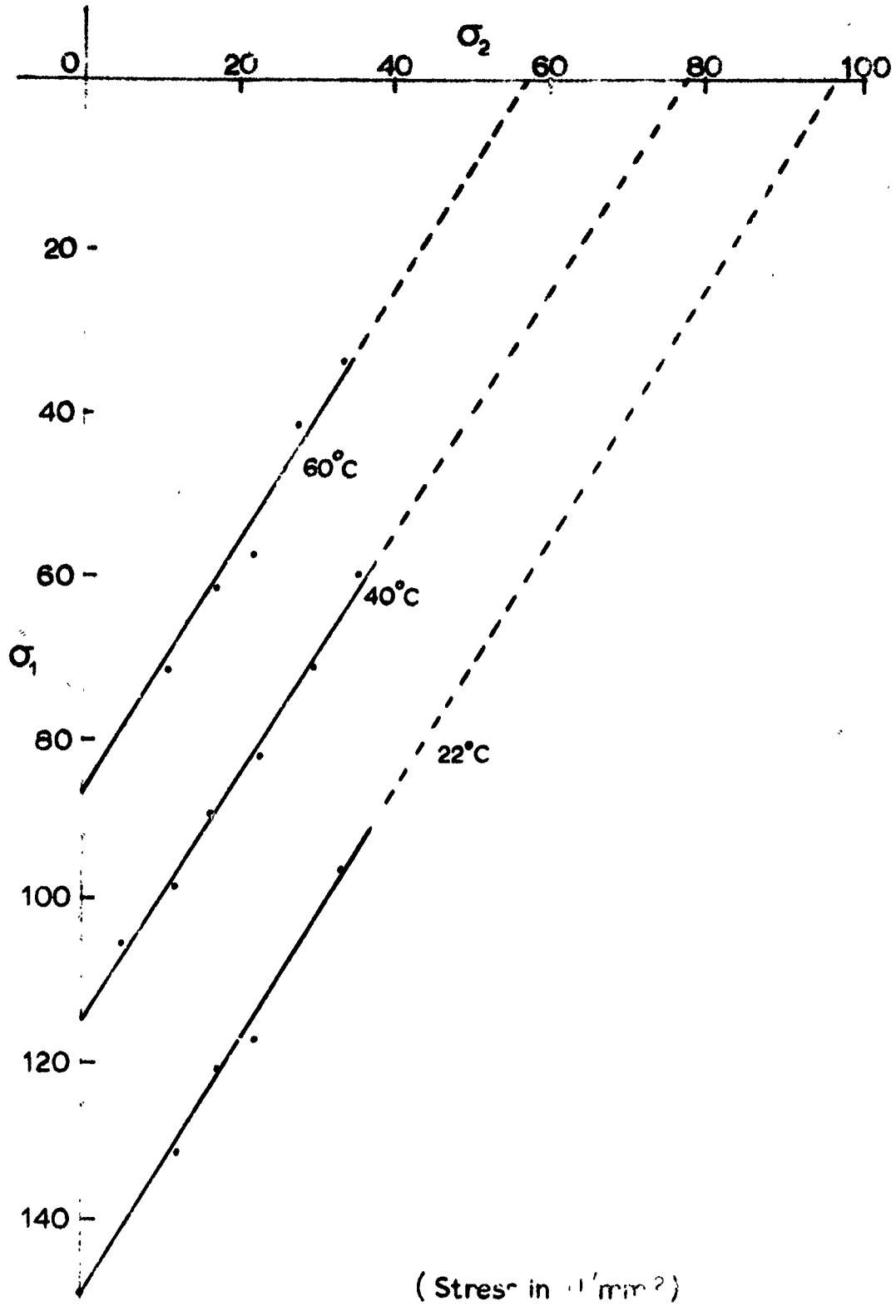

FIGURE 30. Variation of plane strain compressive yield stress with applied tension, for P.M.M.A. at three temperatures. (Best straight lines through experimental points parallel within experimental error).

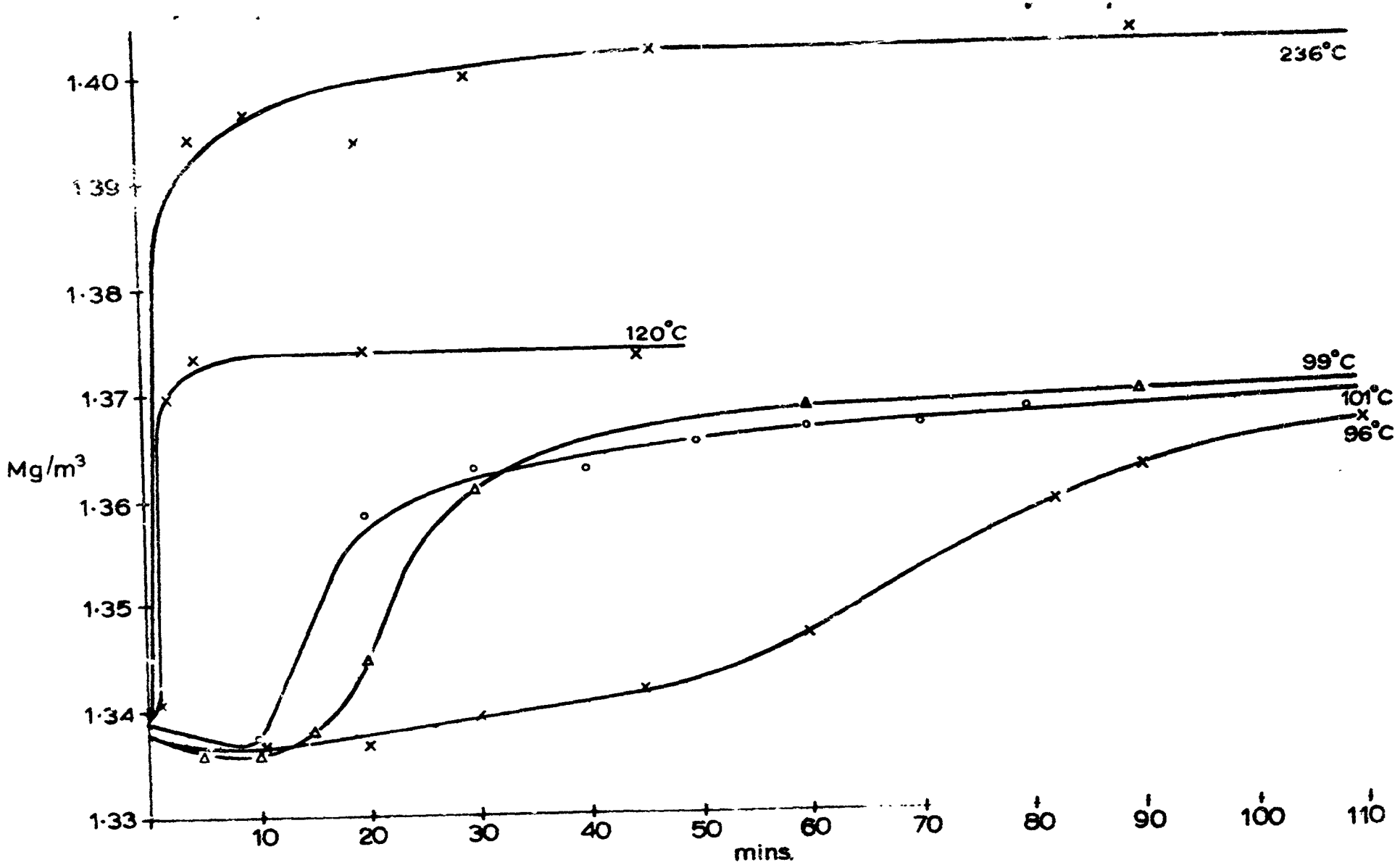

FIGURE 31. Density of P.E.T. samples held at various temperatures for various lengths of time.

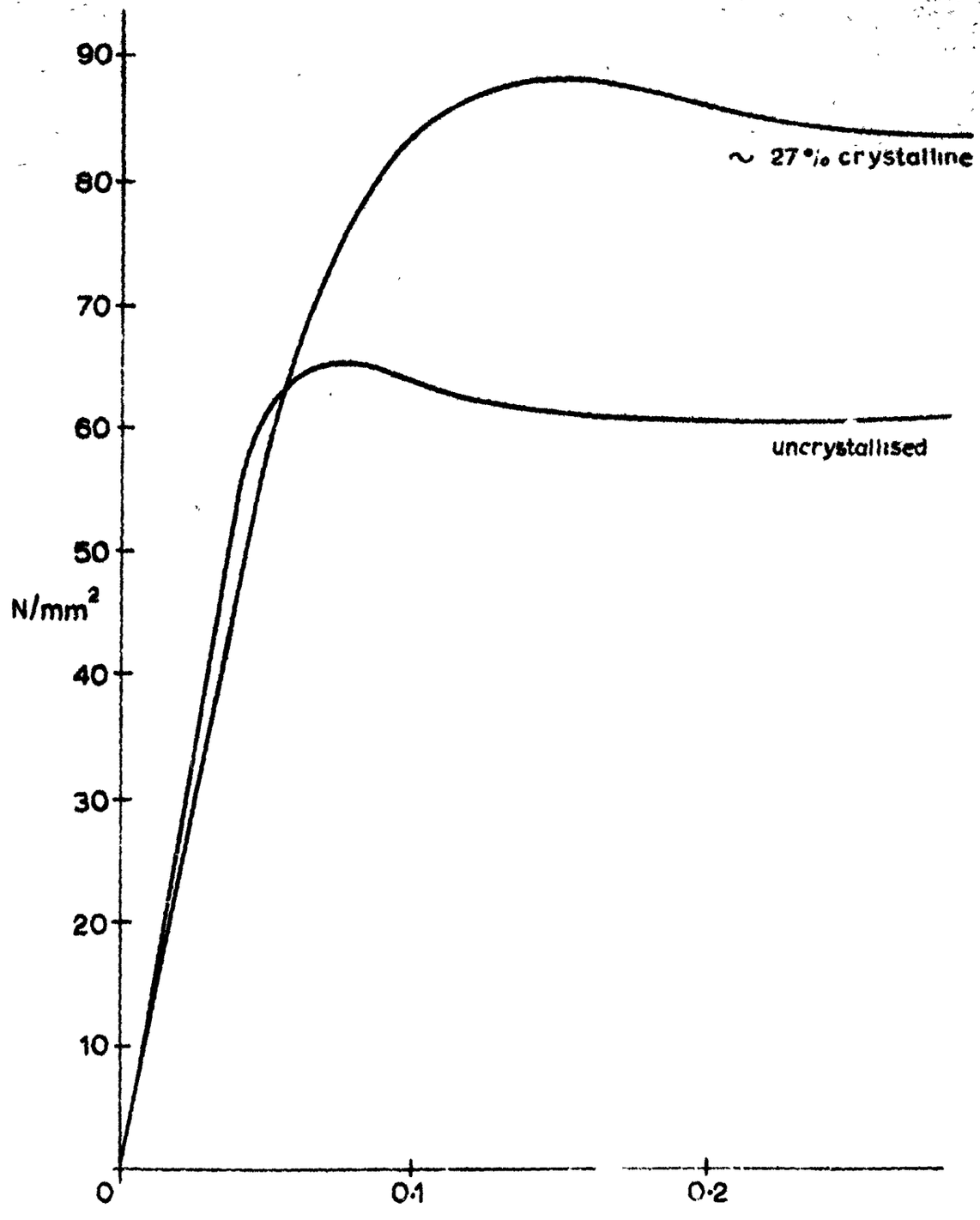

FIGURE 32. Stress-strain curves for crystallised and uncrystallised P.E.T. using 6.4 mm dies at room temperature, and constant crosshead speed of 0.05 mm/min. Crystallinity quoted found from density readings; uncrystallised material showed no crystallinity by x-rays vide 3.1.5).

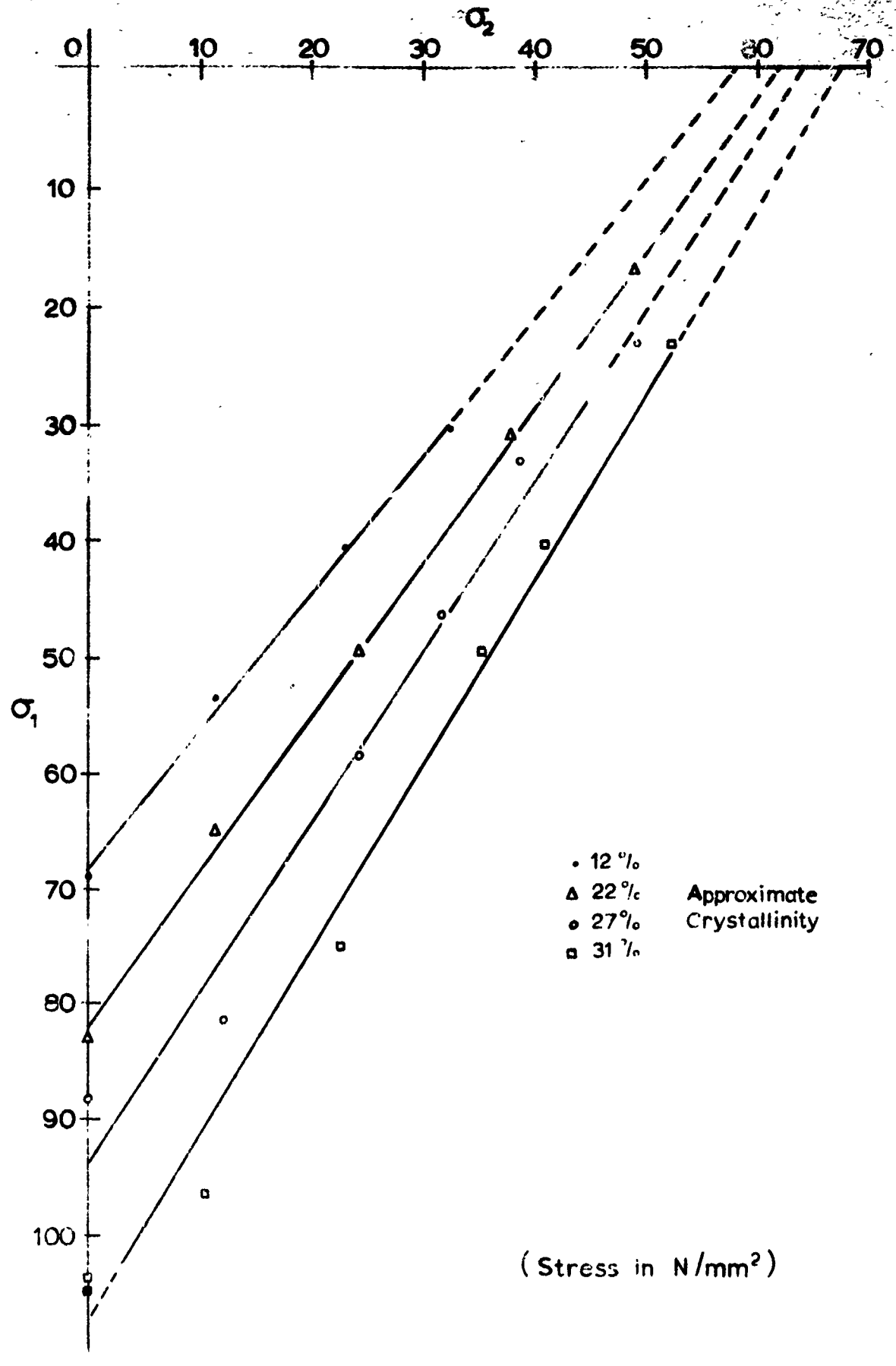

FIGURE 33. Effect of increasing crystallinity in P.E.T. on variation of σ_1 with σ_2. (The large scatter in part due to scatter of crystallinity values about quoted mean).

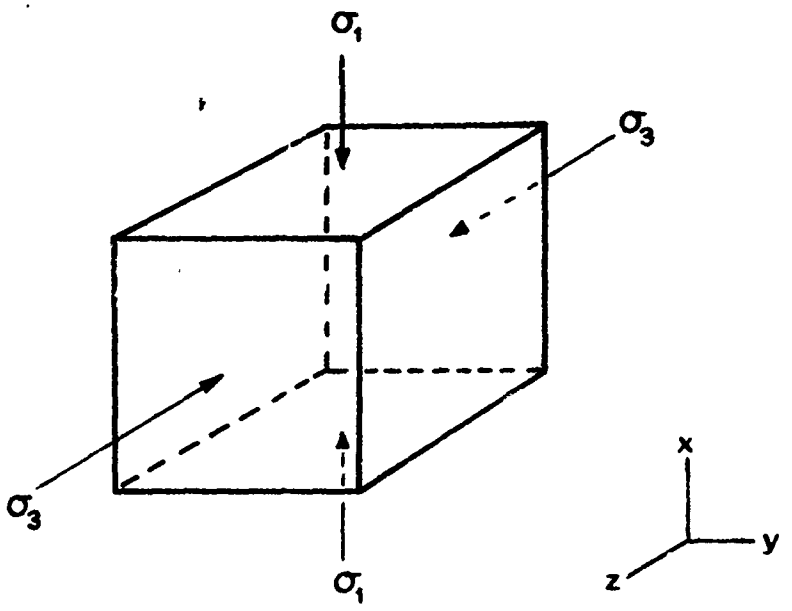

FIGURE 34. Simple plane strain compression

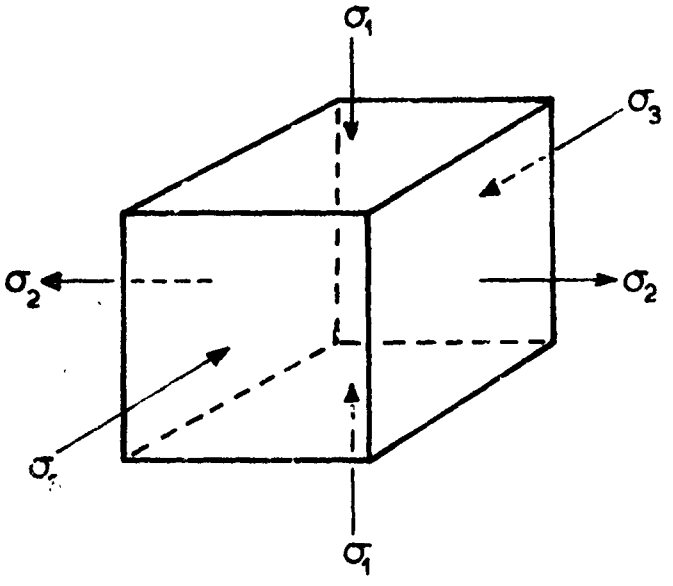

FIGURE 35. Plane strain compression with additional tension.

Stresses acting on elemental cube under the dies. Stresses σ_1 and σ_2 are applied; stress σ_3 results from constrained flow in the z direction.

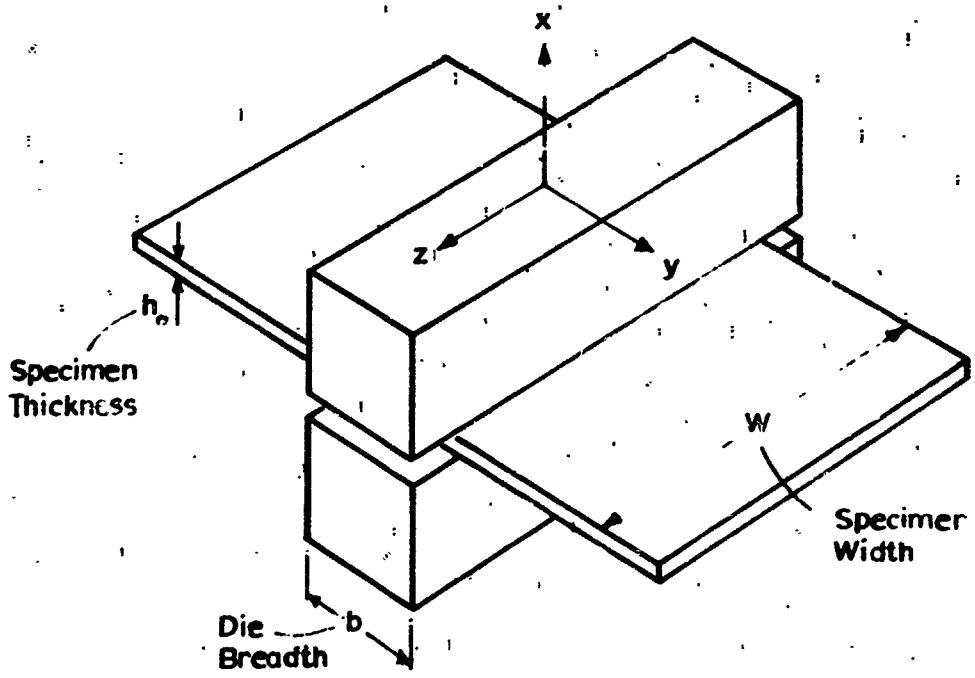

FIGURE 36. Schematic diagram of test arrangement for plane strain compression.

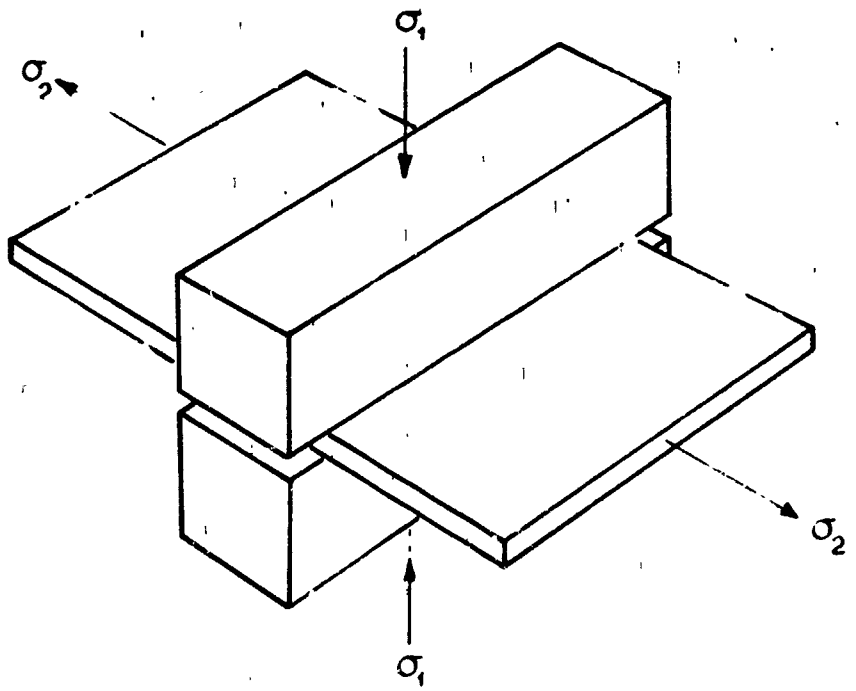

FIGURE 37. The applied stresses for plane strain compression with additional tension or compression. σ_1 always compressive, σ_2 either tensile or compressive.

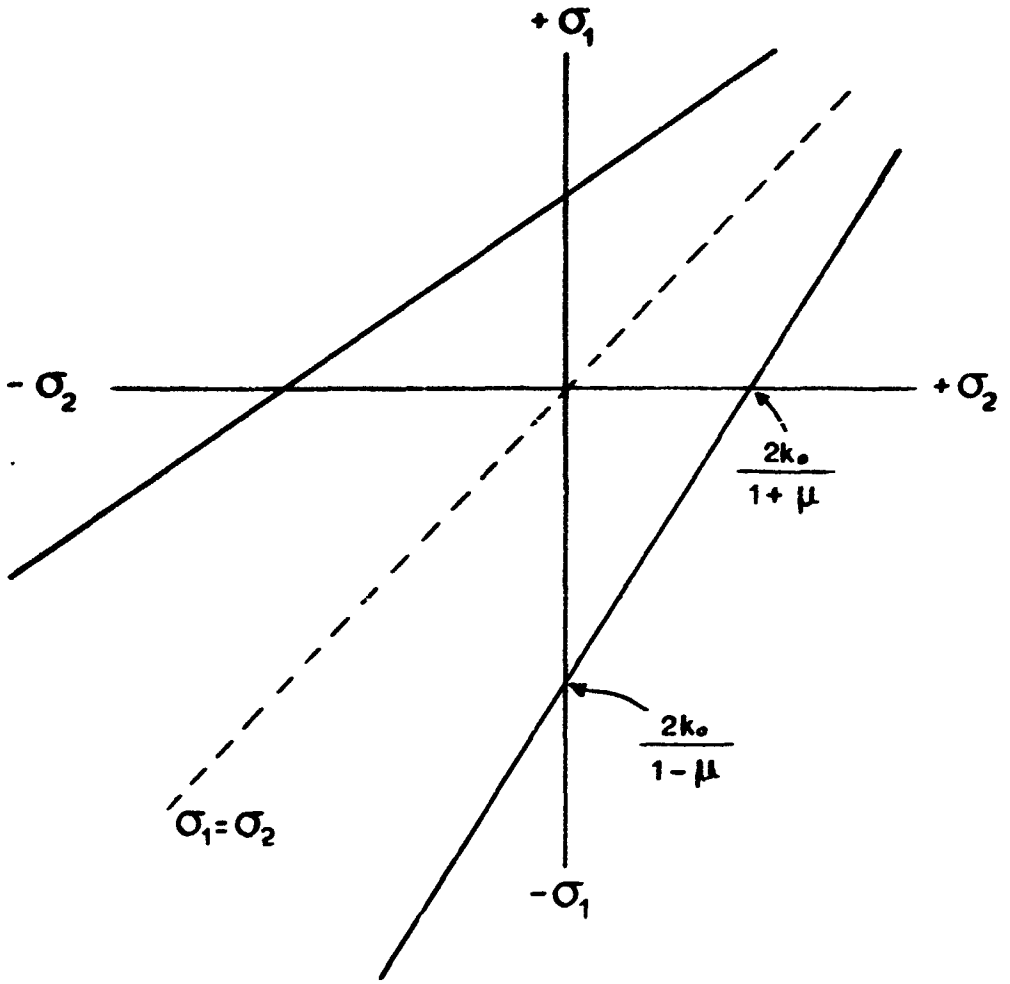

FIGURE 38. Shape of yield locus in two dimensional stress space (equation 8) for von Mises yield criterion modified to include linear pressure dependence. The unmodified form of von Mises criterion (equation 4) would appear as two straight lines parallel to the line $\sigma_1 = \sigma_2$ in this diagram.

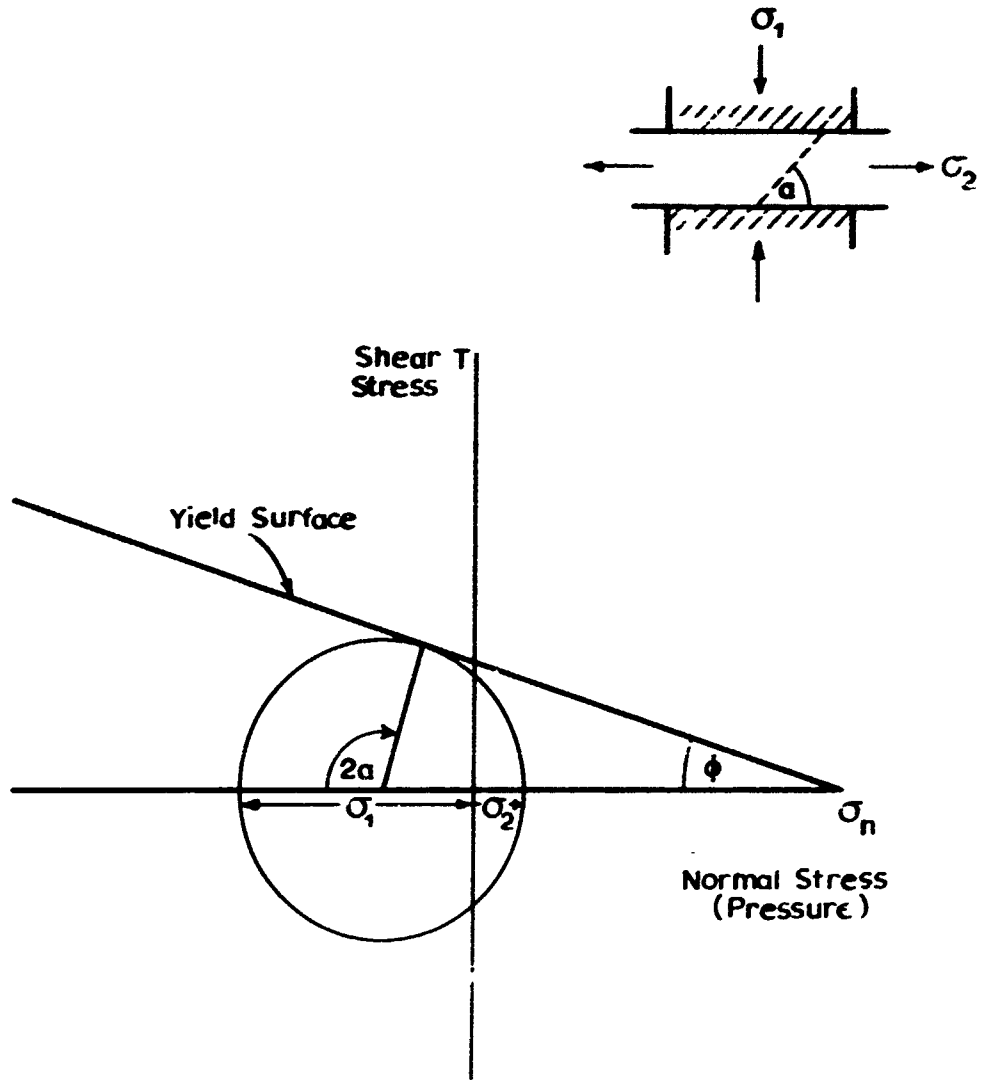

FIGURE 39. Mohr's circle construction showing Coulomb's yield locus and a stress circle representing yield on a plane inclined at angle α. The angle ϕ is the angle of internal friction equal to $\tan^{-1}\mu$.

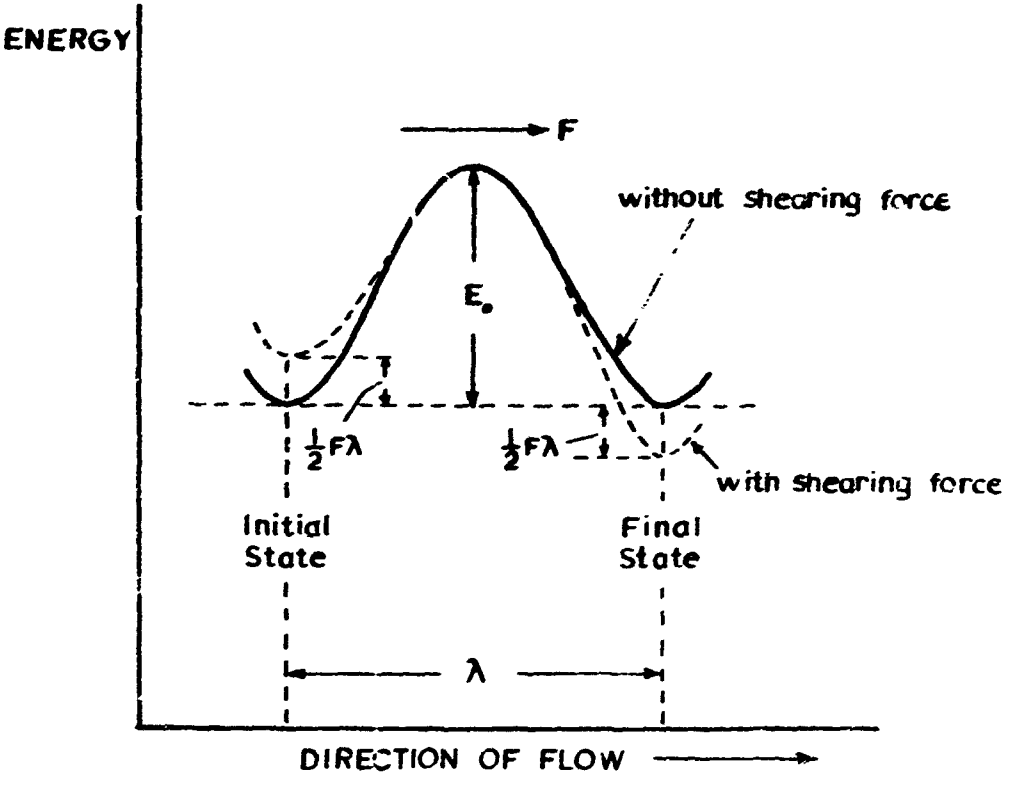

FIGURE 40. Diagram showing decrease in height of energy barrier to flow as a result of the applied shear force F from Glasstone, Laidler and Eyring (1941).

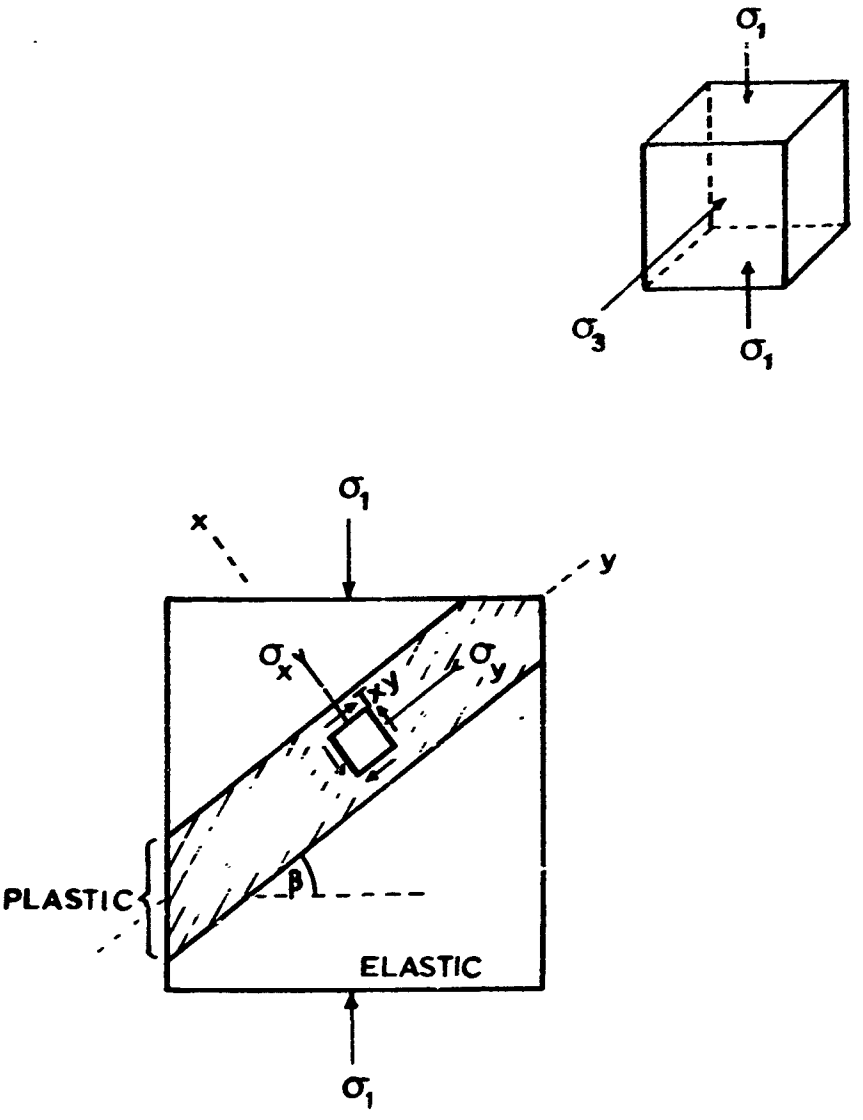

FIGURE 41. Stresses acting on an element of material within a plastic shear zone produced in plane strain compression. Zone inclined at an angle $(90 - \beta)$ to principal stress σ_1. Flow within the plastic zone, in the y direction, is assumed restricted by the elastic material outside the zone

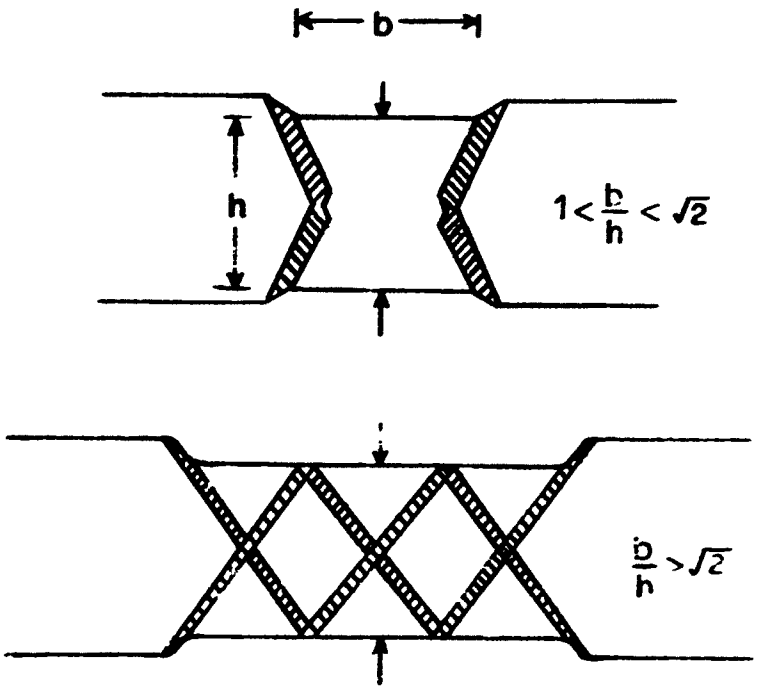

FIGURE 42. Two possible modes of deformation in plane strain compression, after Green (1951).

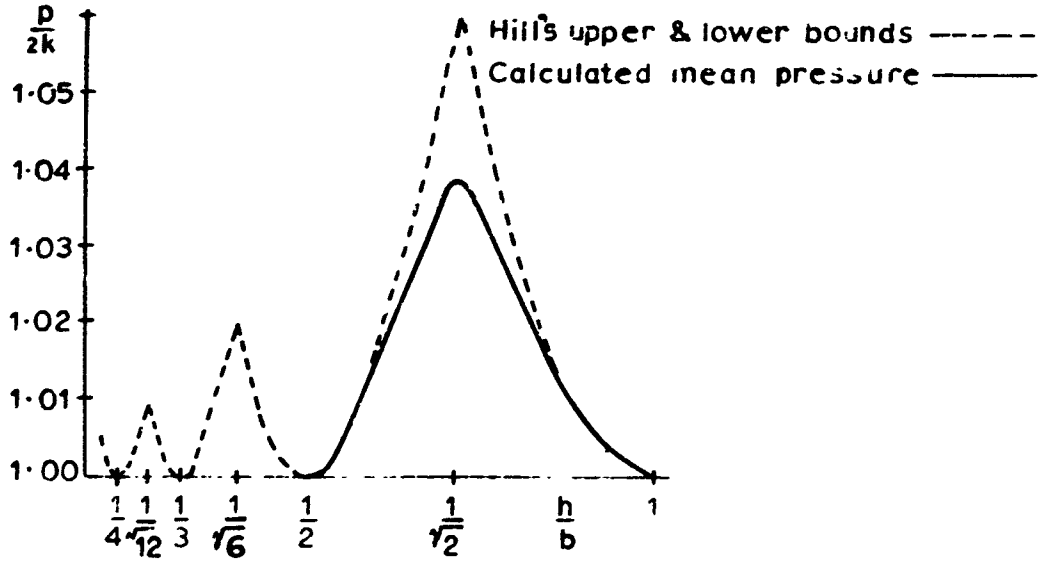

FIGURE 43. Ratio of mean pressure on dies over that for homogeneous compression ($^{p}/_{2k}$), as a function of ratio of specimen thickness to die breadth ($^{h}/_{b}$), after Green (1951).

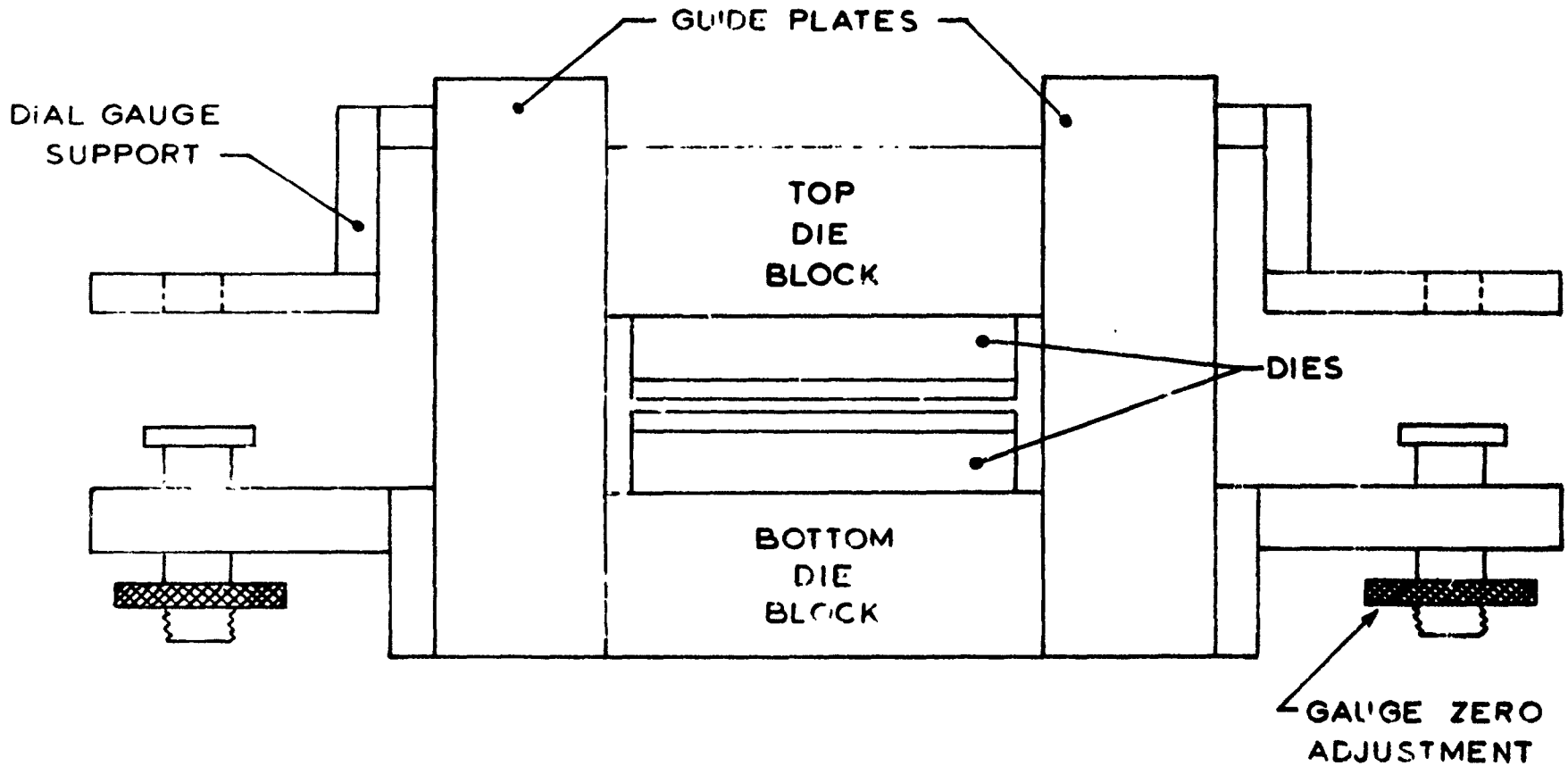

FIGURE 44. Diagram of apparatus used for plane strain compression - actual size.

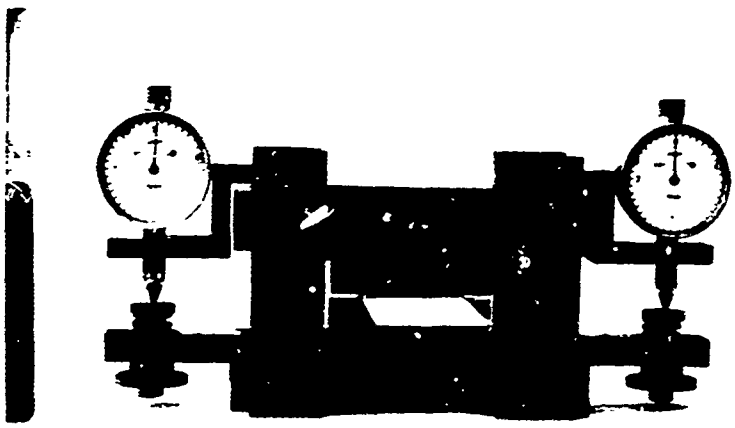

FIGURE 45. Apparatus for plane strain compression, showing dial gauges used to measure strain, and specimen in position between the dies.

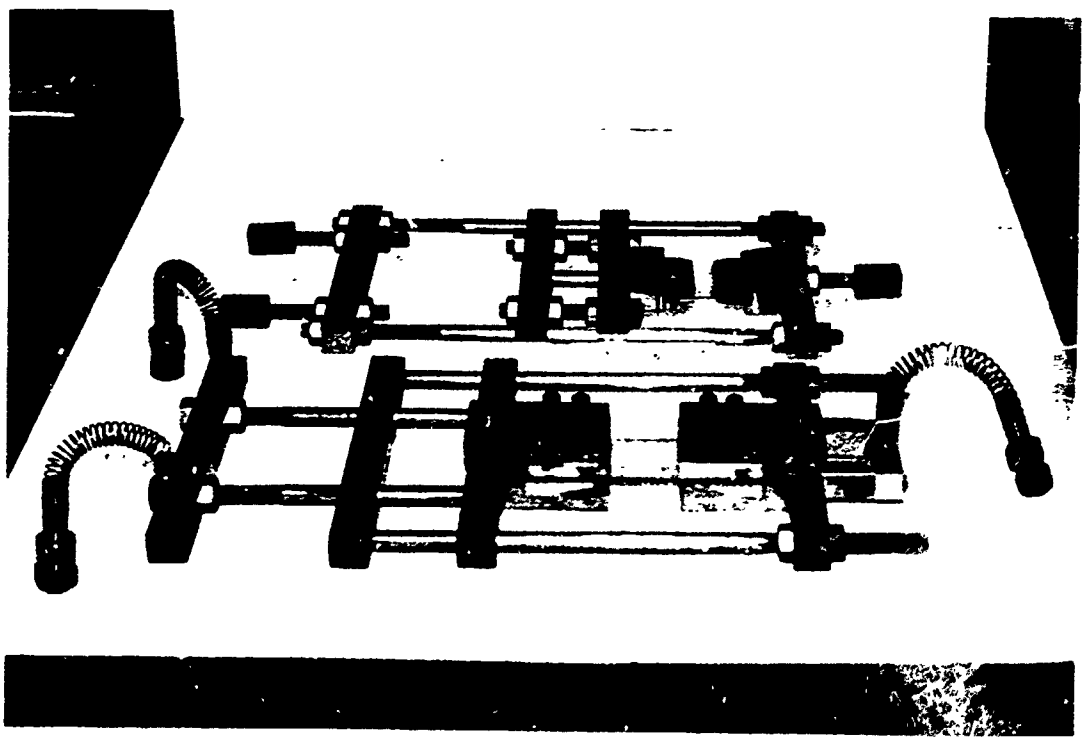

FIGURE 46. Rigs used for applying an additional tension or compression in the plane of a sheet specimen.

In foreground specimen mounted in tensile grips, and springs used for suspending the rig.

In background rig for applying additional compression, complete with specimen holders.

FIGURE 47. Complete biaxial loading system showing the hydraulic ram mounted in the tensile rig.

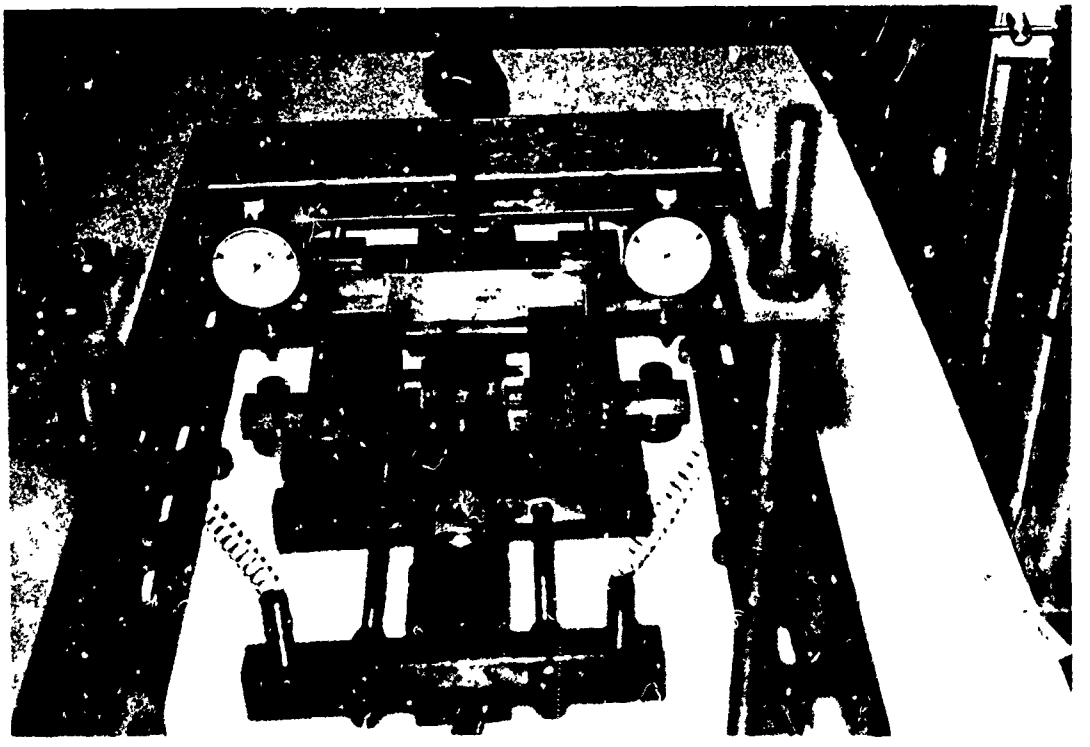

FIGURE 47. General view of the apparatus and one complete tensile rig

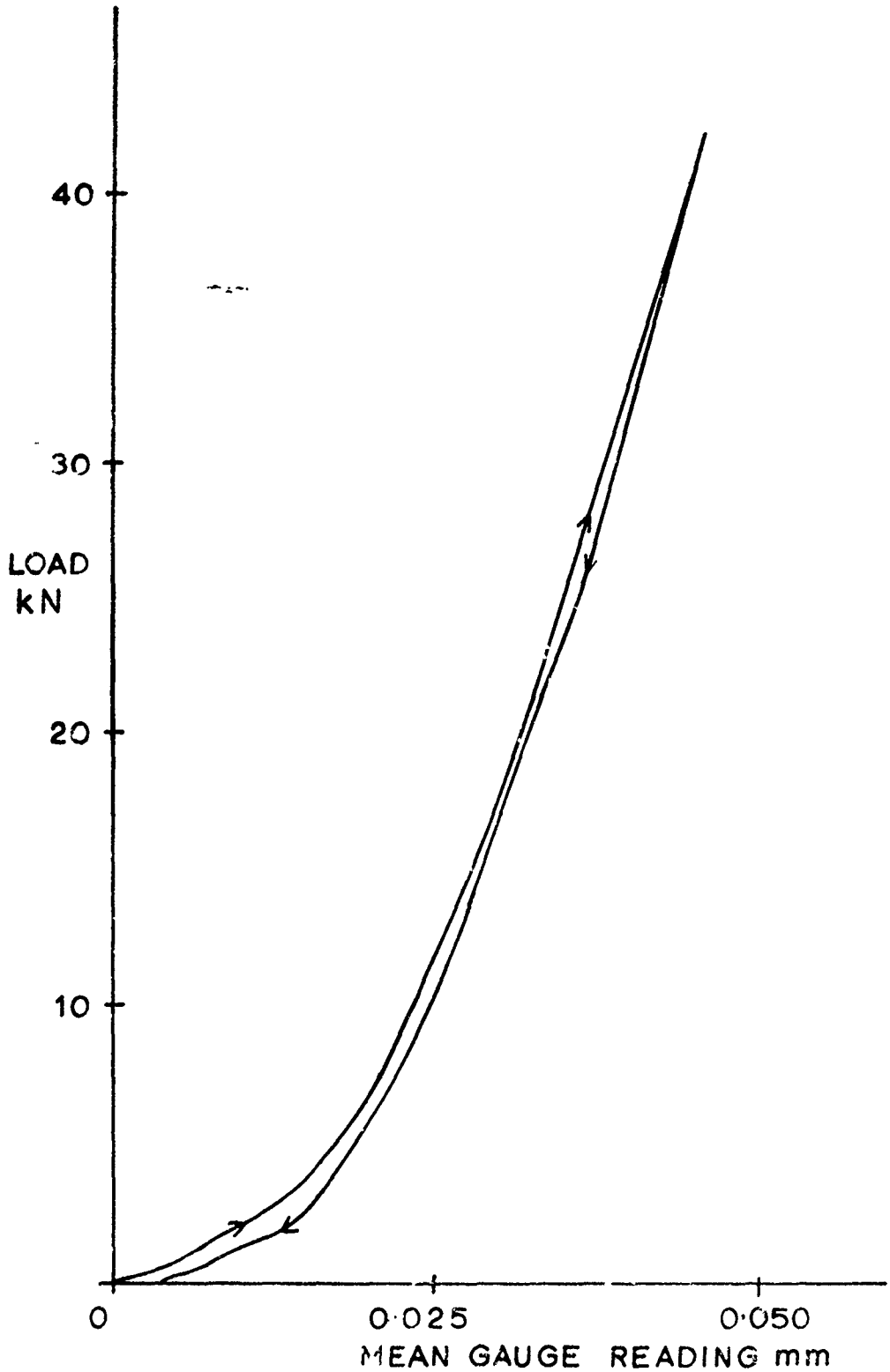

FIGURE 48. A typical curve used to correct dial gauge readings for rig deflection under load. The gauge reading from this curve for a particular load is subtracted from the equivalent gauge reading obtained with a specimen in position.

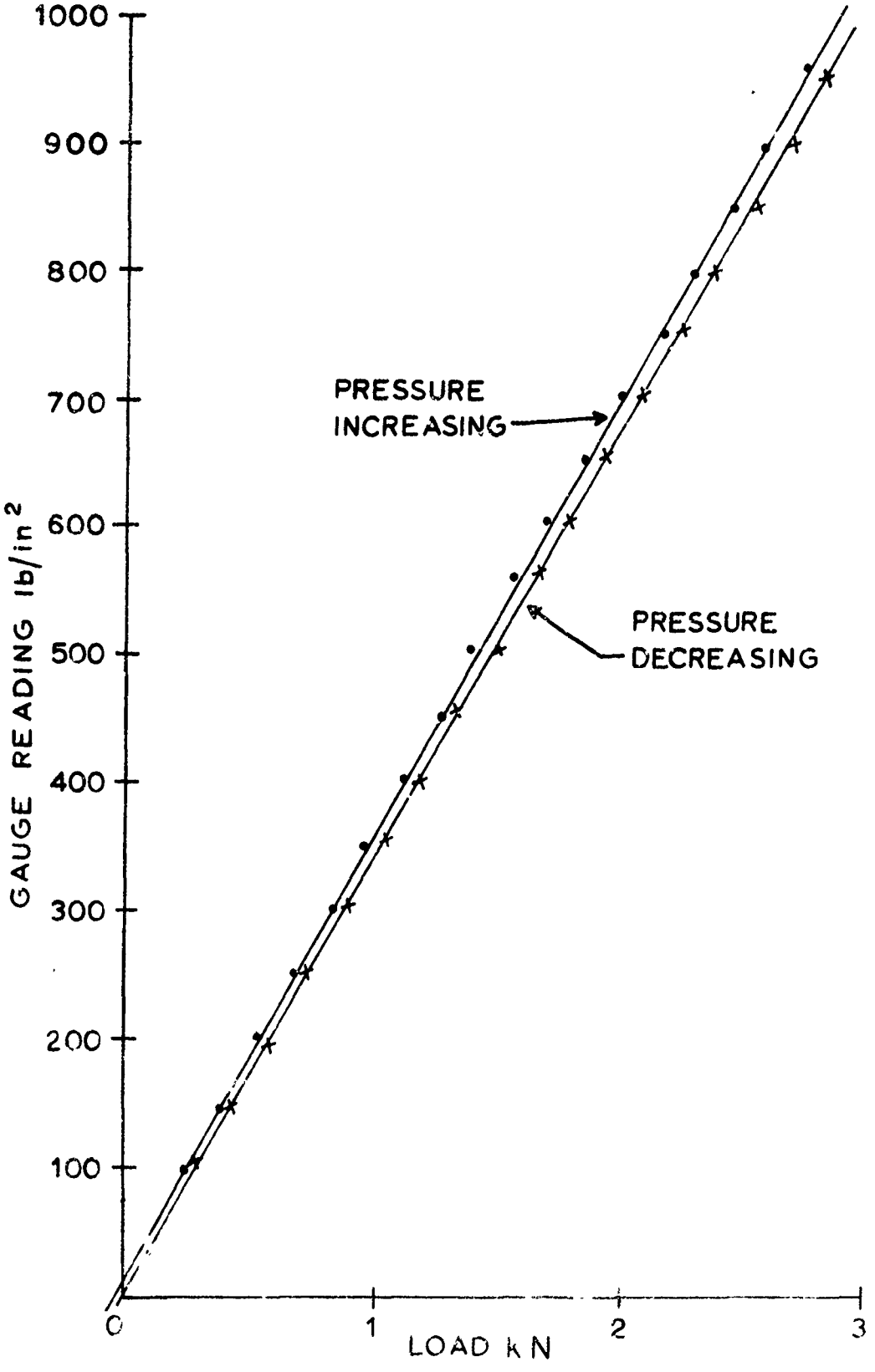

FIGURE 49. Calibration curve for the hydraulic ram in the tensile rig.

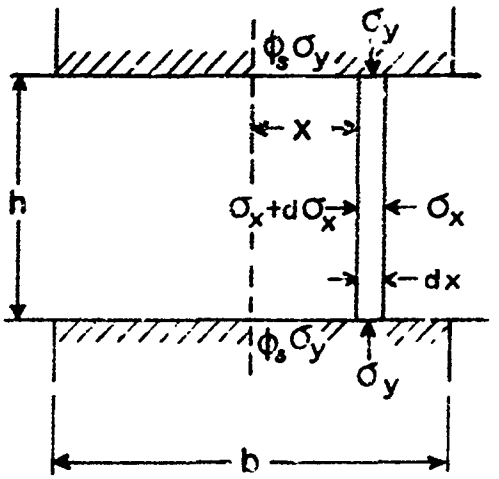

FIGURE 50. Stresses acting on an element of material between the dies in simple plane strain compression. Die breadth b and specimen thickness h.

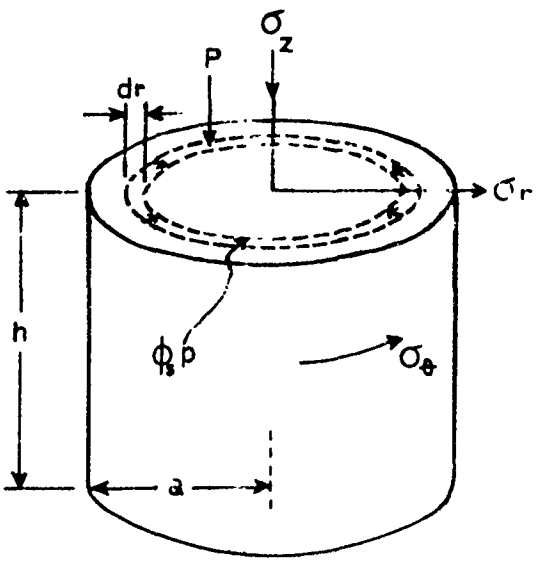

FIGURE 51. Stresses acting on an element of material under the dies in uniaxial compression. Cylinder radius a and height h

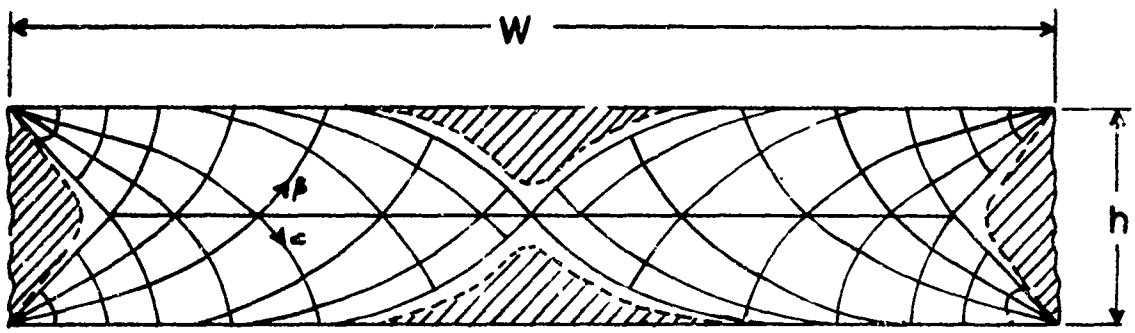

FIGURE 52. The theoretically constructed slip line field for plane strain compression between perfectly rough dies. The slip lines are drawn at 15° intervals for a $\frac{w}{h}$ ratio of 5.

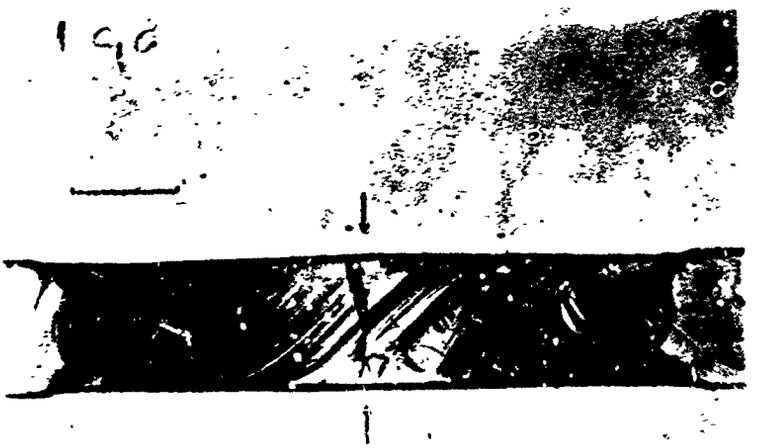

FIGURE 53. Section of a polystyrene specimen taken just to yield in plane strain compression, viewed in transmitted white light. Compression was in the direction indicated, between unlubricated dies.